Right-handed charged current in $b \to u$ transition (Doctor thesis)

Tetsuya Enomoto *
Department of Physics, Graduate School of Science,
Osaka University, Toyonaka, Osaka 560-0043, Japan

(Dated: February 17, 2016)

* Electronic address: tetsuya@het.phys.sci.osaka-u.ac.jp

Abstract

Right-handed charged current in $b \to u$ transition has been considered in order to explain the discrepancy among $|V_{ub}|$ measurements in several B meson decay modes. We study this problem with the most recent experimental data. As a result, we find that a large CP violation in the $b \to u$ right-handed charged current is suggested. Accordingly we study possible CP violating signals in $B \to \pi\pi$, $\rho_L\rho_L$ and DK decays. We obtain constraints from the present experimental data and present future prospects. The scenario of the $b \to u$ right-handed charged current is consistent with the present data and new CP violating signals in the above decay modes might be discovered in future experiments.

Contents

1 Introduction 5

2 The SM and extension with RHCC 7
2.1 The SM 7
2.2 Effective theory with RHCC 7

3 Constraint to $b \to u$ RHCC by measurement of $|V_{ub}|$ 9
3.1 Direct measurement of $|V_{ub}|$ 9
3.2 Indirect determination of V_{ub}^L by the unitarity of CKM matrix 13
3.3 Summary and consideration about measurement of $|V_{ub}|$ 15

4 Constraint to $b \to u$ RHCC by hadronic B decays 18
4.1 $B \to \pi\pi$ 18
4.2 $B \to \rho_L \rho_L$ 23
4.3 $B \to DK$ 28

5 $b \to u$ RHCC in minimal supersymmetric standard model 33

6 Conclusion 36

App. A Form factor and decay constant 38
A.1 Parity and time-reversal conversion property of states and operator . 38
A.2 Decay constant 40
A.3 Form factors 42

App. B Calculations of each B meson decay rate 46
B.1 $b - u - \ell - \nu$ 4 fermi operator 46
B.2 $B \to \tau\nu$ 46
B.3 $B \to \pi\ell\nu$ 47
B.4 $B \to X_u \ell\nu$ 49
B.5 $B \to \rho\ell\nu, \omega\ell\nu$ 50

App. C Renormalization for hadronic decays 55

C.1 $b_L \to u_L \bar{c}_L s_L$ 59
C.2 $b_R \to u_R \bar{c}_L s_L$ 61
C.3 $b_L \to u_L \bar{u}_L d_L$ 64

App. D Isospin analysis in $B \to \pi\pi$ and $\rho_L\rho_L$ 65

App. E Dalitz Plot Analysis in $B \to DK$ 73

App. F Input list 78

1 Introduction

In the standard model (SM) with its gauge group $SU(3)_C \times SU(2)_L \times U(1)$ all charged currents are left-handed. However in new physics models, right-handed charged currents (RHCC) could arise. Moreover quark charged currents in the SM is governed by the Cabibbo-Kobayashi-Maskawa (CKM) matrix [1, 2]. $b \to u$ transition in the SM is suppressed by CKM element V_{ub} and is likely to be affected by RHCC induced in new physics. In addition, it is possible to examine decays of bottom quark in detail because of the competent data of B factory experiments.

There was discrepancy in $|V_{ub}|$ measurement among several semileptonic and leptonic B meson decays [3] as shown in Fig. 1. It is reported that $b \to u$ RHCC can explain it [4, 5, 6], as will be fully described below. After the publication of Ref. [4, 5, 6], the branching fraction of $B \to \tau\nu$ was updated by Belle collaboration and the discrepancy of $|V_{ub}|$ determination became less significant [7]. Therefore the possibility of the new physics scenario that induces the $b \to u$ RHCC must be reconsidered. Also in these previous studies, it is assumed that $b \to u$ RHCC does not induce new CP violation.

In this work, we reexamine possibility of $b \to u$ RHCC taking new experimental data into account. We will introduce $b \to u$ RHCC in Sec. 2. In Sec. 3 we explain $b \to u$ RHCC effect to the determination of $|V_{ub}|$ from semileptonic and leptonic B meson decays and reveal that it suggests large CP violation in $b \to u$ RHCC [8]. In Sec. 4, we examine how CP violating observables in $B \to \pi\pi, B \to \rho\rho$ and $B \to DK$ are affected by $b \to u$ RHCC. We find that a new direct CP asymmetries, which are absent in the SM, arise and the determination of angles of unitarity triangle is affected [8]. Moreover possible signals in $b \to u$ RHCC are compared with experimental data and we show that $b \to u$ CP violating RHCC is a viable new physics scenario [8]. In Sec. 5, we compare $b \to u$ RHCC induced by squark mixing in the minimal supersymmetric standard model (MSSM) to experimental constraints given in Sec. 3. Our conclusion is stated in Sec. 6.

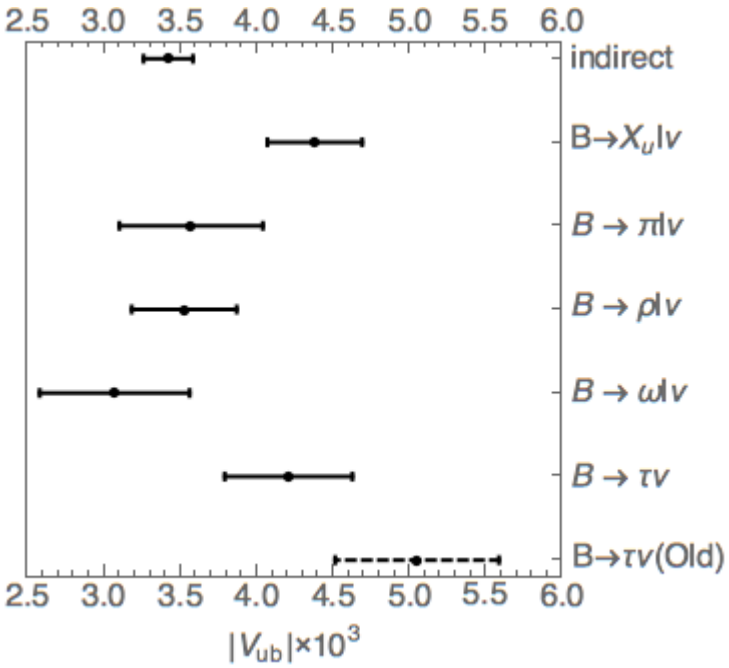

Fig.1 current data of $|V_{ub}|$ by each measurements

2 The SM and extension with RHCC

2.1 The SM

The tree-level flavor changing interaction in the SM is described by the following left-handed charged current;

$$\mathcal{L}_{\text{c.c.}} = \bar{U}_L \gamma^\mu V_{\text{CKM}} D_L W_\mu^+ + \text{h.c.} \tag{1}$$

$$D_L = \begin{pmatrix} d_L & s_L & b_L \end{pmatrix}^T \tag{2}$$

$$U_L = \begin{pmatrix} u_L & c_L & t_L \end{pmatrix}^T \tag{3}$$

$$V_{\text{CKM}} = \begin{pmatrix} V_{ud} & V_{us} & V_{ub} \\ V_{cd} & V_{cs} & V_{cb} \\ V_{td} & V_{ts} & V_{tb} \end{pmatrix} \tag{4}$$

where CKM matrix, V_{CKM}, represents the transition among quark generations. Absolute values of CKM matrix element in the SM are given as [9]

$$|V_{\text{CKM}}| = \begin{pmatrix} 0.97 & 0.23 & 0.0041 \\ 0.23 & 0.99 & 0.041 \\ 0.0084 & 0.040 & 1.0 \end{pmatrix}. \tag{5}$$

If the flavor structure in new physics differs from that of the SM, flavor signals can be affected significantly by new physics. In particular, since V_{ub} has the smallest absolute value, the $b \to u$ transitions tend to be sensitive to new physics. One of possible scenarios is that an effect of new physics appears in the $b \to u$ transitions as the corresponding RHCC.

2.2 Effective theory with RHCC

In general, effects of new physics at low energys are expressed in the following effective lagrangian,

$$\mathcal{L} = \mathcal{L}_{SM} + \frac{1}{\Lambda} \sum_i C_i^{(5)} \mathcal{Q}_i^{(5)} + \frac{1}{\Lambda^2} \sum_i C_i^{(6)} \mathcal{Q}_i^{(6)} + O\left(\frac{1}{\Lambda^3}\right), \tag{6}$$

where Λ is the scale of new physics and $\mathcal{Q}_i^{(n)}$'s represent gauge invariant operators of dimension n. The $b \to u$ RHCC is induced by the following operator,

$$\mathcal{Q}_{RR} = (\bar{u}\gamma^\mu P_R b)\left(\bar{\phi}^\dagger i D_{(L)\mu}\phi\right) + \text{h.c} \tag{7}$$

$$D_{(L)\mu} = \partial_\mu + \frac{ig'}{2}B_\mu Y + \frac{ig}{2}\vec{W}_\mu \cdot \vec{\sigma}. \tag{8}$$

We note that the above operator is the only one that contributes to $b \to u$ RHCC up to and including dimension 6. Substituting the Higgs vacuum expectation value, this operator is evaluated as

$$\begin{aligned}\mathcal{Q}_{RR}|_{\phi\to\langle\phi\rangle} =& \bar{u}\gamma^\mu P_R b(\frac{1}{\sqrt{2}}v, 0) i D_{(L)\mu}\begin{pmatrix} 0 \\ \frac{1}{\sqrt{2}}v \end{pmatrix} \\ =& -\frac{gv^2}{2\sqrt{2}}\bar{u}\gamma^\mu P_R b W_\mu^+. \end{aligned} \tag{9}$$

Thus $b \to u$ RHCC is introduced in Lagrangian density:

$$\mathcal{L}_{buW}^R = \frac{-g}{\sqrt{2}}V_{ub}^R \bar{u}\gamma^\mu P_R b W_\mu^+ \tag{10}$$

$$V_{ub}^R = \frac{C_{RR}^{(6)}v^2}{2\Lambda^2} \simeq 0.003 \times C_{RR}^{(6)}(3\text{TeV}/\Lambda)^2 \tag{11}$$

where $v = 246$ GeV is used. The Lagrangian density of b-u-W vertex including both left- and right- handed charged currents is

$$\mathcal{L}_{buW} = \frac{-g}{\sqrt{2}}\bar{u}\gamma^\mu (V_{ub}^R P_R + V_{ub}^L P_L) b W_\mu^+, \tag{12}$$

where V^L denotes the quark mixing matrix in the left-handed sector. Compering Eq. (5) and Eq. (11), we find that the $b \to u$ RHCC is sensitive to $\sim$3 TeV scale new physics.

The left-handed charged current might be also affected by new physics. However such effects are expected to be suppressed taking constraints of flavor changing neutral current (FCNC) into account. Hence we assume that V^L is unitary as in the SM.

3 Constraint to $b \to u$ RHCC by measurement of $|V_{ub}|$

Experimental determinations of the strength of $b \to u$ transition $|V_{ub}|$ are affected by the $b \to u$ RHCC. In this section, we evaluate the effects of the $b \to u$ RHCC in direct $|V_{ub}|$ determinations in $B \to \tau\nu$, $\pi\ell\nu$, $X_u\ell\nu$, $\rho\ell\nu$ and $\omega\ell\nu$. In addition, we discuss the indirect determination of $|V_{ub}^L|$.

3.1 Direct measurement of $|V_{ub}|$

3.1.1 $B \to \tau\nu$

The decay rate of $B \to \tau\nu$ is calculated with the following equation,

$$\Gamma(B \to \tau\nu) = \frac{1}{8\pi} {G_f}^2 |V_{ub}^L - V_{ub}^R|^2 {F_B}^2 M_B M_\tau^2 \left(1 - \left(\frac{M_\tau}{M_B}\right)^2\right)^2 . \tag{13}$$

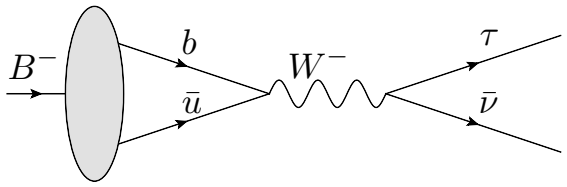

Fig.2 Feynman diagram of $B^- \to \tau\nu$

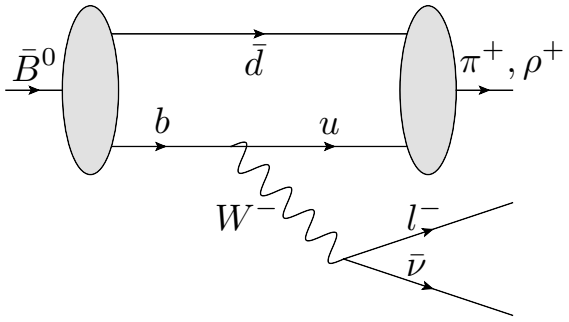

Fig.3 Feynman diagram of $\bar{B}^0 \to \pi^+(\rho^+, \omega^+)\ell^-\bar{\nu}$

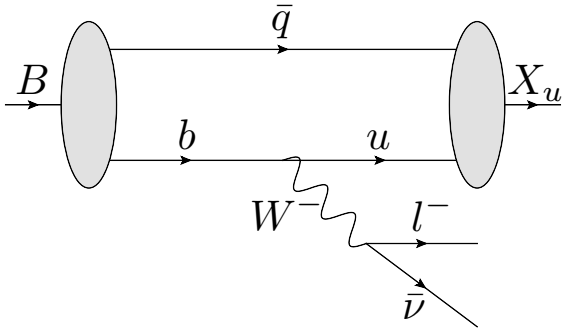

Fig.4 Feynman diagram of $B \to X_u\ell^-\bar{\nu}$

The relative sign between V_{ub}^L and V_{ub}^R is minus because only axial-vector current can contribute. After solving $|V_{ub}^L - V_{ub}^R|$ and inserting experimental value, the result is

$$|V_{ub}^L - V_{ub}^R| = (4.22 \pm 0.42) \times 10^{-3}. \tag{14}$$

with following data,

$$\mathrm{Br}(B \to \tau\nu) = (114 \pm 22) \times 10^{-6} \text{ [10]} \tag{15}$$

$$F_B = 0.1905 \pm 0.0042 \text{ GeV [11]}. \tag{16}$$

3.1.2 $B \to \pi\ell\nu$

Decay rate of $B \to \pi\ell\nu$ is calculated following equation,

$$d\Gamma(B \to \pi\ell\nu) = \frac{G_f^2}{192\pi^3 c_\pi^2 M_B^3} |V_{ub}^L + V_{ub}^R|^2 f_+(q^2)^2 \lambda(q^2)^{3/2} dq^2. \tag{17}$$

The relative sign between V_{ub}^L and V_{ub}^R is plus because only vector current can contribute. For form factor, we use

$$f_+(q^2) = \frac{r_1}{1 - q^2/(m_1^\pi)^2} + \frac{r_2}{1 - q^2/m_{\text{fit}}^2} \qquad (0 < q^2 < 14\text{GeV}^2) \tag{18}$$

$$\begin{array}{cc} m_{\text{fit}}^2 = 40.73\text{GeV}^2 & m_1^\pi = 5.32\text{GeV}^2 \\ r_1 = 0.744 & r_2 = -0.486 \end{array} \tag{19}$$

$$c_\pi = \begin{cases} 1 & \pi = \pi^+ \\ \sqrt{2} & \pi = \pi^0 \end{cases} \tag{20}$$

calculated by P. Ball and R. Zwicky [12]. This equation has 13% error. Branching ratio with $0 < q^2 < 16[\text{GeV}^2]$ is measured, so we use this equation with q^2 extension. In the result, $|V_{ub}^L + V_{ub}^R|$ is

$$|V_{ub}^L + V_{ub}^R| = (3.58 \pm 0.47) \times 10^{-3}, \tag{21}$$

with experimental data [10],

$$\mathrm{Br}(B \to \pi\ell\nu)|_{16\text{GeV}^2 > q^2 > 0} = (1.06 \pm 0.04) \times 10^{-4}. \tag{22}$$

3.1.3 $B \to X_u \ell\nu$

The result of calculating $B \to X_u \ell\nu$ with free quark approximation is given by the following equation,

$$\begin{aligned}\Gamma(B \to X_u \ell\nu) = \frac{G_f^2 m_b^5}{192\pi^3}[(|V_{ub}^L|^2 + |V_{ub}^R|^2)(1 - 8\rho + 8\rho^3 - \rho^4 - 12\rho^2 \log\rho) \\ - 4\mathrm{Re}(V_{ub}^L V_{ub}^{R*})\sqrt{\rho}(1 + 6\rho - 6\rho^2 - \rho^3 + 6(\rho+1)\rho\log\rho)].\end{aligned} \tag{23}$$

Because $\rho = (m_u/m_b)^2 \sim 10^{-3} \ll 1$, we can neglect ρ. The decay rate can be described as

$$\Gamma(B \to X_u \ell\nu) = \frac{G_f^2 m_b^5}{192\pi^3}[(|V_{ub}^L|^2 + |V_{ub}^R|^2). \tag{24}$$

This equation shows that $|V_{ub}|^2$ in the SM is changed $|V_{ub}^L|^2 + |V_{ub}^R|^2$ with the $b \to u$ RHCC in inclusive decay. $|V_{ub}|$ measured by inclusive decay is averaged as $|V_{ub}| = (4.39 \pm 0.31) \times 10^{-3}$ [10]. In the result, $|V_{ub}^L|^2 + |V_{ub}^R|^2$ can be calculated as,

$$|V_{ub}^L|\sqrt{1 + \left|\frac{V_{ub}^R}{V_{ub}^L}\right|^2} = (4.39 \pm 0.31) \times 10^{-3}. \tag{25}$$

We noted that we use the GGOU method and the experimental and theoretical error are linearly combined, because the discrepancy among calculation methods is significant.

3.1.4 $B \to \rho\ell\nu, \omega\ell\nu$

We are going to consider the $b \to u$ RHCC effect on $B \to \rho\ell\nu$,$B \to \omega\ell\nu$ decays. Decay rate is calculated as following equations,

$$\frac{d\Gamma}{dq^2} = \frac{G_f^2 p_V q^2}{96\pi^3 c_V^2 M_B^2}\left(|H_0|^2 + |H_+|^2 + |H_-|^2\right) \tag{26}$$

$$H_\pm = (V_{ub}^L - V_{ub}^R)(M_B + M_\rho)A_1(q^2) \mp (V_{ub}^L + V_{ub}^R)\frac{2M_B p_\rho}{M_B + M_\rho}V(q^2) \tag{27}$$

$$H_0 = (V_{ub}^L - V_{ub}^R)\frac{M_B + M_\rho}{2\sqrt{q^2}}\left((M_B^2 - M_\rho^2 - q^2)A_1(q^2) - \frac{4M_B^2 p_\rho^2}{(M_B + M_\rho)^2}A_2(q^2)\right) \tag{28}$$

$$c_V = \begin{cases} 1 & V = \rho^+ \\ \sqrt{2} & V = \rho^0, \omega \end{cases}. \tag{29}$$

with $V = \rho^{\pm}, \rho^0, \omega$. Form factor we use are listed below,

$$A_1(q^2) = \frac{r_1^{A_1}}{1 - q^2/{m_{\rm fit}^{A_1}}^2} \tag{30}$$

$$A_2(q^2) = \frac{r_1^{A_2}}{1 - q^2/{m_{\rm fit}^{A_2}}^2} + \frac{r_2^{A_2}}{(1 - q^2/{m_{\rm fit}^{A_2}}^2)^2} \tag{31}$$

$$V(q^2) = \frac{r_1^{V}}{1 - q^2/m_{1^-}^2} + \frac{r_2^{V}}{1 - q^2/{m_{\rm fit}^{V}}^2} \tag{32}$$

- parameter set for $B \to \rho\ell\nu$

$$r_1^{A_1} = 0.240 \quad {m_{\rm fit}^{A_1}}^2 = 37.51{\rm GeV}^2 \tag{33}$$

$$r_1^{A_2} = 0.009 \quad r_2^{A_2} = 0.212 \quad {m_{\rm fit}^{A_2}}^2 = 40.82{\rm GeV}^2 \tag{34}$$

$$r_1^{V} = 1.045 \quad r_2^{V} = -0.721 \quad m_{1^-} = 5.32{\rm GeV} \quad {m_{\rm fit}^{V}}^2 = 38.34{\rm GeV}^2 \tag{35}$$

- parameter set for $B \to \omega\ell\nu$

$$r_1^{A_1} = 0.217 \quad {m_{\rm fit}^{A_1}}^2 = 37.01{\rm GeV}^2 \tag{36}$$

$$r_1^{A_2} = 0.006 \quad r_2^{A_2} = 0.192 \quad {m_{\rm fit}^{A_2}}^2 = 41.24{\rm GeV}^2 \tag{37}$$

$$r_1^{V} = 1.006 \quad r_2^{V} = -0.713 \quad m_{1^-} = 5.32{\rm GeV} \quad {m_{\rm fit}^{V}}^2 = 37.45{\rm GeV}^2 \tag{38}$$

with 9.5% error in A_1, 10.4% error in A_2 and 9.3% error in V [12]. We can calculate as

$$\Gamma(B \to V\ell\nu) = |V_{ub}^L|^2 \left(1 + \left|\frac{V_{ub}^R}{V_{ub}^L}\right|^2 + a{\rm Re}\left(\frac{V_{ub}^R}{V_{ub}^L}\right)\right) \Gamma(B \to V\ell\nu)|_{V_{ub}^L=1, V_{ub}^R=0} \tag{39}$$

$$a = \begin{cases} -1.18 & V = \rho^+, \rho^0 \\ -1.25 & V = \omega \end{cases} \tag{40}$$

with constant a. $|V_{ub}| = \sqrt{\Gamma(B \to V\ell\nu)/\Gamma(B \to V\ell\nu)|_{V_{ub}^L=1, V_{ub}^R=0}}$ measured by $B \to V\ell\nu$ is listed in following equation [13],

$$\begin{array}{ll} |V_{ub}| = 3.54 \pm 0.34 & B \to \rho\ell\nu \\ |V_{ub}| = 3.08 \pm 0.49 & B \to \omega\ell\nu \end{array} . \tag{41}$$

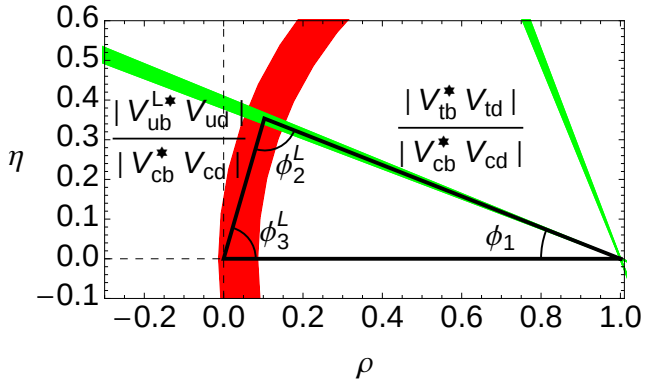

Fig.5 Light green region is constraint by $\sin 2\phi_1$ and red region is constraint by $\Delta m_{B_d}/\Delta m_{B_s}$.

In the result, V_{ub}^R/V_{ub}^L can be calculated as following,

$$|V_{ub}^L|\sqrt{1-1.18\mathrm{Re}\left(\frac{V_{ub}^R}{V_{ub}^L}\right)+\left|\frac{V_{ub}^R}{V_{ub}^L}\right|^2}=(3.54\pm0.34)\times10^{-3}\qquad\cdots B\to\rho\ell\nu \tag{42}$$

$$|V_{ub}^L|\sqrt{1-1.25\mathrm{Re}\left(\frac{V_{ub}^R}{V_{ub}^L}\right)+\left|\frac{V_{ub}^R}{V_{ub}^L}\right|^2}=(3.08\pm0.49)\times10^{-3}\qquad\cdots B\to\omega\ell\nu. \tag{43}$$

3.2 Indirect determination of V_{ub}^L by the unitarity of CKM matrix

Unitarity of CKM matrix includes the following relation,

$$V_{ub}^{L*}V_{ud}+V_{cb}^*V_{cd}+V_{tb}^*V_{td}=0, \tag{44}$$

which may be shown in the complex plane as Fig. 5. The triangle in this figure is called as unitarity triangle and its angles are denoted by $\phi_1(\beta)$, $\phi_2(\alpha)$ and $\phi_3(\gamma)$ as shown in Fig. 5. The horizontal axis ρ and the vertical axis η are defined by Wolfenstein parametrization [14],

$$V^L=\begin{pmatrix}1-\frac{\lambda^2}{2} & \lambda & A\lambda^3(\rho-i\eta)\\ -\lambda & 1-\frac{\lambda^2}{2} & A\lambda^2\\ A\lambda^3(1-\rho-i\eta) & -A\lambda^2 & 1\end{pmatrix}+O(\lambda^4). \tag{45}$$

Since measurements of ϕ_2 and ϕ_3 could be affected by the $b\to u$ RHCC, angles of unitarity triangle might differ from measured values of ϕ_2 and ϕ_3. In this thesis, we

Input parameters
$\sin 2\phi_1 = 0.691 \pm 0.017$ [10]
$\Delta M_{B^0} = 0.5055(20)$ ps^{-1} [10]
$\Delta M_{B_s} = 17.757(21)$ ps^{-1} [10]
$\xi = 1.268 \pm 0.063$ [11]

Table 1 Input parameters for indirect measurement

call the angles of unitarity triangle as ϕ_2^L and ϕ_3^L. Effects of the $b \to u$ RHCC to ϕ_2 and ϕ_3 measurements are discussed in Sec. 4.

With the unitary of CKM matrix, it is possible to calculate $|V_{ub}^L|$, ϕ_2^L and ϕ_3^L without direct measurements. Figure 5 shows that the side of $|V_{tb}^* V_{td}/V_{cb}^* V_{cd}|$ measured from $B_{d(s)} - \bar{B}_{d(s)}$ mixing observables $\Delta m_{B_{d(s)}}$, and ϕ_1 measured from $b \to c\bar{c}s$ decays like $B \to J/\psi K_s$ are needed for this analysis. These observables are not affected by the $b \to u$ RHCC since the $b \to u$ transition plays minor roles in the relevant processes. We determine ρ and η with the experimental data of $\Delta m_{B_{d(s)}}$ and ϕ_1 solving the following equations,

$$\frac{\Delta m_{B_d}}{\Delta m_{B_s}} = \frac{m_{B_d}}{m_{B_s}} \xi^{-2} \left| \frac{V_{td}}{V_{ts}} \right|^2 = \frac{m_{B_d}}{m_{B_s}} \xi^{-2} \lambda^2 \{(1-\rho)^2 + \eta^2\} \tag{46}$$

$$\tan(\phi_1) = \tan\left(\arg\left(\frac{V_{td} V_{tb}^*}{V_{cd} V_{cb}^*} \right) \right) = \frac{\eta}{1-\rho}, \tag{47}$$

where ξ is flavor SU(3) breaking ratio. Then we calculate $|V_{ub}^L|$, ϕ_2^L and ϕ_3^L using the following relations [15],

$$V_{ub}^L = A\lambda^3(\rho - i\eta) \tag{48}$$

$$\tan(\phi_2^L) = \frac{\eta}{\eta^2 + (\rho-1)\rho} \tag{49}$$

$$\phi_3^L = \arg(V_{ub}^{L*}). \tag{50}$$

With the input data listed in Table 1, we obtain $|V_{ub}^L|$, ϕ_2^L and ϕ_3^L as shown in Table 2. We note that there are four values of ϕ_1 for the given $\sin 2\phi_1$ and we obtain four sets of (ρ, η). In Table 2, we list ϕ_1 and corresponding output parameters.

ϕ_1	(ρ, η)	$\|V_{ub}^L\| \times 10^3$	ϕ_2^L	ϕ_3^L
$21.38°$	$(0.10, 0.35)$	3.43 ± 0.16	$(84.4 \pm 7.5)°$	$(73.8 \pm 7.5)°$
$68.62°$	$(0.65, 0.90)$	10.3 ± 0.4	$(57.2 \pm 2.1)°$	$(54.2 \pm 2.1)°$
$201.38°$	$(1.90, -0.35)$	18.0 ± 0.7	$(-10.9 \pm 0.5)°$	$(-10.6 \pm 0.5)°$
$248.62°$	$(1.35, -0.90)$	15.1 ± 0.6	$(-35.0 \pm 1.0)°$	$(-33.5 \pm 1.0)°$

Table 2 CKM calculation results

3.3 Summary and consideration about measurement of $|V_{ub}|$

So far, constraints on V_{ub}^L and V_{ub}^R are given in the five decay processes and $|V_{ub}^L|$ is obtained from indirect measurement. The result is summarized as follows.

$$|V_{ub}^L| = \frac{|V_{ub}^i|}{\sqrt{1 + x^2 + y^2 + a^i x}} \tag{51}$$

where $x \equiv \mathrm{Re}\left(V_{ub}^R / V_{ub}^L\right)$, $y \equiv \mathrm{Im}\left(V_{ub}^R / V_{ub}^L\right)$. The relevant decay mode is specified with i. The coefficient of the interference term, a^i, is given as

$$a^i = \begin{cases} -2 & i = B \to \tau\nu \\ 2 & i = B \to \pi\ell\nu \\ 0 & i = B \to X_u\ell\nu \\ -1.18 & i = B \to \rho\ell\nu \\ -1.25 & i = B \to \omega\ell\nu \end{cases} . \tag{52}$$

The corresponding experimental situation is shown in Fig. 6.

In order to determine the best fit values of x, y and $|V_{ub}^L|$ we define χ^2 as

$$\chi^2 = \left(\frac{|V_{ub}^{\mathrm{UT}}| - |V_{ub}^L|}{\sigma_{|V_{ub}^{\mathrm{UT}}|}} \right)^2 + \sum_i \left(\frac{|V_{ub}^i| - |V_{ub}^L|\sqrt{1 + x^2 + y^2 + a^i x}}{\sigma_{|V_{ub}^i|}} \right)^2 . \tag{53}$$

First, we analyze the case of no $b \to u$ RHCC namely $x = y = 0$. We obtain $\chi^2_{\mathrm{min}}/\mathrm{d.o.f}$ and $|V_{ub}^L|$ as

$$\frac{\chi^2_{\mathrm{min}}}{\mathrm{d.o.f}} = \frac{10.8}{5} = 2.16 \tag{54}$$

$$|V_{ub}^L| = 3.64 \times 10^{-3}. \tag{55}$$

Turning on the $b \to u$ RHCC, the χ^2 fit leads to

$$\frac{\chi^2_{\rm min}}{\rm d.o.f} = \frac{6.82}{3} = 2.27 \tag{56}$$

$$x = -4.21 \times 10^{-3} \tag{57}$$

$$|y| = 0.551 \tag{58}$$

$$|V^L_{ub}| = 3.43 \times 10^{-3}. \tag{59}$$

After integrating out $|V^L_{ub}|$, we obtain allowed region of V^R_{ub}/V^L_{ub} as shown in Fig. 9. This figure means that measurements of $|V_{ub}|$ suggest large imaginary part of V^R_{ub}/V^L_{ub}. Thus the $b \to u$ RHCC can be an new source of CP violation in B decays. In addition, one σ allowed regions in $|V^L_{ub}| - x$ plane where y is taken best fit value are shown in Fig. 8 and $|V^L_{ub}|$ measured by each decay mode where x and y are taken best fit values is listed in Fig. 7. These figures show that y plays a significant role in determination of $|V_{ub}|$. The best fit value of $|V^L_{ub}|$ in Eq. (59) corresponds to the solution of $\phi_1 = 21.38°$, which is also favored in the SM. Even with V^R_{ub}, three other solutions of ϕ_1 give larger χ^2 values and are disfavored.

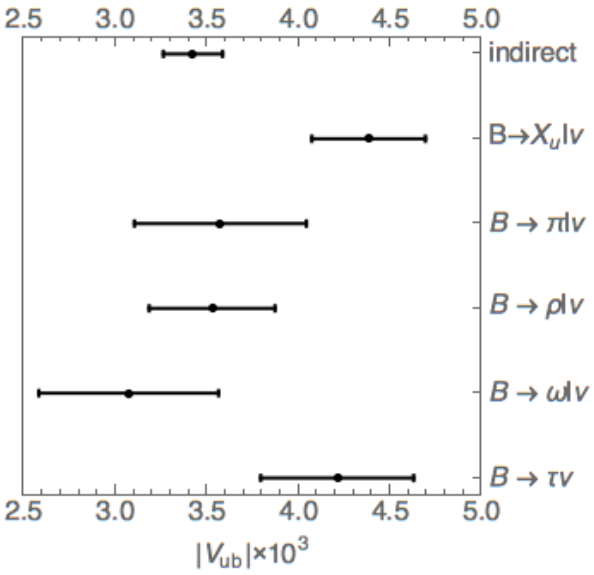

Fig.6 Current data of $|V_{ub}| \times 10^3$ by each measurement

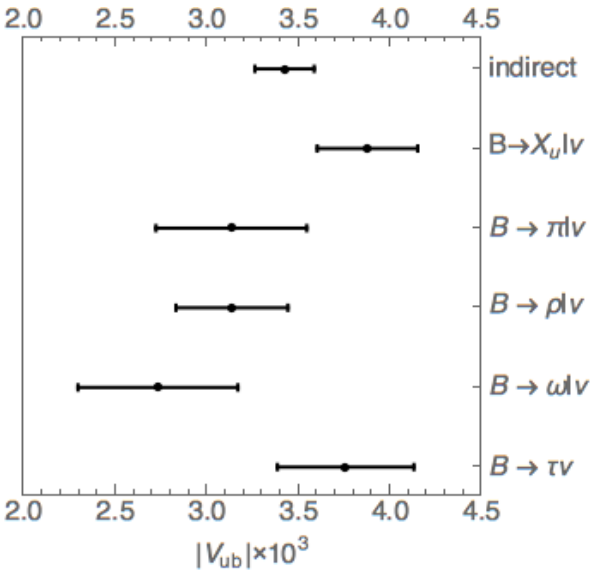

Fig.7 $|V^L_{ub}| \times 10^3$ using the best fit value of the $b \to u$ RHCC.

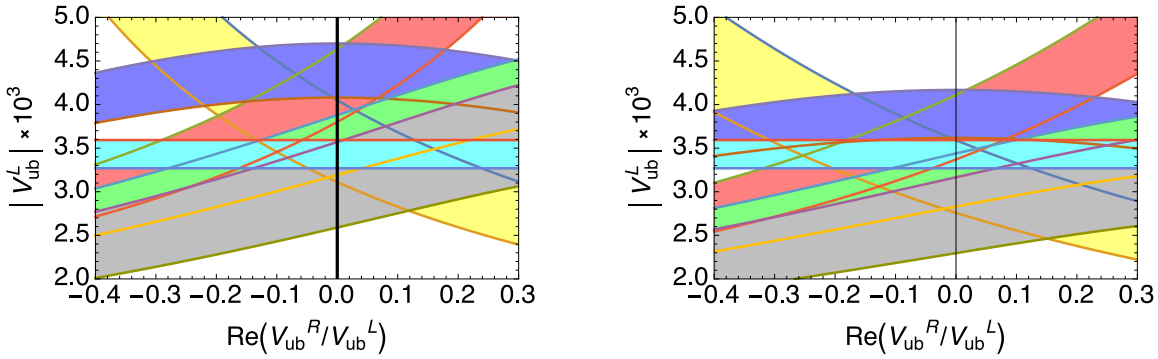

(a) $y = 0$ is satisfied.

(b) y is taken best fit value.

Fig.8 $|V_{ub}^L|$ as functions of $\mathrm{Re}(V_{ub}^R/V_{ub}^L)$ calculated from each process with y satisfied zero (left figure) or the best fit value (right figure). Yellow: $B \to \tau\nu$、Red: $B \to \pi\ell\nu$、Blue: $B \to X_u\ell\nu$、Green: $B \to \rho\ell\nu$、Gray: $B \to \omega\ell\nu$、Light blue: V_{ub}^L calculated by unitarity of CKM matrix.

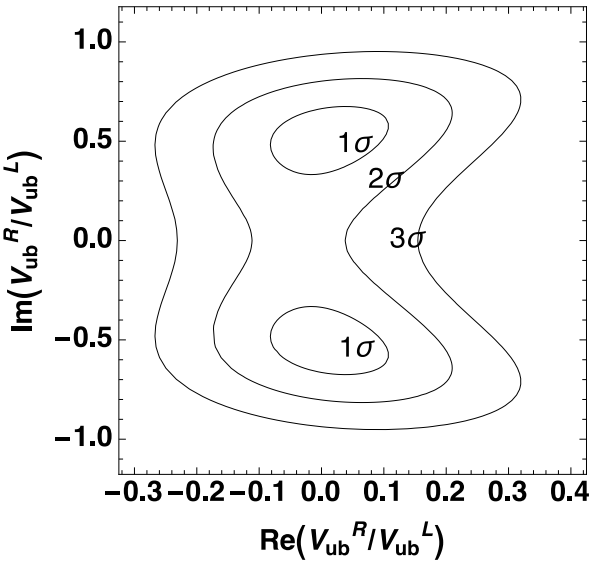

Fig.9 Allowed region of V_{ub}^R/V_{ub}^L.

4 Constraint to $b \to u$ RHCC by hadronic B decays

The hadronic decays including $b \to u$ transition can be affected by the $b \to u$ RHCC. In addition, measurements of $|V_{ub}|$ suggest large CP violation in the $b \to u$ RHCC. Therefore we consider its effect on $B \to \pi\pi$ and $B \to \rho\rho$, from which one of the angles of the unitarity triangle ϕ_2 is extracted, and $B \to DK$ used for measurement of ϕ_3.

4.1 $B \to \pi\pi$

The isospin of the final state of $B \to \pi\pi$ is $I = 0$ or 2. We define the following isospin amplitude,

$$A_I \equiv \langle (\pi\pi)_I | \mathcal{H} | B^0 \rangle \tag{60}$$

$$\bar{A}_I \equiv \langle (\pi\pi)_I | \mathcal{H} | \bar{B}^0 \rangle \tag{61}$$

where $\mathcal{H}$ denotes the effective weak interaction Hamiltonian. As shown in Fig. 10, both the tree and penguin diagrams are involved in this process. The penguin diagram contributes to $I = 0$ and the tree one does to both $I = 0$ and 2. Hence we can determine A_0, A_2, $\bar{A}_0$ and $\bar{A}_2$ by the isospin analysis [16]. The detailed explanation of the isospin analysis is given in App. D . Although the $b \to u$ RHCC contributes to both $I = 0$ and 2 amplitudes, it is sufficient to consider $I = 2$ amplitudes, which is free from the penguin pollution, as explained below.

The time dependent CP asymmetry of $B \to \pi\pi(\pi^+\pi^-$ or $\pi^0\pi^0)$ is represented as

$$\frac{\Gamma(B^0 \to \pi\pi) - \Gamma(\bar{B}^0 \to \pi\pi)}{\Gamma(B^0 \to \pi\pi) + \Gamma(\bar{B}^0 \to \pi\pi)} = C_{\pi\pi} \cos(\Delta M_{B_d} t) - S_{\pi\pi} \sin(\Delta M_{B_d} t) . \tag{62}$$

The coefficients $S_{\pi\pi}$ and $C_{\pi\pi}$ are given as

$$C_{\pi^+\pi^-} = \left(1 - |R_{\pi\pi}|^2 \left|\frac{1+\bar{z}}{1+z}\right|^2\right) / \left(1 + |R_{\pi\pi}|^2 \left|\frac{1+\bar{z}}{1+z}\right|^2\right) \tag{63}$$

$$S_{\pi^+\pi^-} = \sqrt{1 - C^2_{\pi^+\pi^-}} \sin\left(2\phi_2^L + \arg(R_{\pi\pi}) + \arg\left(\frac{1+\bar{z}}{1+z}\right)\right) \tag{64}$$

$$C_{\pi^0\pi^0} = \left(1 - |R_{\pi\pi}|^2 \left|\frac{2-\bar{z}}{2-z}\right|^2\right) / \left(1 + |R_{\pi\pi}|^2 \left|\frac{2-\bar{z}}{2-z}\right|^2\right) \tag{65}$$

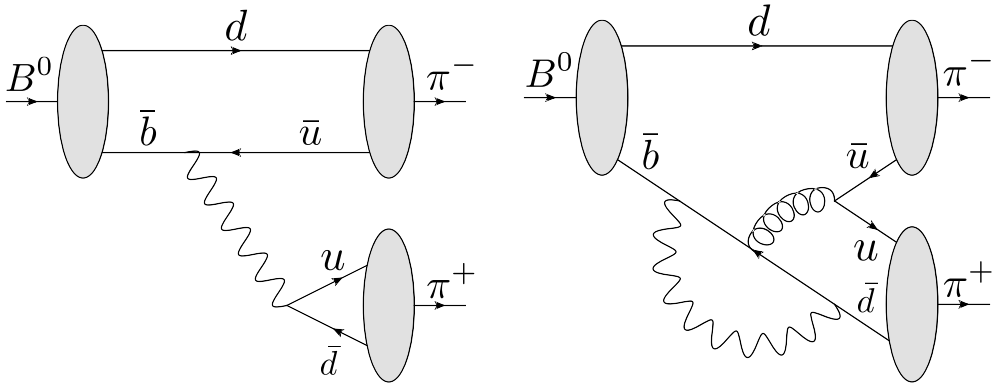

(a) tree diagram (b) penguin diagram

Fig.10 Feynman diagram for $B^0 \to \pi^+\pi^-$

where

$$z = \sqrt{2}A_0/A_2, \quad \bar{z} = \sqrt{2}\bar{A}_0/\bar{A}_2 \tag{66}$$

$$R_{\pi\pi} = \frac{1 + \bar{A}_{2R}/\bar{A}_{2L}}{1 + A_{2R}/A_{2L}}. \tag{67}$$

We have introduced the $I = 2$ amplitudes of left- and right- handed $b \to u$ currents, A_{2L} ($\bar{A}_{2L}$) and A_{2R} ($\bar{A}_{2R}$) for B and ($\bar{B}$). We note that experimental data of $S_{\pi^0\pi^0}$ is not available at present. In addition to $C_{\pi^+\pi^-}$, $C_{\pi^0\pi^0}$ and $S_{\pi^+\pi^-}$, the following observables are also available:

$$\frac{\mathrm{Br}(B^0 \to \pi^+\pi^-)}{\mathrm{Br}(B^+ \to \pi^+\pi^0)} \frac{\tau^+}{\tau^0} = \frac{1}{9}(|1+z|^2 + |1+\bar{z}|^2) \tag{68}$$

$$\frac{\mathrm{Br}(B^0 \to \pi^0\pi^0)}{\mathrm{Br}(B^+ \to \pi^+\pi^0)} \frac{2\tau^+}{\tau^0} = \frac{1}{18}(|2-z|^2 + |2-\bar{z}|^2) \tag{69}$$

$$A_{\mathrm{CP}}(B^+ \to \pi^+\pi^0) = \left(1 - |R_{\pi\pi}|^2\right) / \left(1 + |R_{\pi\pi}|^2\right). \tag{70}$$

We use the following experimental data [10] in our numerical analysis:

$$C_{\pi^+\pi^-} = -0.31 \pm 0.05 \tag{71}$$
$$S_{\pi^+\pi^-} = -0.66 \pm 0.06 \tag{72}$$
$$C_{\pi^0\pi^0} = -0.43 \pm 0.24 \tag{73}$$
$$\mathrm{Br}(B^0 \to \pi^+\pi^-) = (5.10 \pm 0.19) \times 10^{-6} \tag{74}$$
$$\mathrm{Br}(B^0 \to \pi^0\pi^0) = (1.91 \pm 0.225) \times 10^{-6} \tag{75}$$
$$\mathrm{Br}(B^+ \to \pi^+\pi^0) = (5.48 \pm 0.345) \times 10^{-6} \tag{76}$$
$$A_{\mathrm{CP}}(B^+ \to \pi^+\pi^0) = -0.026 \pm 0.039 \tag{77}$$

With these input parameters as well as ϕ_2^L which is given by the analysis of the unitarity triangle in Sec. 3, we can determine z, $\bar{z}$ and $R_{\pi\pi}$. We present the allowed region of $R_{\pi\pi}$ in Fig. 11, where the horizontal axis is chosen to be $A_{\mathrm{CP}}(B^+ \to \pi^+\pi^-)$ and the vertical axis is $\arg(R_{\pi\pi})$. The allowed region at $1(2)\sigma$ is shown in red (pink).

We compare the experimental constraint with the prediction of the $b \to u$ RHCC which is examined in Sec. 3. We evaluate A_{2R}/A_{2L} and $\bar{A}_{2R}/\bar{A}_{2L}$ as functions of V_{ub}^R/V_{ub}^L. The necessary effective Hamiltonians of $b \to u\bar{u}d$ for the calculation of the $I = 2$ amplitudes are written as

$$\mathcal{H}_{b_L \to u_L \bar{u}_L d_L} = 2\sqrt{2} G_f V_{ub}^{L*} V_{ud} (C_1 \mathcal{O}_1 + C_2 \mathcal{O}_2) \tag{78}$$
$$\mathcal{H}_{b_R \to u_R \bar{u}_L d_L} = 2\sqrt{2} G_f V_{ub}^{R*} V_{ud} (C_{1R} \mathcal{O}_{1R} + C_{2R} \mathcal{O}_{2R}) \tag{79}$$
$$\mathcal{O}_1 = (\bar{u}^\alpha \gamma^\mu P_L d^\beta)(\bar{b}^\beta \gamma_\mu P_L u^\alpha) \tag{80}$$
$$\mathcal{O}_2 = (\bar{u}^\alpha \gamma^\mu P_L d^\alpha)(\bar{b}^\beta \gamma_\mu P_L u^\beta) \tag{81}$$
$$\mathcal{O}_{1R} = (\bar{u}^\alpha \gamma^\mu P_L d^\beta)(\bar{b}^\beta \gamma_\mu P_R u^\alpha) \tag{82}$$
$$\mathcal{O}_{2R} = (\bar{u}^\alpha \gamma^\mu P_L d^\alpha)(\bar{b}^\beta \gamma_\mu P_R u^\beta). \tag{83}$$

where α and β are color indices. The Wilson coefficients C_1, C_2, C_{1R} and C_{2R} are determined by the following renormalization group equation (RGE)

$$\mu \frac{d}{d\mu} C_j(\mu) = \sum_i \gamma_{ij}(\mu) C_i(\mu) \tag{84}$$
$$\gamma_{ij} = \frac{\alpha_s}{2\pi} \begin{pmatrix} -1 & 3 \\ 3 & -1 \end{pmatrix}, \qquad i,j = 1,2 \tag{85}$$
$$\gamma_{ij} = \frac{\alpha_s}{2\pi} \begin{pmatrix} -8 & 0 \\ -3 & 1 \end{pmatrix}, \qquad i,j = 1R, 2R. \tag{86}$$

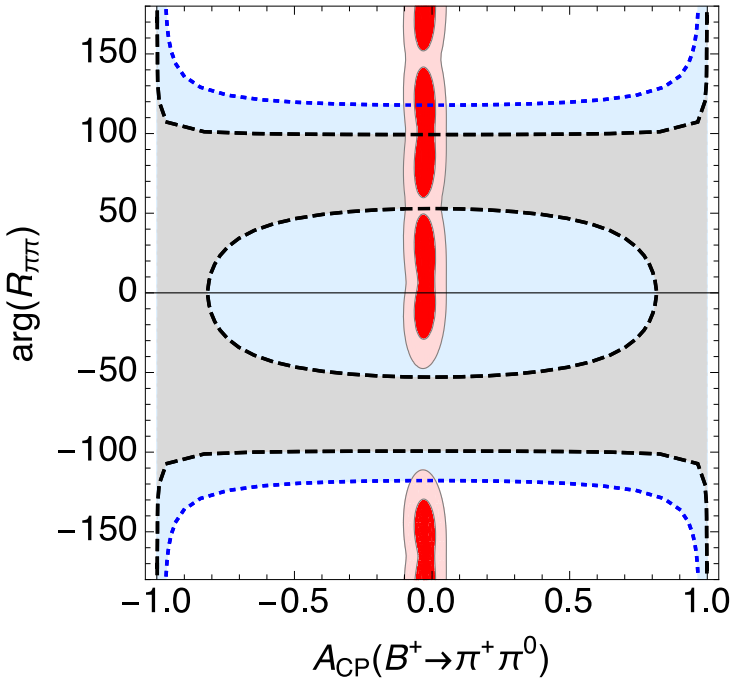

Fig.11 Allowed region by experimental results in $B \to \pi\pi$ and the prediction region of the $b \to u$ CP violating RHCC. The red (pink) shows 1 (2)σ allowed region. The gray (light blue) shows 1(2)σ prediction region.

The solution of RGE is obtained as follows:

$$C_1(m_b) = \frac{1}{2}\left(\left(\frac{\alpha_s(m_b)}{\alpha_s(m_W)}\right)^{-6/23} - \left(\frac{\alpha_s(m_b)}{\alpha_s(m_W)}\right)^{12/23}\right) = -0.27 \tag{87}$$

$$C_2(m_b) = \frac{1}{2}\left(\left(\frac{\alpha_s(m_b)}{\alpha_s(m_W)}\right)^{-6/23} + \left(\frac{\alpha_s(m_b)}{\alpha_s(m_W)}\right)^{12/23}\right) = 1.12 \tag{88}$$

$$C_{1R}(m_b) = \frac{1}{3}\left(\left(\frac{\alpha_s(m_b)}{\alpha_s(m_W)}\right)^{24/23} - \left(\frac{\alpha_s(m_b)}{\alpha_s(m_W)}\right)^{-3/23}\right) = 0.34 \tag{89}$$

$$C_{2R}(m_b) = \frac{1}{3}\left(3\left(\frac{\alpha_s(m_b)}{\alpha_s(m_W)}\right)^{-3/23}\right) = 0.92 \tag{90}$$

where α_s is the running QCD coupling. The derivation of the RGE and the above solution is described in App. C .

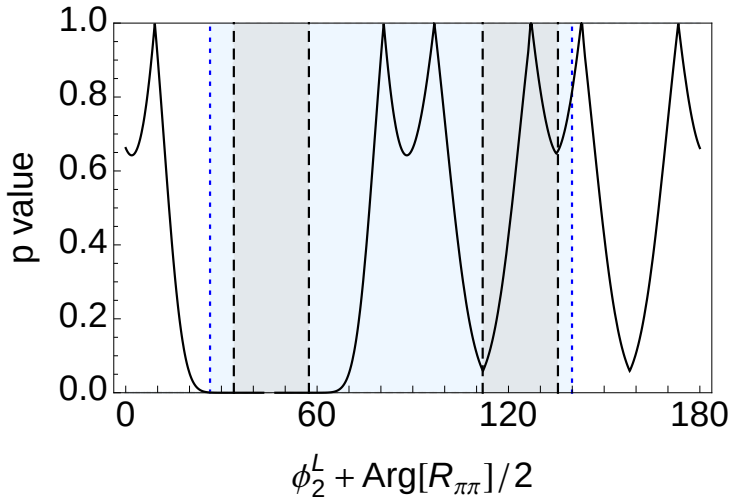

Fig.12 The p value of $\phi_2^L + \arg(R_{\pi\pi})/2$ assuming $\delta_L - \delta_R = 0$ or π and the $b \to u$ CP violating RHCC's prediction. The gray (light blue) shows $1(2)\sigma$ prediction region. The black line is p value.

The amplitude ratio A_{2R}/A_{2L} is written as

$$\frac{A_{2R}}{A_{2L}} = \frac{\sqrt{\frac{2}{3}}\langle\pi^+\pi^0|\mathcal{H}_{b_R\to u_R\bar{u}_L d_L}|B^+\rangle e^{i\delta_R}}{\sqrt{\frac{2}{3}}\langle\pi^+\pi^0|\mathcal{H}_{b_L\to u_L\bar{u}_L d_L}|B^+\rangle e^{i\delta_L}} \tag{91}$$

$$= \left(\frac{V_{ub}^R}{V_{ub}^L}\right)^* e^{i(\delta_R-\delta_L)} \frac{\langle\pi^+\pi^0|C_{1R}\mathcal{O}_{1R} + C_{2R}\mathcal{O}_{2R}|B^+\rangle}{\langle\pi^+\pi^0|C_1\mathcal{O}_1 + C_2\mathcal{O}_2|B^+\rangle}, \tag{92}$$

where $\delta_{R,L}$ are strong phases. We evaluate the matrix elements in Eq. (92) with factorization approximation:

$$\begin{aligned}
&\langle\pi^+\pi^0|C_1\mathcal{O}_1 + C_2\mathcal{O}_2|B^+\rangle \\
=&(C_2 + C_1/3)\langle\pi^+|\bar{u}\gamma^\mu P_L d|0\rangle\langle\pi^0|\bar{b}\gamma_\mu P_L u|B^+\rangle \\
&+ (C_1 + C_2/3)\langle\pi^0|\bar{u}\gamma^\mu P_L u|0\rangle\langle\pi^+|\bar{b}\gamma_\mu P_L d|B^+\rangle \qquad (93)\\
=&-(1/4)(1/\sqrt{2})(-if_\pi)f_0(M_\pi^2)(M_{B^+}^2 - M_\pi^2)(4/3)(C_2 + C_1) \qquad (94)
\end{aligned}$$

and

$$
\begin{aligned}
&\langle\pi^+\pi^0|C_{1R}\mathcal{O}_{1R}+C_{2R}\mathcal{O}_{2R}|B^+\rangle \\
=&(C_{2R}+C_{1R}/3)\langle\pi^+|\bar{u}\gamma^\mu P_L d|0\rangle\langle\pi^0|\bar{b}\gamma_\mu P_R u|B^+\rangle \\
&-2(C_{1R}+C_{2R}/3)\langle\pi^0|\bar{u}P_R u|0\rangle\langle\pi^+|\bar{b}P_L d|B^+\rangle \qquad (95)\\
=&-(1/4)(1/\sqrt{2})(-if_\pi)f_0(M_\pi^2)(M_{B^+}^2-M_\pi^2) \\
&\times\left((C_{2R}+C_{1R}/3)+\frac{M_\pi^2}{m_u(m_b-m_d)}(C_{1R}+C_{2R}/3)\right). \qquad (96)
\end{aligned}
$$

The form factor f_0 is defined Eq. (236) in App. A . Thus we obtain

$$
\begin{aligned}
\frac{A_{2R}}{A_{2L}}&=\left(\frac{V_{ub}^R}{V_{ub}^L}\right)^* e^{i(\delta_R-\delta_L)}\frac{(C_{2R}+C_{1R}/3)+(C_{1R}+C_{2R}/3)\frac{M_\pi^2}{(m_b-m_d)m_u}}{(C_2+C_1/3)+(C_1+C_2/3)} \qquad (97)\\
&=1.56\left(\frac{V_{ub}^R}{V_{ub}^L}\right)^* e^{i(\delta_R-\delta_L)} \qquad (98)
\end{aligned}
$$

and similarly

$$
\frac{\bar{A}_{2R}}{\bar{A}_{2L}}=1.56\frac{V_{ub}^R}{V_{ub}^L}e^{i(\delta_R-\delta_L)}. \qquad (99)
$$

Given the allowed region of V_{ub}^R/V_{ub}^L in Fig. 9, we show the prediction of $A_{\rm CP}(B^+\to\pi^+\pi^0)$ and $\arg(R_{\pi\pi})$ in Fig. 11. In this calculation, we vary $\delta_R-\delta_L$ in the range $[0,2\pi]$. We observe that the prediction of the $b\to u$ RHCC is consistent with the $B\to\pi\pi$ experimental result. Figure 12 shows a comparison between $\phi_2(=\phi_2^L+\arg(R_{\pi\pi})/2)$ measurement and the prediction of the $b\to u$ RHCC. In this figure, we assume $\delta_L-\delta_R=0$ or π so that $A_{\rm CP}(B^+\to\pi^+\pi^0)=0$. The prediction of the $b\to u$ RHCC is consistent with $\phi_2^L\sim 127^\circ$ at 1σ and there are several solutions at 2σ level.

4.2 $B\to\rho_L\rho_L$

The decay process $B\to\rho\rho$ is governed by the tree-level $b\to u$ transition and the one-loop $b\to d$ penguin diagram as $B\to\pi\pi$. The possible final states are $\rho_T\rho_T$ and $\rho_L\rho_L$ with $\rho_{T(L)}$ being the transverse (longitudinal) helicity state. The $\rho_T\rho_T$ final state is a mixture of CP even and odd states. On the other hand, $\rho_L\rho_L$ is purely CP even. Therefore the isospin analysis and the ϕ_2 extraction strategy in $B\to\pi\pi$ can be applied to $B\to\rho_L\rho_L$ almost in the same manner. Furthermore we can evaluate

the effect of the $b \to u$ RHCC as in the previous subsection. Employing a similar notation as $B \to \pi\pi$, we obtain the coefficients in the time dependent CP asymmetry and the direct CP asymmetry:

$$C_{\rho^+\rho^-} = \left(1 - |R_{\rho_L\rho_L}|^2 \left|\frac{1+\bar{z}}{1+z}\right|^2\right) / \left(1 + |R_{\rho_L\rho_L}|^2 \left|\frac{1+\bar{z}}{1+z}\right|^2\right) \tag{100}$$

$$S_{\rho^+\rho^-} = \sqrt{1 - C^2_{\rho^+\rho^-}} \sin\left(2\phi_2^L + \arg\left(R_{\rho_L\rho_L}\right) + \arg\left(\frac{1+\bar{z}}{1+z}\right)\right) \tag{101}$$

$$C_{\rho^0\rho^0} = \left(1 - |R_{\rho_L\rho_L}|^2 \left|\frac{2-\bar{z}}{2-z}\right|^2\right) / \left(1 + |R_{\rho_L\rho_L}|^2 \left|\frac{2-\bar{z}}{2-z}\right|^2\right) \tag{102}$$

$$S_{\rho^0\rho^0} = \sqrt{1 - C^2_{\rho^0\rho^0}} \sin\left(2\phi_2^L + \arg\left(R_{\rho_L\rho_L}\right) + \arg\left(\frac{2-\bar{z}}{2-z}\right)\right) \tag{103}$$

$$A_{\rm CP}(B^+ \to \rho_L^+\rho_L^0) = \left(1 - |R_{\rho_L\rho_L}|^2\right) / \left(1 + |R_{\rho_L\rho_L}|^2\right) \tag{104}$$

where z, $\bar{z}$ and $R_{\rho_L\rho_L}$ are defined in the same way as Eqs.(66, 67) with the corresponding $B \to \rho_L\rho_L$ amplitudes. Ratios of branching fractions are given as

$$\frac{f_L^{+-}{\rm Br}(B^0 \to \rho^+\rho^-)}{f_L^{+0}{\rm Br}(B^+ \to \rho^+\rho^0)} \frac{\tau^+}{\tau^0} = \frac{1}{9}(|1+z|^2 + |1+\bar{z}|^2) \tag{105}$$

$$\frac{f_L^{00}{\rm Br}(B^0 \to \rho^0\rho^0)}{f_L^{+0}{\rm Br}(B^+ \to \rho^+\rho^0)} \frac{\tau^+}{\tau^0} = \frac{1}{18}(|2-z|^2 + |2-\bar{z}|^2) \tag{106}$$

where f_L^{ij} is the fraction of longitudinal polarization, so that ${\rm Br}(B^0 \to \rho_L^i\rho_L^j) = f_L^{ij}{\rm Br}(B^0 \to \rho^i\rho^j)$. A different point from $B \to \pi\pi$ is that $S_{\rho^0\rho^0}$ can be measured and thus the number of solutions tends to decrease compered to $B \to \pi\pi$. The input

parameters used in our numerical analysis are listed below:

$$
\begin{aligned}
C_{\rho^+\rho^-} &= -0.06 \pm 0.13 \text{ [10]} && (107)\\
S_{\rho^+\rho^-} &= -0.05 \pm 0.17 \text{ [10]} && (108)\\
C_{\rho^0\rho^0} &= 0.2 \pm 0.8 \pm 0.3 \text{ [10]} && (109)\\
S_{\rho^0\rho^0} &= 0.3 \pm 0.7 \pm 0.2 \text{ [10]} && (110)\\
\mathrm{Br}(B^0 \to \rho^+\rho^-) &= (24.2 \pm 3.15) \times 10^{-6} \text{ [10]} && (111)\\
\mathrm{Br}(B^0 \to \rho^0\rho^0) &= (0.73 \pm 0.275) \times 10^{-6} \text{ [10]} && (112)\\
\mathrm{Br}(B^+ \to \rho^+\rho^0) &= (24.0 \pm 1.95) \times 10^{-6} \text{ [10]} && (113)\\
A_{\mathrm{CP}}(B^+ \to \rho_L^+\rho_L^0) &= 0.051 \pm 0.054 \text{ [10]} && (114)\\
f_L^{+0} &= 0.950 \pm 0.016 \text{ [17, 18]} && (115)\\
f_L^{00} &= 0.618 \pm 0.118 \text{ [19, 20]} && (116)\\
f_L^{+-} &= 0.990 \pm 0.020 \text{ [21, 22]}. && (117)
\end{aligned}
$$

As in the case of $B \to \pi\pi$, we obtain the allowed region of $A_{\mathrm{CP}}(B^+ \to \rho_L^+\rho_L^0)$ and $\arg(R_{\rho_L\rho_L})$ from the above input data and ϕ_2^L determined by the unitarity triangle. In Fig. 13, we present the $1(2)\sigma$ allowed region in red (pink).

In order to evaluate the effect of the $b \to u$ RHCC, we calculate the amplitude ratio A_{2R}/A_{2L}. The effective Hamiltonian is the same as $B \to \pi\pi$ and we obtain

$$
\begin{aligned}
\frac{A_{2R}}{A_{2L}} &= \frac{\sqrt{\frac{2}{3}}\langle\rho_L^+\rho_L^0|\mathcal{H}_{b_R\to u_R\bar{u}_L d_L}|B^+\rangle e^{i\delta_R}}{\sqrt{\frac{2}{3}}\langle\rho_L^+\rho_L^0|\mathcal{H}_{b_L\to u_L\bar{u}_L d_L}|B^+\rangle e^{i\delta_L}}\\
&= \left(\frac{V_{ub}^R}{V_{ub}^L}\right)^* e^{i(\delta_R-\delta_L)}\frac{\langle\rho_L^+\rho_L^0|C_{1R}\mathcal{O}_{1R}+C_{2R}\mathcal{O}_{2R}|B^+\rangle}{\langle\rho_L^+\rho_L^0|C_1\mathcal{O}_1+C_2\mathcal{O}_2|B^+\rangle} \qquad (118)
\end{aligned}
$$

where $\delta_{R,L}$ are strong phases. We evaluate the matrix elements in Eq. (118) with the factorization method. In B meson rest frame, the polarization of ρ meson and the momentum of B and ρ mesons may be written as

$$
\begin{aligned}
\epsilon^\mu_{\rho^+,L} &= (p_\rho, , 0, 0, -E_\rho) && (119)\\
p^\mu_{\rho^+} &= (E_\rho, 0, 0, p_\rho) && (120)\\
p^\mu_{B^+} &= (M_{B^+}, 0, 0, 0). && (121)
\end{aligned}
$$

because the ρ meson is longitudinal. Hence the vector form factor vanishes as

$$
\langle\rho_L^+|\bar{b}\gamma_\mu d|B^+\rangle \propto \epsilon_{\mu\nu\rho\sigma}\epsilon^{\nu *}_{\rho^+,L}p^\rho_{\rho^+}p^\sigma_{B^+} = 0. \qquad (122)
$$

Then the matrix elements in Eq. (118) are evaluated as

$$\begin{aligned}
&\langle\rho_L^+\rho_L^0|C_1\mathcal{O}_1+C_2\mathcal{O}_2|B^+\rangle \\
=&(C_2+C_1/3)\langle\rho_L^+|\bar{u}\gamma^\mu P_L d|0\rangle\langle\rho_L^0|\bar{b}\gamma_\mu P_L u|B^+\rangle \\
&+(C_1+C_2/3)\langle\rho_L^0|\bar{u}\gamma^\mu P_L u|0\rangle\langle\rho_L^+|\bar{b}\gamma_\mu P_L d|B^+\rangle \qquad (123)\\
=&(1/4)\langle\rho_L^+|\bar{u}\gamma^\mu\gamma_5 d|0\rangle\langle\rho_L^0|\bar{b}\gamma_\mu\gamma_5 u|B^+\rangle(4/3)(C_1+C_2) \qquad (124)
\end{aligned}$$

and

$$\begin{aligned}
&\langle\rho_L^+\rho_L^0|C_{1R}\mathcal{O}_{1R}+C_{2R}\mathcal{O}_{2R}|B^+\rangle \\
=&(C_{2R}+C_{1R}/3)\langle\rho_L^+|\bar{u}\gamma^\mu P_L d|0\rangle\langle\rho_L^0|\bar{b}\gamma_\mu P_R u|B^+\rangle \\
&-2(C_{1R}+C_{2R}/3)\langle\rho_L^0|\bar{u}P_R u|0\rangle\langle\rho_L^+|\bar{b}P_L d|B^+\rangle \qquad (125)\\
=&-(1/4)\langle\rho_L^+|\bar{u}\gamma^\mu\gamma_5 d|0\rangle\langle\rho_L^0|\bar{b}\gamma_\mu\gamma_5 u|B^+\rangle(C_{2R}+C_{1R}/3). \qquad (126)
\end{aligned}$$

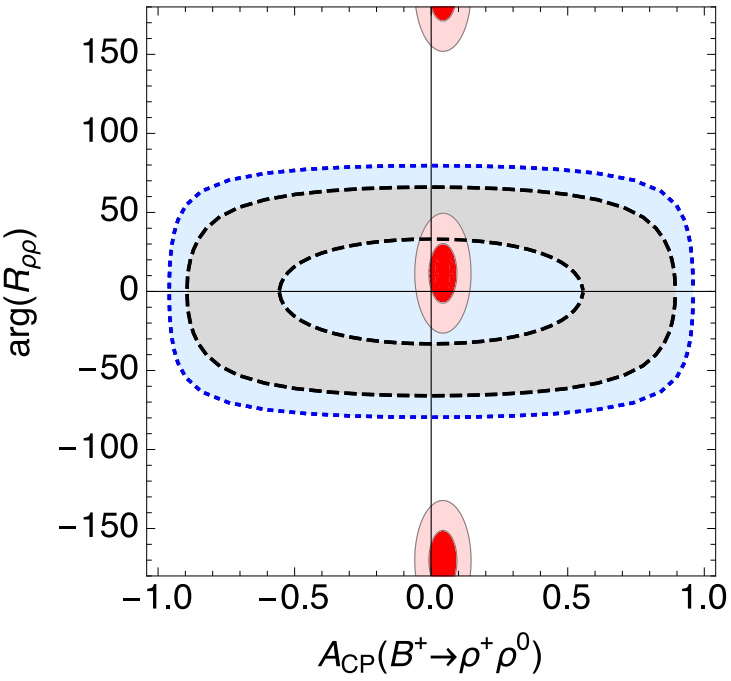

Fig.13 Allowed region by experimental results in $B\to\rho\rho$ and the prediction region of the $b\to u$ CP violating RHCC. The red (pink) shows 1 (2)σ allowed region. The gray (light blue) shows 1(2)σ prediction region.

Using the Wilson coefficients in Eqs.(88-90), we obtain

$$\frac{A_{2R}}{A_{2L}} = \left(\frac{V_{ub}^R}{V_{ub}^L}\right)^* e^{i(\delta_R-\delta_L)} \frac{-(C_{2R}+C_{1R}/3)}{(4/3)(C_2+C_1)} \tag{127}$$

$$= -\,0.91 \left(\frac{V_{ub}^R}{V_{ub}^L}\right)^* e^{i(\delta_R-\delta_L)}. \tag{128}$$

With this result, we evaluate $A_{\rm CP}(B^+ \to \rho_L^+ \rho_L^0)$ and $\arg(R_{\rho_L\rho_L})$ for the allowed region of V_{ub}^R/V_{ub}^L given in Fig. 9 taking range of $\delta_R - \delta_L$ in $[0, 2\pi]$. Figure. 13 shows the $1(2)\sigma$ region by the gray (light blue). The $b \to u$ RHCC scenario is marginally allowed at 1σ level and perfectly consistent with the present experimental data at 2σ. Assuming $\delta_L - \delta_R = 0$ or π, which means $A_{\rm CP}(B^+ \to \rho_L^+ \rho_L^0) = 0$, we show a comparison of the ϕ_2 measurement (solid line) and the prediction of the $b \to u$ RHCC (colored region) in Fig. 14. As stated above the prediction of the $b \to u$ RHCC is consistent with the value of ϕ_2 determined by the present experimental data. We note that the number of ϕ_2 solutions in the isospin analysis is only two, which is much less than the case of $B \to \pi\pi$ shown in Fig. 12. Therefore we expect that the improvement in future experiment will be able to constrain the $b \to u$ RHCC strongly.

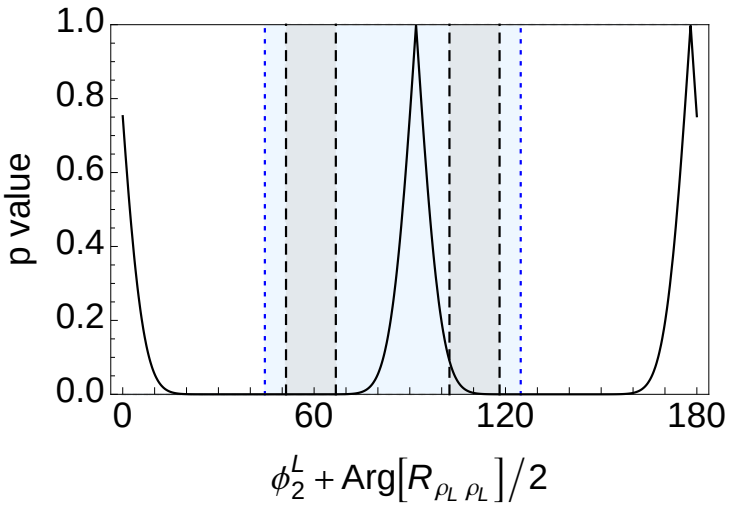

Fig.14 The p value of $\phi_2^L + \arg(R_{\rho_L\rho_L})/2$ assuming $\delta_L - \delta_R = 0$ or π and the $b \to u$ CP violating RHCC's prediction. The gray (light blue) shows $1(2)\sigma$ prediction region. The black line shows p value.

4.3 $B \to DK$

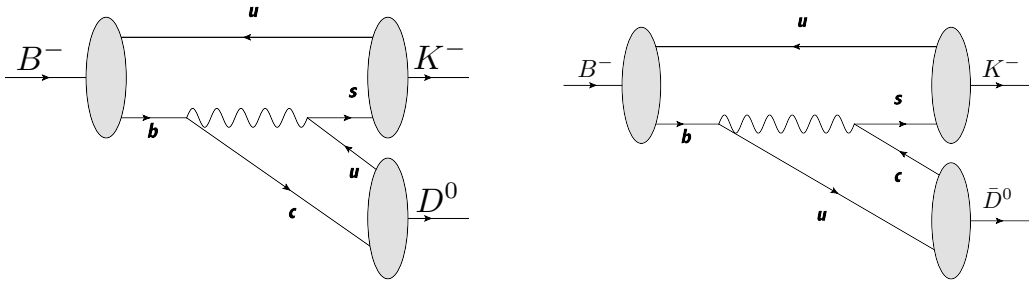

(a) $B^- \to D^0 K^-$ (b) $B^- \to \bar{D}^0 K^-$

Fig.15 Feynman diagram for $B \to DK$

In the SM, GLW method [23, 24], ADS method [25] and Dalitz plot analysis (GGSZ method) [26] are known as methods of ϕ_3 determination. The affinity of them is that ϕ_3 is extracted from the interference between $B^\pm \to D^0 K^\pm$ and $B^\pm \to \bar{D}^0 K^\pm$ through common decay modes of D^0 and $\bar{D}^0$ as shown in Fig. 15. In the SM, ϕ_3 is determined by the following equation,

$$\frac{A(B^+ \to D^0 K^+)}{A(B^- \to \bar{D}^0 K^-)} = e^{2i\phi_3}. \tag{129}$$

As seen in Fig. 15(b), however, the $b \to u$ RHCC affects the measurement of ϕ_3 and induces a new direct CP violation $A_{CP}(B^+ \to D^0 K^+)$ defined below.

The relevant amplitudes are defined as

$$A(B^- \to D^0 K^-) = \mathcal{A}_B \tag{130}$$
$$A(B^- \to \bar{D}^0 K^-) = \bar{A}^L_{DK} + \bar{A}^R_{DK} \tag{131}$$
$$= \mathcal{A}_B r_- e^{i(-\phi_{DK}+\delta)} \tag{132}$$
$$A(B^+ \to \bar{D}^0 K^+) = \mathcal{A}_B \tag{133}$$
$$A(B^+ \to D^0 K^+) = A^L_{DK} + A^R_{DK} \tag{134}$$
$$= \mathcal{A}_B r_+ e^{i(\phi_{DK}+\delta)}, \tag{135}$$

where $A^{L(R)}_{DK}$ and $\bar{A}^{L(R)}_{DK}$ denote the contribution of the left(right)-handed charged current, and δ is a CP even phase. We note that the CP odd phase ϕ_{DK} reduces to

ϕ_3^L in the absence of the $b \to u$ RHCC, namely

$$A_{DK}^L / \bar{A}_{DK}^L = e^{2i\phi_3^L}. \tag{136}$$

The effects of the $b \to u$ RHCC are expressed as

$$\begin{aligned}
\phi_{DK} =& \phi_3^L + \arg(R_{DK})/2 && (137)\\
A_{CP}(B^+ \to D^0 K^+) =& \frac{\Gamma(B^+ \to D^0 K^+) - \Gamma(B^- \to \bar{D}^0 K^-)}{\Gamma(B^+ \to D^0 K^+) - \Gamma(B^- \to \bar{D}^0 K^-)} && (138)\\
=& \frac{r_+^2 - r_-^2}{r_+^2 + r_-^2} && (139)\\
=& \frac{1 - |R_{DK}|^2}{1 + |R_{DK}|^2} && (140)
\end{aligned}$$

where

$$R_{DK} \equiv \frac{1 + A_{DK}^R / A_{DK}^L}{1 + \bar{A}_{DK}^R / \bar{A}_{DK}^L}. \tag{141}$$

We note that $A_{\rm CP}(B^+ \to D^0 K^+)$ has not been measured in experiments. In the following, we extend Dalitz plot analysis in the presence of the $b \to u$ RHCC and obtain a constraint on $A_{\rm CP}(B^+ \to D^0 K^+)$ as well as ϕ_{DK}.

4.3.1 Extended Dalitz plot analysis in $B \to DK$ with $b \to u$ RHCC

In the Dalitz plot analysis, the decay modes of neutral D mesons, $D^0 \to K_s(p_1)\pi^+(p_2)\pi^-(p_3)$ and $\bar{D}^0 \to K_s(p_1)\pi^-(p_2)\pi^+(p_3)$ are used. The phase space of the Dalitz decay is shown in Fig. 16 where $s_{1i} = (p_1 + p_i)^2$. We divide the phase space into bins as illustrated in Fig. 16 (in our numerical analysis, we employ the optimal binning used in Ref. [27]). The number of events in the ith bin of $B^\pm \to (K_s\pi^+\pi^-)K^\pm$ in the presence of the $b \to u$ RHCC can be expressed as

$$\begin{aligned}
N_i^+ =& K_{-i} + {r_+}^2 K_i + 2r_+ \sqrt{K_i K_{-i}}\,(\cos(\phi_{DK} + \delta)c_i - \sin(\phi_{DK} + \delta)s_i)\\
N_i^- =& K_{-i} + {r_+}^2 K_i + 2r_+ \sqrt{K_i K_{-i}}\,(\cos(-\phi_{DK} + \delta)c_i - \sin(-\phi_{DK} + \delta)s_i)\\
N_{-i}^+ =& K_i + {r_-}^2 K_{-i} + 2r_- \sqrt{K_i K_{-i}}\,(\cos(\phi_{DK} + \delta)c_i + \sin(\phi_{DK} + \delta)s_i)\\
N_{-i}^- =& K_i + {r_-}^2 K_{-i} + 2r_- \sqrt{K_i K_{-i}}\,(\cos(-\phi_{DK} + \delta)c_i + \sin(-\phi_{DK} + \delta)s_i)\,, \qquad (142)
\end{aligned}$$

where $i = 1 \cdots n$ and the ith and $-i$th bins are symmetric about the diagonal line $s_{12} = s_{13}$. The real numbers c_i's and s_i's, which satisfy $c_i = c_{-i}$ and $s_i = -s_{-i}$, come

from the interference between D^0 and $\bar{D}^0$. $K_{i(-i)}$ is the number of events in the ith bin of $D^0(\bar{D}^0) \to K_s\pi^+\pi^-$. There are $4n$ equations for $N^{\pm}_{\pm i}$ that depend on $4+2n$ unknown parameters, ϕ_{DK}, δ, $r_\pm$, s_i and c_i. Hence we can solve these equations as far as $n \geq 2$ and determine $A_{CP}(B^+ \to D^0K^+)$ and $\arg(R_{DK})$. $N^{\pm}_i$ and K_i are measured by Belle collaboration [27]. As for c_i and s_i, although we treated them as parameters in the above counting, they are actually measured by CLEO collabotation [28]. We obtained the allowed region of $A_{CP}(B^+ \to D^0K^+)$ and $\arg(R_{DK})$. The $1(2)\sigma$ region is presented in red (pink) in Fig. 17. We see that the constraint on the direct CP violation $A_{CP}(B^+ \to D^0K^+)$ is rather weak.

4.3.2 Prediction to $B \to DK$ by $b \to u$ RHCC

The effective Hamiltonian that describes $b \to u\bar{c}s$ process is written as

$$\mathcal{H}_{b_L \to u_L \bar{c}_L s_L} = 2\sqrt{2} G_f V^L_{ub} V^*_{cs} (C_1 \mathcal{O}_1 + C_2 \mathcal{O}_2) \tag{143}$$

$$\mathcal{H}_{b_R \to u_R \bar{c}_L s_L} = 2\sqrt{2} G_f V^R_{ub} V^*_{cs} (C_{1R} \mathcal{O}_{1R} + C_{2R} \mathcal{O}_{2R}) \tag{144}$$

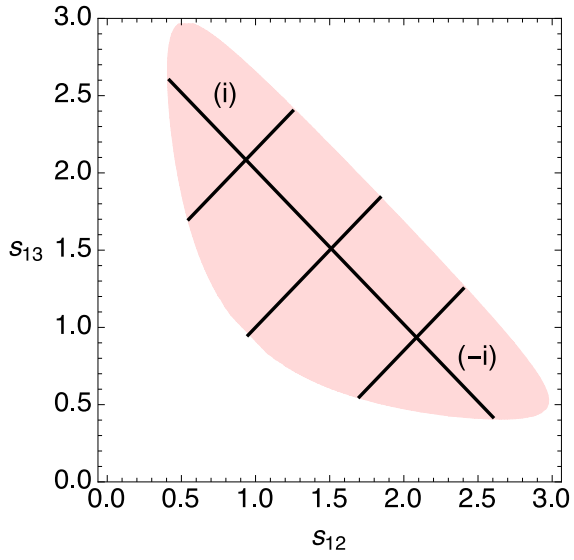

Fig.16 Example of phase space binning.

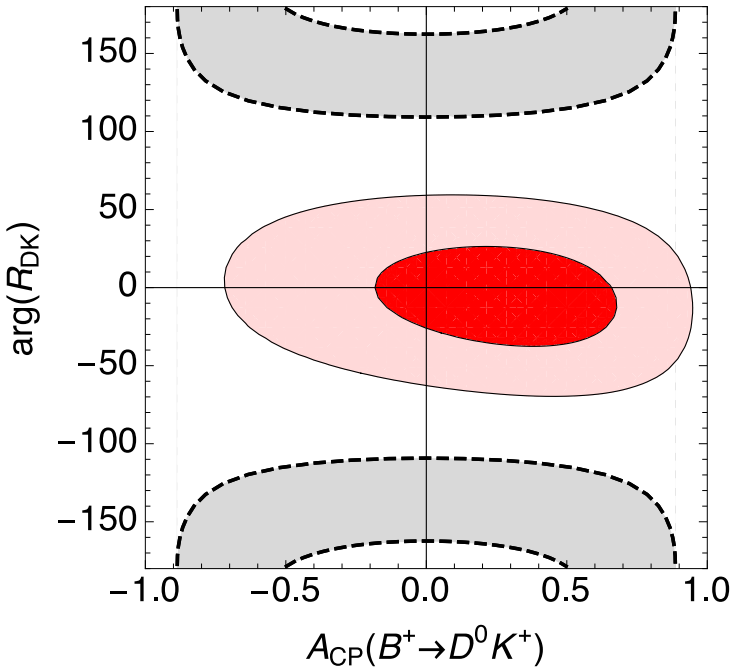

Fig.17 Allowed region by experimental results in $B \to DK$ and the predicted region of the $b \to u$ CP violating RHCC. The red (pink) shows 1 (2)σ allowed region. The gray shows 1σ prediction region. All region is allowed at 2σ.

where

$$\mathcal{O}_1 = \bar{u}^\alpha \gamma^\mu P_L b^\beta \bar{s}^\beta \gamma_\mu P_L c^\alpha \tag{145}$$

$$\mathcal{O}_2 = \bar{u}^\alpha \gamma^\mu P_L b^\alpha \bar{s}^\beta \gamma_\mu P_L c^\beta \tag{146}$$

$$\mathcal{O}_{1R} = \bar{u}^\alpha \gamma^\mu P_R b^\beta \bar{s}^\beta \gamma_\mu P_L c^\alpha \tag{147}$$

$$\mathcal{O}_{2R} = \bar{u}^\alpha \gamma^\mu P_R b^\alpha \bar{s}^\beta \gamma_\mu P_L c^\beta. \tag{148}$$

We evaluate A^R_{DK} and A^L_{DK} in the factorization approximation:

$$A^L_{DK} = \langle \bar{D}^0 K^- | \mathcal{H}_{b_L \to u_L \bar{c}_L s_L} | B^- \rangle \tag{149}$$

$$= -(2\sqrt{2} G_f V^L_{ub} V^{L*}_{cs}/4)(C_1 + C_2/3) \langle \bar{D} | \bar{u} \gamma_\mu \gamma_5 c | 0 \rangle \langle K^- | \bar{s} \gamma^\mu b | B^- \rangle e^{i\delta_L} \tag{150}$$

$$= -(2\sqrt{2} G_f V^L_{ub} V^{L*}_{cs}/4)(C_1 + C_2/3)(-i f_D) f_0^{B\to K}[M_D^2](M_B^2 - M_K^2) e^{i\delta_L} \tag{151}$$

and

$$A^R_{DK} = \langle \bar{D}^0 K^- | \mathcal{H}_{b_R \to u_R \bar{c}_L s_L} | B^- \rangle \tag{152}$$

$$= -(2\sqrt{2} G_f V^R_{ub} V^*_{cs}/4)\,(C_{1R} + C_{2R}/3)\,(-2) \langle \bar{D}|\bar{u}\gamma_5 c|0\rangle \langle K^-|\bar{s}b|B^-\rangle e^{i\delta_R} \tag{153}$$

$$= -(2\sqrt{2} G_f V^R_{ub} V^*_{cs}/4)\,(C_{1R} + C_{2R}/3)\,(-2) \left(\frac{-i f_D M_D^2}{m_c + m_u}\right) \left(\frac{(M_B^2 - M_K^2) f_0^{B\to K}[M_D^2]}{m_b - m_s}\right) e^{i\delta_R} \tag{154}$$

where δ_R and δ_L are strong phases and we ignore annihilation contributions. The Wilson coefficients C_1, C_2, C_{1R} and C_{2R} turn out to be the same as those in $B \to \pi\pi$. Thus we obtain the amplitude ratio A^R_{DK}/A^L_{DK} as

$$\frac{A^R_{DK}}{A^L_{DK}} = -4.99 \frac{V^R_{ub}}{V^L_{ub}} e^{i(\delta_R - \delta_L)}. \tag{155}$$

The predicted region of $A_{CP}(B^+ \to D^0 K^+)$ and $\arg(R_{DK})$ corresponding to V^R_{ub}/V^L_{ub} in Fig. 9 with $\delta_R - \delta_L \in [0, 2\pi]$ is given in Fig. 17. The 1σ allowed region is indicated by the gray and the whole plane is allowed at 2σ.

5 $b \to u$ RHCC in minimal supersymmetric standard model

Minimal supersymmetric standard model(MSSM) has flavor violating interactions in supersymmetry-breaking sector. Since the down quarks are of 6 types as chirality $\times$ generation, the down type scalar quarks also have 6 types. The mass matrix of down type squarks can be written as [29]

$$M^2_{\tilde{d}} = \begin{pmatrix} (M^{\tilde{d}}_{1L})^2 & \Delta^{\tilde{d}LL}_{12} & \Delta^{\tilde{d}LL}_{13} & \Delta^{\tilde{d}LR}_{11} & \Delta^{\tilde{d}LR}_{12} & \Delta^{\tilde{d}LR}_{13} \\ \Delta^{\tilde{d}LL*}_{12} & (M^{\tilde{d}}_{2L})^2 & \Delta^{\tilde{d}LL}_{23} & \Delta^{\tilde{d}RL*}_{12} & \Delta^{\tilde{d}LR}_{22} & \Delta^{\tilde{d}LR}_{23} \\ \Delta^{\tilde{d}LL*}_{13} & \Delta^{\tilde{d}LL*}_{23} & (M^{\tilde{d}}_{3L})^2 & \Delta^{\tilde{d}RL*}_{13} & \Delta^{\tilde{d}RL*}_{23} & \Delta^{\tilde{d}LR}_{33} \\ \Delta^{\tilde{d}LR*}_{11} & \Delta^{\tilde{d}RL}_{12} & \Delta^{\tilde{d}RL}_{13} & (M^{\tilde{d}}_{1R})^2 & \Delta^{\tilde{d}RR}_{12} & \Delta^{\tilde{d}RR}_{13} \\ \Delta^{\tilde{d}LR*}_{12} & \Delta^{\tilde{d}LR*}_{22} & \Delta^{\tilde{d}RL}_{23} & \Delta^{\tilde{d}RR*}_{12} & (M^{\tilde{d}}_{2R})^2 & \Delta^{\tilde{d}RR}_{23} \\ \Delta^{\tilde{d}LR*}_{13} & \Delta^{\tilde{d}LR*}_{23} & \Delta^{\tilde{d}LR*}_{33} & \Delta^{\tilde{d}RR*}_{13} & \Delta^{\tilde{d}RR*}_{23} & (M^{\tilde{d}}_{3R})^2 \end{pmatrix}. \tag{156}$$

The up type squarks have a similar mass matrix, changing the superscript $\tilde{d} \to \tilde{u}$. The $d_i \to u_f$ RHCC is induced by the flavor violation in the squark mass matrices as shown Fig. 18. Using the mass insertion approximation, we obtain the following

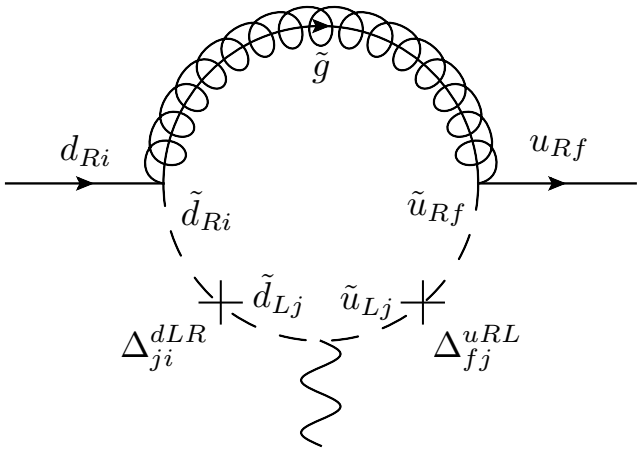

Fig.18 $d_i \to u_f$ RHCC induced in MSSM

effective Lagrangian.

$$\mathcal{L}_{\rm RHCC} = \frac{-ig}{\sqrt{2}} W^\mu \left(\bar{u}_{Rf}\gamma_\mu d_{Ri}\right)\left(\frac{\alpha_s}{36\pi}\delta^{dLR}_{ji}\delta^{uRL}_{fj}\right) \tag{157}$$

$$\delta^{qXY}_{ij} = \frac{\Delta^{\tilde{q}XY}_{ij}}{\sum_s (M^{\tilde{q}}_s)^2/6}, \qquad s = 1L, 2L, 3L, 1R, 2R, 3R \tag{158}$$

$$= \frac{\Delta^{\tilde{q}XY}_{ij}}{m^2}. \tag{159}$$

where we assume that squarks and gluino have same mass m. Thus V^R_{ub} is given by

$$V^R_{ub} = \frac{\alpha_s}{36\pi}\sum_j \delta^{dLR}_{j3}\delta^{uRL}_{1j}. \tag{160}$$

Flavor off diagonal components of the down type squark mass matrix are constrained rather strongly by FCNC processes,

$$|\delta^{dLR}_{13}| \leq 0.0010 \tag{161}$$

$$|\delta^{dLR}_{23}| \leq 0.010 \tag{162}$$

for $m = 1$TeV [29]. Therefore δ^{dLR}_{13} and δ^{dLR}_{23} can be ignored. Then V^R_{ub} can be written as

$$V^R_{ub} = \frac{\alpha_s}{36\pi}\delta^{dLR}_{33}\delta^{uRL}_{13}. \tag{163}$$

In Fig. 19, we present the region of $\delta^{dLR}_{33}\delta^{uRL}_{13}$ that is allowed by the constraint on V^R_{ub}/V^L_{ub} in Fig. 9. Since the mass insertion approximation is used in Eq. (163), its applicability is limited to the cases of small $|\delta^{dLR}_{33}\delta^{uRL}_{13}|$. Thus Fig. 19 should be interpreted with caution. As a reference, we show the line of $|\delta^{dLR}_{33}\delta^{uRL}_{13}| = 0.3$ in Fig. 19. In order to precisely examine the region of large $|\delta^{dLR}_{33}\delta^{uRL}_{13}|$, we need an evaluation beyond the mass insertion approximation.

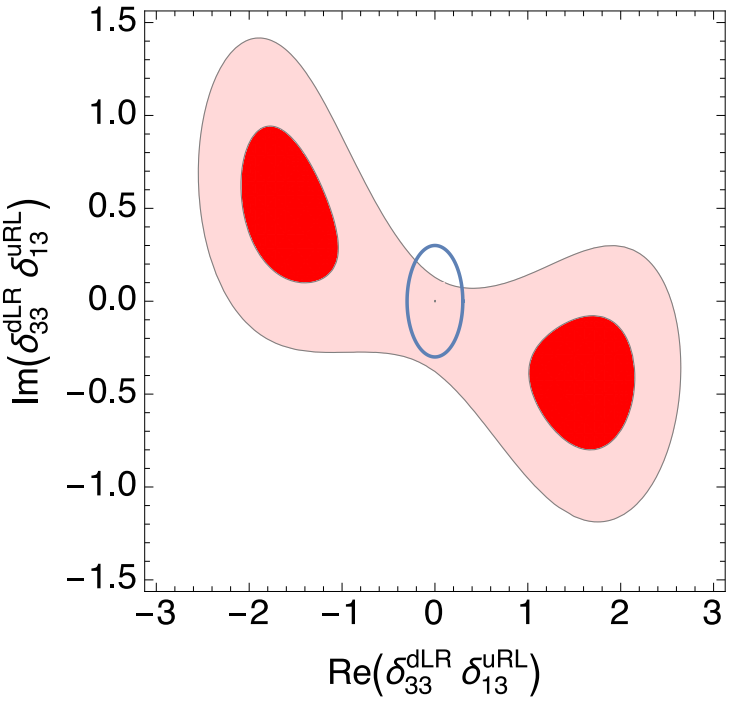

Fig.19 The allowed region of MSSM parameter. The red (pink) shows $1(2)\sigma$. The blue circle shows $|\delta_{33}^{\rm dLR}\delta_{13}^{\rm uRL}| = 0.3$.

6 Conclusion

We have considered the $b \to u$ RHCC suggested by various $|V_{ub}|$ determinations and examined its consequences in CP violation in B decays.

It is found that the discrepancy among the result of direct measurements of $|V_{ub}|$ from $B \to \tau\nu$, $\pi\ell\nu$, $X_u\ell\nu$, $\rho\ell\nu$ and $\omega\ell\nu$, and that of indirect measurement using unitarity of V^L is decreased by $b \to u$ RHCC as shown in Fig. 6 and Fig. 7. At the same time, our analysis suggests a large CP violation in $b \to u$ RHCC as shown in Fig. 9. The p-value of the model with CP violating $b \to u$ RHCC is practically the same as that of SM.

According to this result, we have studied CP violating observables in $B \to \pi\pi$, $B \to \rho\rho$ and $B \to DK$. We reveal that new direct CP asymmetries, deviation of ϕ_2 in $B \to \pi\pi$ and $B \to \rho\rho$ and that of ϕ_3 in $B \to DK$ arise. They are shown in Figs. 11, 13 and 17 with present experimental constraints. The direct CP violation of $B^+ \to \pi^+\pi^0$ and $B^+ \to \rho^+\rho^0$ are strongly constrained by experimental data. On the other hand, a large deviation $\sim 50^\circ$ of ϕ_2 is still allowed. Although the effect to $B \to DK$ is enhanced by QCD radiative collection, experimental constraint is rather weak at present. Comparing these possible CP violating signals and present experimental data, we find that the $b \to u$ CP violating RHCC is a viable new physics scenario. These CP violating signals may be discovered by SuperKEKB/Belle II and LHCb experiments.

If the $b \to u$ RHCC is found in experiments, it means that the flavor structure and CP violation in new physics is not described by the CKM matrix. We have illustrated such a case in the MSSM evaluating loop-induced $b \to u$ RHCC and shown the constraint on the relevant parameters in Fig. 19.

In order to clarify the remaining the discrepancy in several $|V_{ub}|$ determinations, more detailed studies of the leptonic and semi-leptonic B decays discussed in this thesis as well as other decay modes such as $B \to \rho\ell\nu$ and $\Lambda_b \to p\ell\nu$ [30] are necessary. In particular, since the ρ meson polarization in $B \to \rho\ell\nu$ [31] and the lepton energy distribution in $\Lambda_b \to p\ell\nu$ are sensitive to the $b \to u$ RHCC, both theoretical and experimental studies of these modes are important to discover or constrain $b \to u$ RHCC.

In conclusion, the $b \to u$ RHCC is consistent with current experimental constraints. It might be discovered by further theoretical and experimental studies of leptonic and semi-leptonic B decays and CP violations in hadronic B decays.

App. A Form factor and decay constant

The Calculations of the hadron transition amplitude like $B \to \pi$ and $B \to \rho$ required calculation of strong interaction because B, π, ρ are bound states by strong interaction. Strong interaction is difficult to calculate in order not available perturbations. However we can determine function form of the hadron transition amplitude using that strong interaction preserve Lorentz invariance, parity symmetry(P symmetry) and time-reversal symmetry(T symmetry). Then the hadron matrix elements are called as Form Factor and Decay Constant. Now, we will look about their definition. It needs caution that we deal with π, ρ, ω and others meson made from $\bar{u}u$ and $\bar{d}d$. Because

$$\pi^0 \sim \frac{\bar{u}u - \bar{d}d}{\sqrt{2}} \tag{164}$$

$$\rho^0 \sim \frac{\bar{u}u - \bar{d}d}{\sqrt{2}} \tag{165}$$

$$\omega^0 \sim \frac{\bar{u}u + \bar{d}d}{\sqrt{2}}, \tag{166}$$

we must multiply $\pm 1/\sqrt{2}$. Here, we consider this point by multiplying amplitude and $c_{\text{meson}} = 1$ or $\pm\sqrt{2}$.

A.1 Parity and time-reversal conversion property of states and operator

The parity and time-reversal conversion property of pseudo scalar meson P and vector meson V are

$$\mathcal{P}|P(p^0, \vec{p})\rangle = -|P(p^0, -\vec{p})\rangle \tag{167}$$

$$\mathcal{P}|V(p^0, \vec{p}, \epsilon)\rangle = |V(p^0, -\vec{p}, \epsilon')\rangle \tag{168}$$

$$\mathcal{P}|0\rangle = |0\rangle \tag{169}$$

$$\mathcal{T}|P(p^0, \vec{p})\rangle = +|P(p^0, -\vec{p})\rangle \tag{170}$$

$$\mathcal{T}|V(p^0, \vec{p}, \epsilon)\rangle = +|V(p^0, -\vec{p}, \epsilon')\rangle \tag{171}$$

$$\mathcal{T}|0\rangle = |0\rangle. \tag{172}$$

Time-reversal of states can have arbitrary phase because it is anti-unitarity but we define like above.

Next, we consider about the P and T conversion property of operators. For this, we consider about P and T conversion property of spin 1/2 current $J^\mu(t,\vec{x}) = \bar{\psi}\gamma^\mu\psi$ first. P conversion of $J^\mu(t,\vec{x})$ is

$$\begin{aligned}\mathcal{P}J^\mu(t,\vec{x})\mathcal{P}^\dagger &= J_\mu(t,-\vec{x}) \\ &= \bar{\psi}(t,-\vec{x})\gamma^0\gamma^\mu\gamma^0\psi(t,-\vec{x}).\end{aligned} \tag{173}$$

Thus wave functionψ is converted below.

$$\mathcal{P}\psi(t,\vec{x})\mathcal{P}^\dagger = \gamma^0\psi(t,-\vec{x}) \tag{174}$$

Thus 5 type operators are converted below with $\sigma_{\mu\nu} = i[\gamma_\mu,\gamma_\nu]/2$.

$$\mathcal{P}\bar{\psi_1}(t,\vec{x})\psi_2(t,\vec{x})\mathcal{P}^\dagger = \bar{\psi_1}(t,-\vec{x})\psi_2(t,-\vec{x}) \tag{175}$$

$$\mathcal{P}\bar{\psi_1}(t,\vec{x})\gamma_5\psi_2(t,\vec{x})\mathcal{P}^\dagger = -\bar{\psi_1}(t,-\vec{x})\gamma_5\psi_2(t,-\vec{x}) \tag{176}$$

$$\mathcal{P}\bar{\psi_1}(t,\vec{x})\gamma_\mu\psi_2(t,\vec{x})\mathcal{P}^\dagger = \bar{\psi_1}(t,-\vec{x})\gamma^\mu\psi_2(t,-\vec{x}) \tag{177}$$

$$\mathcal{P}\bar{\psi_1}(t,\vec{x})\gamma_\mu\gamma_5\psi_2(t,\vec{x})\mathcal{P}^\dagger = -\bar{\psi_1}(t,-\vec{x})\gamma^\mu\gamma_5\psi_2(t,-\vec{x}) \tag{178}$$

$$\mathcal{P}\bar{\psi_1}(t,\vec{x})\sigma_{\mu\nu}\psi_2(t,\vec{x})\mathcal{P}^\dagger = \bar{\psi_1}(t,-\vec{x})\sigma^{\mu\nu}\psi_2(t,-\vec{x}) \tag{179}$$

Changing sign of space component is represented by the raising and lowering of subscript. Similarly T conversion of $J^\mu(t,\vec{x})$ is

$$\mathcal{T}J^\mu(t,\vec{x})\mathcal{T}^\dagger = \bar{\psi}(-t,\vec{x})\gamma_\mu\psi(-t,\vec{x}). \tag{180}$$

Because T conversion is anti-unitary, T conversion of wave function is

$$\mathcal{T}\psi(t,\vec{x})\mathcal{T}^\dagger = \gamma^1\gamma^3\psi(-t,\vec{x}). \tag{181}$$

For this reason, T conversion of operators are below.

$$\mathcal{T}\bar{\psi_1}(t,\vec{x})\psi_2(t,\vec{x})\mathcal{T}^{-1} = \bar{\psi_1}(-t,\vec{x})\psi_2(-t,\vec{x}) \tag{182}$$

$$\mathcal{T}\bar{\psi_1}(t,\vec{x})\gamma_5\psi_2(t,\vec{x})\mathcal{T}^{-1} = \bar{\psi_1}(-t,\vec{x})\gamma_5\psi_2(-t,\vec{x}) \tag{183}$$

$$\mathcal{T}\bar{\psi_1}(t,\vec{x})\gamma_\mu\psi_2(t,\vec{x})\mathcal{T}^{-1} = \bar{\psi_1}(-t,\vec{x})\gamma^\mu\psi_2(-t,\vec{x}) \tag{184}$$

$$\mathcal{T}\bar{\psi_1}(t,\vec{x})\gamma_\mu\gamma_5\psi_2(t,\vec{x})\mathcal{T}^{-1} = \bar{\psi_1}(-t,\vec{x})\gamma^\mu\gamma_5\psi_2(-t,\vec{x}) \tag{185}$$

$$\mathcal{T}\bar{\psi_1}(t,\vec{x})\sigma_{\mu\nu}\psi_2(t,\vec{x})\mathcal{T}^{-1} = -\bar{\psi_1}(-t,\vec{x})\sigma^{\mu\nu}\psi_2(-t,\vec{x}) \tag{186}$$

An equation of $\psi(t,\vec{x})$ is

$$\psi(t,\vec{x}) = \int \frac{d^3\vec{p}}{(2\pi)^3}\frac{1}{\sqrt{2E_p}}\sum_{s=\pm}\left(a^s(p)u^s(p)e^{-ip\cdot x} + b^{s\dagger}(p)v^s(p)e^{ip\cdot x}\right) \tag{187}$$

$$\bar{\psi}(t,\vec{x}) = \int \frac{d^3\vec{p}}{(2\pi)^3}\frac{1}{\sqrt{2E_p}}\sum_{s=\pm}\left(a^{s\dagger}(p)\bar{u}^s(p)e^{ip\cdot x} + b^s(p)\bar{v}^s(p)e^{-ip\cdot x}\right) \tag{188}$$

$$(i\partial\!\!\!/ - m)\psi(t,\vec{x}) = 0 \tag{189}$$

$$\bar{\psi}(t,\vec{x})(i\overleftarrow{\partial\!\!\!/} + m) = 0. \tag{190}$$

A.2 Decay constant

A.2.1 Pseudo scalar meson

We want to consider about pseudo scalar meson vanishing amplitudes $\langle 0|\bar{q}_1\Gamma q_2|P\rangle(\Gamma = 1,\gamma_5...)$. This need QCD calculation, so it is difficult. For this reason, we use P and T symmetry in QCD. In P and T conversion, amplitudes convert

$$\langle 0|\bar{q}_1 q_2|P\rangle \xrightarrow{P} -\langle 0|\bar{q}_1 q_2|P\rangle \tag{191}$$

$$\langle 0|\bar{q}_1\gamma_5 q_2|P\rangle \xrightarrow{P} \langle 0|\bar{q}_1\gamma_5 q_2|P\rangle \tag{192}$$

$$\langle 0|\bar{q}_1\gamma_\mu q_2|P\rangle \xrightarrow{P} -\langle 0|\bar{q}_1\gamma^\mu q_2|P\rangle \tag{193}$$

$$\langle 0|\bar{q}_1\gamma_\mu\gamma_5 q_2|P\rangle \xrightarrow{P} \langle 0|\bar{q}_1\gamma^\mu\gamma_5 q_2|P\rangle \tag{194}$$

$$\langle 0|\bar{q}_1\sigma_{\mu\nu} q_2|P\rangle \xrightarrow{P} -\langle 0|\bar{q}_1\sigma^{\mu\nu} q_2|P\rangle \tag{195}$$

$$\langle 0|\bar{q}_1 q_2|P\rangle \xrightarrow{T} -\langle 0|\bar{q}_1 q_2|P\rangle \tag{196}$$

$$\langle 0|\bar{q}_1\gamma_5 q_2|P\rangle \xrightarrow{T} -\langle 0|\bar{q}_1\gamma_5 q_2|P\rangle \tag{197}$$

$$\langle 0|\bar{q}_1\gamma_\mu q_2|P\rangle \xrightarrow{T} -\langle 0|\bar{q}_1\gamma^\mu q_2|P\rangle \tag{198}$$

$$\langle 0|\bar{q}_1\gamma_\mu\gamma_5 q_2|P\rangle \xrightarrow{T} -\langle 0|\bar{q}_1\gamma^\mu\gamma_5 q_2|P\rangle \tag{199}$$

$$\langle 0|\bar{q}_1\sigma_{\mu\nu} q_2|P\rangle \xrightarrow{T} \langle 0|\bar{q}_1\sigma^{\mu\nu} q_2|P\rangle. \tag{200}$$

Moreover, Lorentz parameter in these bracket is only P meson momentum p^μ, so the amplitudes are calcated

$$c_P\langle 0|\bar{q}_1 q_2|P\rangle = 0 \tag{201}$$
$$c_P\langle 0|\bar{q}_1\gamma_5 q_2|P\rangle = if'_P \tag{202}$$
$$c_P\langle 0|\bar{q}_1\gamma_\mu q_2|P\rangle = 0 \tag{203}$$
$$c_P\langle 0|\bar{q}_1\gamma_\mu\gamma_5 q_2|P\rangle = if_P p_\mu \tag{204}$$
$$c_P\langle 0|\bar{q}_1\sigma_{\mu\nu} q_2|P\rangle = 0. \tag{205}$$

f_p is called Decay Constant. There is following relation among momentum of quark k_1^μ and k_2^μ and meson's one p^μ,

$$k_1^\mu + k_2^\mu = p^\mu. \tag{206}$$

Then we derive relation between f_P and f'_P as

$$f'_P = \frac{M_P^2}{m_1 + m_2} f_P. \tag{207}$$

with equation of motion (EOM).

A.2.2 Vector meson

Similarly we can consider about vector meson. T and P conversion of amplitudes is

$$\langle 0|\bar{q}_1 q_2|V\rangle \xrightarrow{P} \langle 0|\bar{q}_1 q_2|V\rangle \tag{208}$$
$$\langle 0|\bar{q}_1\gamma_5 q_2|V\rangle \xrightarrow{P} -\langle 0|\bar{q}_1\gamma_5 q_2|V\rangle \tag{209}$$
$$\langle 0|\bar{q}_1\gamma_\mu q_2|V\rangle \xrightarrow{P} \langle 0|\bar{q}_1\gamma^\mu q_2|V\rangle \tag{210}$$
$$\langle 0|\bar{q}_1\gamma_\mu\gamma_5 q_2|V\rangle \xrightarrow{P} -\langle 0|\bar{q}_1\gamma^\mu\gamma_5 q_2|V\rangle \tag{211}$$
$$\langle 0|\bar{q}_1\sigma_{\mu\nu} q_2|V\rangle \xrightarrow{P} \langle 0|\bar{q}_1\sigma^{\mu\nu} q_2|V\rangle \tag{212}$$

$$\langle 0|\bar{q}_1 q_2|V\rangle \xrightarrow{T} \langle 0|\bar{q}_1 q_2|V\rangle \tag{213}$$
$$\langle 0|\bar{q}_1\gamma_5 q_2|V\rangle \xrightarrow{T} \langle 0|\bar{q}_1\gamma_5 q_2|V\rangle \tag{214}$$
$$\langle 0|\bar{q}_1\gamma_\mu q_2|V\rangle \xrightarrow{T} \langle 0|\bar{q}_1\gamma^\mu q_2|V\rangle \tag{215}$$
$$\langle 0|\bar{q}_1\gamma_\mu\gamma_5 q_2|V\rangle \xrightarrow{T} \langle 0|\bar{q}_1\gamma^\mu\gamma_5 q_2|V\rangle \tag{216}$$
$$\langle 0|\bar{q}_1\sigma_{\mu\nu} q_2|V\rangle \xrightarrow{T} -\langle 0|\bar{q}_1\sigma^{\mu\nu} q_2|V\rangle. \tag{217}$$

Amplitude of vector meson include first order of polarization vector ϵ^μ and $\epsilon \cdot p = 0$. Thus amplitudes is calculated

$$c_V \langle 0|\bar{q}_1 q_2|V\rangle = 0 \tag{218}$$
$$c_V \langle 0|\bar{q}_1 \gamma_5 q_2|V\rangle = 0 \tag{219}$$
$$c_V \langle 0|\bar{q}_1 \gamma_\mu q_2|V\rangle = f_V \epsilon_\mu \tag{220}$$
$$c_V \langle 0|\bar{q}_1 \gamma_\mu \gamma_5 q_2|V\rangle = 0 \tag{221}$$
$$c_V \langle 0|\bar{q}_1 \sigma_{\mu\nu} q_2|V\rangle = i f'_V (p_\mu \epsilon_\nu - p_\nu \epsilon_\mu). \tag{222}$$

Since momentum of quarks k_1^μ and k_2^μ are satisfy $k_1^\mu + k_2^\mu = p^\mu$, we evaluate f'_V as

$$f'_V = \frac{m_1 + m_2}{M_V^2} f_V. \tag{223}$$

with EOM.

A.3 Form factors

A.3.1 Pseudo scalar meson to pseudo scalar meson

We deal with amplitude of transition from pseudo scalar meson to pseudo scalar meson for considering $B \to \pi \ell \nu$ and others. P and T transition of these amplitudes are

$$\langle P_1|\bar{q}_1 q_2|P_2\rangle \xrightarrow{P} \langle P_1|\bar{q}_1 q_2|P_2\rangle \tag{224}$$
$$\langle P_1|\bar{q}_1 \gamma_5 q_2|P_2\rangle \xrightarrow{P} -\langle P_1|\bar{q}_1 \gamma_5 q_2|P_2\rangle \tag{225}$$
$$\langle P_1|\bar{q}_1 \gamma_\mu q_2|P_2\rangle \xrightarrow{P} \langle P_1|\bar{q}_1 \gamma^\mu q_2|P_2\rangle \tag{226}$$
$$\langle P_1|\bar{q}_1 \gamma_\mu \gamma_5 q_2|P_2\rangle \xrightarrow{P} -\langle P_1|\bar{q}_1 \gamma^\mu \gamma_5 q_2|P_2\rangle \tag{227}$$
$$\langle P_1|\bar{q}_1 \sigma_{\mu\nu} q_2|P_2\rangle \xrightarrow{P} \langle P_1|\bar{q}_1 \sigma^{\mu\nu} q_2|P_2\rangle \tag{228}$$

$$\langle P_1|\bar{q}_1 q_2|P_2\rangle \xrightarrow{T} \langle P_1|\bar{q}_1 q_2|P_2\rangle \tag{229}$$
$$\langle P_1|\bar{q}_1 \gamma_5 q_2|P_2\rangle \xrightarrow{T} \langle P_1|\bar{q}_1 \gamma_5 q_2|P_2\rangle \tag{230}$$
$$\langle P_1|\bar{q}_1 \gamma_\mu q_2|P_2\rangle \xrightarrow{T} \langle P_1|\bar{q}_1 \gamma^\mu q_2|P_2\rangle \tag{231}$$
$$\langle P_1|\bar{q}_1 \gamma_\mu \gamma_5 q_2|P_2\rangle \xrightarrow{T} \langle P_1|\bar{q}_1 \gamma^\mu \gamma_5 q_2|P_2\rangle \tag{232}$$
$$\langle P_1|\bar{q}_1 \sigma_{\mu\nu} q_2|P_2\rangle \xrightarrow{T} -\langle P_1|\bar{q}_1 \sigma^{\mu\nu} q_2|P_2\rangle. \tag{233}$$

For considering these, amplitudes can be written

$$c_{P_1}c_{P_2}\langle P_1|\bar{q}_1 q_2|P_2\rangle = F_S(q^2) \tag{234}$$

$$c_{P_1}c_{P_2}\langle P_1|\bar{q}_1\gamma_5 q_2|P_2\rangle = 0 \tag{235}$$

$$c_{P_1}c_{P_2}\langle P_1|\bar{q}_1\gamma_\mu q_2|P_2\rangle = f_+(q^2)\left(p_2+p_1-\frac{m_{P_2}^2-m_{P_1}^2}{q^2}q\right)_\mu + f_0(q^2)\frac{m_{P_2}^2-m_{P_1}^2}{q^2}q_\mu \tag{236}$$

$$c_{P_1}c_{P_2}\langle P_1|\bar{q}_1\gamma_\mu\gamma_5 q_2|P_2\rangle = 0 \tag{237}$$

$$c_{P_1}c_{P_2}\langle P_1|\bar{q}_1\sigma_{\mu\nu} q_2|P_2\rangle = iF_T(q^2)(p_{1\mu}p_{2\nu}-p_{2\mu}p_{1\nu}) \tag{238}$$

with $q_\mu = (p_2-p_1)_\mu = (k_2-k_1)_\mu$. For tensor type amplitude, a coefficient of $\epsilon_{\mu\nu\rho\sigma}p_1^\rho p_2^\sigma$ is 0 because P transition. This time, there are two vector parameters p_1 and p_2 so F_S, f_+, f_0 and F_T are function of q^2. Now, we are going to rewrite F_S and F_T using f_+ and f_0. Then, F_S is obtained as follow,

$$F_S = \frac{m_{P_2}^2-m_{P_1}^2}{m_2-m_1}f_0. \tag{239}$$

Similarly F_T is calculated as follow,

$$-\frac{i}{2}q^2F_T\left(p_2+p_1-\frac{m_{P_2}^2-m_{P_1}^2}{q^2}q\right)_\nu \tag{240}$$

$$\begin{aligned}=&i(k_{1\nu}+k_{2\nu})\frac{m_{P_2}^2-m_{P_1}^2}{m_2-m_1}f_0\\ &-(m_1+m_2)i\left(f_+(q^2)\left(p_2+p_1-\frac{m_{P_2}^2-m_{P_1}^2}{q^2}q\right)_\nu + f_0(q^2)\frac{m_{P_2}^2-m_{P_1}^2}{q^2}q_\nu\right).\end{aligned} \tag{241}$$

Then we assume following equation,

$$\frac{m_{P_2}^2-m_{P_1}^2}{m_2^2-m_1^2}(k_1+k_2)_\nu = (p_2+p_1)_\nu. \tag{242}$$

This relation is correct in ignoring $O(\Lambda_{\rm QCD})$. Thus F_T is obtained as

$$F_T = \frac{2(m_{P_2}+m_{P_1})}{q^2}(f_+-f_0). \tag{243}$$

A.3.2 Pseudo scalar meson to vector meson

We consider amplitude of transition from pseudo scalar meson to vector meson for considering $B\to\rho\ell\nu$ and others. P and T transition of these amplitudes are listed

in follow,

$$\langle V|\bar{q}_1 q_2|P\rangle \xrightarrow{P} -\langle V|\bar{q}_1 q_2|P\rangle \tag{244}$$

$$\langle V|\bar{q}_1 \gamma_5 q_2|P\rangle \xrightarrow{P} \langle V|\bar{q}_1 \gamma_5 q_2|P\rangle \tag{245}$$

$$\langle V|\bar{q}_1 \gamma_\mu q_2|P\rangle \xrightarrow{P} -\langle V|\bar{q}_1 \gamma^\mu q_2|P\rangle \tag{246}$$

$$\langle V|\bar{q}_1 \gamma_\mu \gamma_5 q_2|P\rangle \xrightarrow{P} \langle V|\bar{q}_1 \gamma^\mu \gamma_5 q_2|P\rangle \tag{247}$$

$$\langle V|\bar{q}_1 \sigma_{\mu\nu} q_2|P\rangle \xrightarrow{P} -\langle V|\bar{q}_1 \sigma^{\mu\nu} q_2|P\rangle \tag{248}$$

$$\langle V|\bar{q}_1 q_2|P\rangle \xrightarrow{T} \langle V|\bar{q}_1 q_2|P\rangle \tag{249}$$

$$\langle V|\bar{q}_1 \gamma_5 q_2|P\rangle \xrightarrow{T} \langle V|\bar{q}_1 \gamma_5 q_2|P\rangle \tag{250}$$

$$\langle V|\bar{q}_1 \gamma_\mu q_2|P\rangle \xrightarrow{T} \langle V|\bar{q}_1 \gamma^\mu q_2|P\rangle \tag{251}$$

$$\langle V|\bar{q}_1 \gamma_\mu \gamma_5 q_2|P\rangle \xrightarrow{T} \langle V|\bar{q}_1 \gamma^\mu \gamma_5 q_2|P\rangle \tag{252}$$

$$\langle V|\bar{q}_1 \sigma_{\mu\nu} q_2|P\rangle \xrightarrow{T} -\langle V|\bar{q}_1 \sigma^{\mu\nu} q_2|P\rangle. \tag{253}$$

For considering these, amplitudes can be written as

$$c_P c_V \langle V|\bar{q}_1 q_2|P\rangle = 0 \tag{254}$$

$$c_P c_V \langle V|\bar{q}_1 \gamma_5 q_2|P\rangle = f_4(\epsilon^* \cdot p_P) \tag{255}$$

$$c_P c_V \langle V|\bar{q}_1 \gamma_\mu q_2|P\rangle = i\epsilon_{\mu\nu\rho\sigma}\epsilon^{*\nu} p_P^\rho p_V^\sigma \frac{2V}{m_P + m_V} \tag{256}$$

$$c_P c_V \langle V|\bar{q}_1 \gamma_\mu \gamma_5 q_2|P\rangle = -\epsilon_\mu^*(m_P + m_V)A_1 + (p_P + p_V)_\mu(\epsilon^* \cdot q)\frac{A_2}{m_P + m_V} + q_\mu(\epsilon^* \cdot q)\frac{2m_V}{q^2}A_3 \tag{257}$$

$$c_P c_V \langle V|\bar{q}_1 \sigma_{\mu\nu} q_2|P\rangle = \epsilon_{\mu\nu\rho\sigma}\left[f_1 \epsilon^{*\rho} p_P^\sigma + f_2 \epsilon^{*\rho} p_V^\sigma + f_3(\epsilon^* \cdot p_P) p_P^\rho p_V^\sigma\right] \tag{258}$$

with $q_\mu = (p_2 - p_1)_\mu$. Just like previous subsection, we are going to calculate relation of (f_1, f_2, f_3, f_4) and (V, A_1, A_2, A_3). First, f_4 is calculated as following equation,

$$-(m_P + m_V) f_4(\epsilon^* \cdot p_P) \tag{259}$$

$$= -(m_P + m_V) c_P c_V \langle V|\bar{q}_1 \gamma_5 q_2|P\rangle \tag{260}$$

$$= c_P c_V \langle V|i\partial^\mu(\bar{q}_1 \gamma_\mu \gamma_5 q_2)|P\rangle \tag{261}$$

$$= -(\epsilon^* \cdot q)(m_P + m_V)A_1 + (m_P^2 - m_V^2)(\epsilon^* \cdot q)\frac{A_2}{m_P + m_V} + 2m_V(\epsilon^* \cdot q)A_3. \tag{262}$$

Thus we obtain f_4 as follow,

$$f_4 = A_1 - \frac{m_P - m_V}{m_P + m_V}A_2 - \frac{2m_V}{m_P + m_V}A_3. \tag{263}$$

Continuously, we evaluate f_1, f_2 and f_3 and obtain following relations,

$$\begin{aligned}
2V\epsilon_{\nu\mu\rho\sigma}\epsilon^{*\mu}p_P^\rho p_V^\sigma =& -i(m_P+m_V)c_P c_V\langle V|\bar{q}_1\gamma_\nu\gamma_5 q_2|P\rangle && (264)\\
=& c_P c_V\langle V|i\partial^\mu(\bar{q}_1\sigma_{\mu\nu}q_2)|P\rangle && (265)\\
=& q^\mu\epsilon_{\mu\nu\rho\sigma}\left[f_1\epsilon^{*\rho}p_P^\sigma + f_2\epsilon^{*\rho}p_V^\sigma + f_3(\epsilon^*\cdot p_P)p_P^\rho p_V^\sigma\right] && (266)\\
=& (f_1+f_2)\epsilon_{\nu\rho\mu\sigma}\epsilon^{*\rho}p_P^\mu p_V^\sigma && (267)
\end{aligned}$$

$$\epsilon_\nu^*(m_P^2-m_V^2)A_1 - (p_P+p_V)_\nu(\epsilon^*\cdot q)\left(\frac{m_P-m_V}{m_P+m_V}A_2+f_4\right) - q_\nu(\epsilon^*\cdot q)\frac{2m_V(m_P-m_V)}{q^2}A_3 \quad (268)$$

$$= ic_P c_V\langle V|i\partial^\mu(\bar{q}_1\sigma_{\mu\nu}\gamma_5 q_2)|P\rangle \quad (269)$$

$$= \frac{1}{2}\epsilon_{\mu\nu\rho\sigma}q^\mu\epsilon^{\rho\sigma\epsilon\eta}\left[f_1\epsilon_\epsilon^* p_{P\eta} + f_2\epsilon_\epsilon^* p_{V\eta} + f_3(\epsilon^*\cdot p_P)p_{P\epsilon}p_{V\eta}\right] \quad (270)$$

$$\begin{aligned}
=& -\frac{1}{2}\Big[\epsilon_\nu^*\left\{f_1(m_P^2-m_V^2+q^2)+f_2(m_P^2-m_V^2-q^2)\right\} - (p_V+p_P)_\nu(\epsilon^*\cdot p_P)(f_1+f_2+q^2f_3)\\
& - q_\nu(\epsilon^*\cdot p_P)\{f_1-f_2-(m_P^2-m_V^2)f_3\}\Big]. && (271)
\end{aligned}$$

As the result, we obtain as following relations,

$$\begin{aligned}
f_1 =& V - \frac{m_P^2-m_V^2}{q^2}(A_1+V) && (272)\\
f_2 =& V + \frac{m_P^2-m_V^2}{q^2}(A_1+V) && (273)\\
f_3 =& -\frac{2}{q^2}\left(A_1 - \frac{2m_V}{m_P+m_V}A_3 - V\right). && (274)
\end{aligned}$$

App. B Calculations of each B meson decay rate

In this section, we are going to calculate decay rate of each B meson decays with RHCC.

B.1 $b-u-\ell-\nu$ 4 fermi operator

At first, we calculate the $b-u-\ell-\nu$ 4 fermi operator. For Eq. (12), it is

$$\mathcal{M}_f = -\frac{g^2}{2}\mathcal{P}_W \langle u\ell\nu| \left[\bar{u}\gamma^\mu \left(P_L V_{ub}^L + P_R V_{ub}^R\right) b\right] \left[\bar{\ell}\gamma_\mu P_L \nu\right] |b\rangle \tag{275}$$

when $\mathcal{P}_W$ is propagator of W boson. Propagator of W boson with unitary gauge is

$$\mathcal{P}_W = \frac{g^{\mu\nu} - \frac{q^\mu q^\nu}{M_W^2}}{q^2 - M_W^2}. \tag{276}$$

Energy scale of B meson is 5GeV and one of W boson is 80GeV, so $q^2 \ll M_W^2$. For this reason,

$$\mathcal{P}_W \simeq -\frac{g^{\mu\nu}}{M_W^2}. \tag{277}$$

In summary, 4 fermi operator is

$$\mathcal{O}_f = 2\sqrt{2}G_f \left(\bar{u}\gamma^\mu \left(P_L V_{ub}^L + P_R V_{ub}^R\right) b\right) \left(\bar{\ell}\gamma_\mu P_L \nu\right) \tag{278}$$

with $G_f = g^2/(4\sqrt{2}M_W^2)$.

B.2 $B \to \tau\nu$

Using Eq. (278), an amplitude of $B \to \tau\nu$ is calculated as

$$A(B \to \tau\nu) = 2\sqrt{2}G_f \langle\tau^-\bar{\nu}|(\bar{\tau}\gamma_\mu P_L \nu)|0\rangle\langle 0|(\bar{u}\gamma^\mu \left(V_{ub}^L P_L + V_{ub}^R P_R\right) b)|B^-\rangle. \tag{279}$$

Using Eqs. (203, 204), we calculate as follow,

$$A(B \to \tau\nu) = \sqrt{2}iG_f(-V_{ub}^L + V_{ub}^R) f_B p_B^\mu \langle\tau^-\bar{\nu}|(\bar{\tau}\gamma_\mu P_L \nu)|0\rangle. \tag{280}$$

Thus decay rate, $\Gamma(B \to \tau\nu)$, is evaluated as following equations,

$$d\Gamma(B \to \tau\nu) = \frac{1}{2E_B}|\mathcal{M}(B \to \tau\nu)|^2 dQ \tag{281}$$

where $|\mathcal{M}(B \to \tau\nu)|^2$ and dQ are shown as

$$|\mathcal{M}(B \to \tau\nu)|^2 = \sum_s |A(B \to \tau\nu)|^2 \tag{282}$$

$$= 2{G_f}^2 |V_{ub}^L - V_{ub}^R|^2 {F_B}^2 P_B^\mu P_B^\rho \sum_s \mathrm{Tr}(\bar{u}_\tau \gamma_\mu P_L v_\nu \bar{v}_\nu \gamma_\rho P_L u_\tau) \tag{283}$$

$$= 2{G_f}^2 |V_{ub}^L - V_{ub}^R|^2 {F_B}^2 M_\tau^2 (M_B^2 - M_\tau^2) \tag{284}$$

$$dQ = \frac{d^3\vec{P}_\nu}{2(2\pi)^3 E_\nu} \frac{d^3\vec{P}_\tau}{2(2\pi)^3 E_\tau} (2\pi)^4 \delta^4(P_B - P_\nu - P_\tau) \tag{285}$$

$$= \frac{1}{8\pi M_B^2}(M_B^2 - M_\tau^2). \tag{286}$$

As the result, we obtain $\Gamma(B \to \tau\nu)$ as

$$\Gamma(B \to \tau\nu) = \frac{1}{2M_B} 2{G_f}^2 |V_{ub}^L - V_{ub}^R|^2 {F_B}^2 M_\tau^2 (M_B^2 - M_\tau^2) \frac{1}{8\pi M_B^2}(M_B^2 - M_\tau^2)$$

$$= \frac{1}{8\pi} {G_f}^2 |V_{ub}^L - V_{ub}^R|^2 {F_B}^2 M_B M_\tau^2 \left(1 - \left(\frac{M_\tau}{M_B}\right)^2\right)^2. \tag{287}$$

B.3 $B \to \pi\ell\nu$

We are going to calculate decay rate of $B \to \pi\ell\nu$. Using Eq. (278), its amplitude is written as

$$A(B \to \pi\ell\nu) = 2\sqrt{2} G_f c_\pi^{-1} \langle \ell\bar{\nu}|(\bar{\tau}\gamma_\mu P_L \nu)|0\rangle \langle \pi|(\bar{u}\gamma^\mu \left(V_{ub}^L P_L + V_{ub}^R P_R\right) b)|B\rangle \tag{288}$$

with $c_{\pi^+} = 1, c_{\pi^0} = \sqrt{2}$. Using Eq. (236, 237), we evaluate as follow,

$$|\mathcal{M}|^2 = \sum_s |A(B \to \pi\ell\nu)|^2$$

$$= 8G_f^2 c_\pi^{-2} |V_{ub}^L + V_{ub}^R|^2 [f_+(q^2)]^2 P_B^\mu P_B^\rho \sum_s \mathrm{Tr}(\bar{u}_\ell \gamma_\mu P_L v_\nu \bar{v}_\nu \gamma_\rho P_L u_\ell)$$

$$= 8G_f^2 c_\pi^{-2} |V_{ub}^L + V_{ub}^R|^2 [f_+(q^2)]^2 2[2(P_B P_l)(P_B P_\nu) - M_B^2 (P_l P_\nu)]. \tag{289}$$

We can represent momentum as following relations,

$$P_l P_\nu = \frac{1}{2}(P_l + P_\nu)^2 = \frac{1}{2}q^2 \tag{290}$$

$$P_B P_l = \frac{M_B^2 y}{2} \tag{291}$$

$$\begin{aligned} P_B P_\nu &= P_B(P_B - P_l - P_\pi) = M_B^2 - \frac{M_B^2 y}{2} + \frac{1}{2}(q^2 - M_B^2 - M_\pi^2) \\ &= \frac{1}{2}q^2 - \frac{M_B^2 y}{2} - \frac{1}{2}(M_B^2 - M_\pi^2) \end{aligned} \tag{292}$$

$$y \equiv \frac{2P_l P_B}{M_B^2}. \tag{293}$$

Thus we can calculate $|\mathcal{M}|^2$ as

$$|\mathcal{M}|^2 = 8G_f^2 c_\pi^{-2} |V_{ub}^L + V_{ub}^R|^2 (f_+(q^2))^2 M_B^2 \left[y(q^2 - M_B^2 y + M_B^2 - M_\pi^2) - q^2 \right]. \tag{294}$$

A phase space dQ is evaluated as

$$dQ = \frac{d^3\vec{P_\nu}}{2E_\nu(2\pi)^3} \frac{d^3\vec{P_\pi}}{2E_\pi(2\pi)^3} \frac{d^3\vec{P_l}}{2E_l(2\pi)^3} (2\pi)^4 \delta^4(P_B - P_\nu - P_\pi - P_l) \tag{295}$$

$$= \frac{1}{32\pi^3} dE_\pi dE_l \tag{296}$$

$$= \frac{1}{128\pi^3} dq^2 dy \tag{297}$$

where we use $q^2 = M_B^2 + M_\pi^2 - 2M_B E_\pi, y = 2E_l/M_B$. Hence we obtain partial decay rate, $d\Gamma(B \to \pi\ell\nu)$, as

$$\begin{aligned} d\Gamma(B \to \pi\ell\nu) = &\frac{4G_f^2 M_B}{128\pi^3 c_\pi^2} |V_{ub}^L + V_{ub}^R|^2 (f_+(q^2))^2 \\ &\times \left[y(q^2 - M_B^2 y + M_B^2 - M_\pi^2) - q^2 \right] dq^2 dy. \end{aligned} \tag{298}$$

Using $P_\nu^2 = 0$, we evaluate y as

$$0 = P_\nu^2 = (P_B - P_l - P_\pi)^2 = q^2 - \frac{y}{2}(q^2 + M_B^2 - M_\pi^2) - \frac{y}{2}\sqrt{\lambda}\cos\theta_{l\pi} \tag{299}$$

$$y = \frac{M_B^2 + M_\pi^2 - \sqrt{\lambda + 4M_B^2 M_\pi^2}}{M_B^2 - \frac{1}{2}\sqrt{\lambda + 4M_B^2 M_\pi^2} + \frac{1}{2}\sqrt{\lambda}\cos\theta_{l\pi}} \tag{300}$$

$$\lambda \equiv (q^2 + M_B^2 - M_\pi^2)^2 - 4q^2 M_B^2 \tag{301}$$

where $\theta_{\ell\pi}$ is angle of momentum ℓ and π. Thus integral range of y is

$$\frac{M_B^2 - M_\pi^2 + q^2 - \sqrt{\lambda}}{2M_B^2} \leq y \leq \frac{M_B^2 - M_\pi^2 + q^2 + \sqrt{\lambda}}{2M_B^2}. \tag{302}$$

where a range of $\cos\theta_{l\pi}$ is $[1,\ -1]$. As the result, we can integrate $d\Gamma(B\to\pi\ell\nu)$ over the y and obtain

$$d\Gamma(B\to\pi\ell\nu)=\frac{G_f^2}{192\pi^3 c_\pi^2 M_B^3}|V_{ub}^L+V_{ub}^R|^2[f_+(q^2)]^2\lambda(q^2)^{3/2}dq^2. \tag{303}$$

B.4 $B\to X_u\ell\nu$

We are going to calculate decay rate of $B\to X_u\ell\nu$ in free quark approximation. An amplitude is written as

$$\begin{aligned}A(B\to X_u\ell\nu)=&2\sqrt{2}G_f\langle u\ell^-\bar\nu|(\bar\ell\gamma^\nu P_L W_\nu^-\nu)(\bar u\gamma^\mu(V_{ub}^L P_L+V_{ub}^R P_R)W_\mu^+ b)|b\rangle\\ =&2\sqrt{2}G_f(\bar u_l\gamma_\mu P_L v_\nu)(\bar u_u\gamma^\mu(V_{ub}^L P_L+V_{ub}^R P_R)u_b)\end{aligned} \tag{304}$$

where Eq. (278) is used. Thus squared matrix element $|\mathcal{M}|^2$ is evaluated as following relation,

$$\begin{aligned}|\mathcal{M}|^2=&\frac{1}{2}\sum_s|A(B\to X_u\ell\nu)|^2\\ =&32G_f^2(2(|V_{ub}^L|^2(p_l p_u)(p_\nu p_b)+|V_{ub}^R|^2(p_l p_b)(p_\nu p_u))-(p_l p_\nu)m_u m_b\mathrm{Re}(V_{ub}^L V_{ub}^{R*})).\end{aligned} \tag{305}$$

We calculate product of momentum as

$$p_l p_\nu=\frac{q^2}{2} \tag{306}$$

$$p_u p_\nu=\frac{1}{2}(m_b^2-m_u^2-m_b^2 y) \tag{307}$$

$$p_b p_\nu=\frac{1}{2}(q^2+m_b^2-m_b^2 y-m_u^2) \tag{308}$$

$$p_l p_u=\frac{1}{2}(-q^2+m_b^2 y) \tag{309}$$

where we use definitions, $q^\mu\equiv p_b-p_u=p_\nu+p_l$ and $y\equiv 2p_b p_l/m_b^2$. A phase space dQ is calculated similar to $B\to\pi\ell\nu$ as

$$dQ=\frac{1}{128\pi^3}dq^2dy. \tag{310}$$

Thus deferential decay rate $d\Gamma(b \to u\ell\nu)$ is evaluated as

$$\begin{aligned} d\Gamma(b \to u\ell\nu) =& \frac{1}{2M_B} 16 G_f^2 (|V_{ub}^R|^2(-q^2 + m_b^2 y)(q^2 + m_b^2 - m_b^2 y - m_u^2) \\ &+ |V_{ub}^L|^2 (m_b^2 y)(m_b^2 - m_u^2 - m_b^2 y) - q^2 m_u m_b \mathrm{Re}(V_{ub}^L V_{ub}^{R*})) \frac{1}{128\pi^3} dq^2 dy. \end{aligned} \tag{311}$$

An integration ranges of y and q^2 are presented as

$$0 \leq q^2 \leq \frac{(1-y-\rho)y}{1-y} m_b^2 \tag{312}$$

$$0 \leq y \leq 1 - \rho \tag{313}$$

where ρ is m_u^2/m_b^2. In the result, we obtain following equations,

$$\frac{d\Gamma(B \to X_u \ell\nu)}{dy} = \frac{G_F^2 m_b^5}{32\pi^3 M_B} [-2\sqrt{\rho}\mathrm{Re}(V_{ub}^L V_{ub}^{R^*}) \frac{y^2(1-\rho-y)^2}{2(1-y)^2} \tag{314}$$

$$+ |V_{ub}^L|^2 \frac{y^2(1-\rho-y)^2(3+\rho(3-y)-5y+2y^2)}{6(1-y)^3} \tag{315}$$

$$+ |V_{ub}^R|^2 \frac{y^2(1-\rho-y)^2}{(1-y)}] \tag{316}$$

$$\begin{aligned} \Gamma(B \to X_u \ell\nu) =& \frac{G_f^2 m_b^5}{384\pi^3 M_B} [(|V_{ub}^L|^2 + |V_{ub}^R|^2)(1 - 8\rho + 8\rho^3 - \rho^4 - 12\rho^2 \log\rho) \\ &- 4\mathrm{Re}(V_{ub}^L V_{ub}^{R*})\sqrt{\rho}(1 + 6\rho - 6\rho^2 - \rho^3 + 6(\rho+1)\rho\log\rho)]. \end{aligned} \tag{317}$$

B.5 $B \to \rho\ell\nu, \omega\ell\nu$

We are going to calculate decay rate of $B \to \rho\ell\nu$. In the case of $B \to \omega\ell\nu$, it is same how to calculate, so we deal with only $B \to \rho\ell\nu$. The amplitude of $B \to \rho\ell\nu$ is

$$\begin{aligned} A(B \to \rho\ell\nu) =& -i2\sqrt{2}G_f \langle \ell^- \bar{\nu}|(\bar{\ell}\gamma^\mu P_L \nu)|0\rangle \langle \rho|(\bar{u}\gamma_\mu \left(V_{ub}^L P_L + V_{ub}^R P_R\right) b)|\bar{B}\rangle \\ =& -i2\sqrt{2}G_f c_\rho^{-1} \langle \ell^- \bar{\nu}|(\bar{\ell}\gamma^\mu P_L \nu)|0\rangle \\ &\times \left(\frac{-V_{ub}^L + V_{ub}^R}{2} \left((M_B + M_\rho) A_1(q^2) \epsilon(P_\rho, \lambda_\rho)_\mu^* - \frac{A_2(q^2)}{M_B + M_\rho} (q\epsilon(P_\rho, \lambda_\rho)^*)(P_B + P_\rho)_\mu \right.\right. \\ &\left.\left. - (q\epsilon(P_\rho, \lambda_\rho)^*) \frac{2M_\rho}{q^2} A_3(q^2) q_\mu \right) + \frac{V_{ub}^L + V_{ub}^R}{2} \frac{2iV(q^2)}{M_B + M_\rho} \epsilon_{\mu\nu\eta\sigma} P_B^\nu P_\rho^\eta \epsilon(P_\rho, \lambda_\rho)^{*\sigma} \right) \end{aligned} \tag{318}$$

where we use Eqs. (256, 257), c_{ρ^+} is 1 and c_{ρ^0} and c_ω is $\sqrt{2}$. A term that is proportional to q^μ does not affect, so we calculate the amplitude as

$$\begin{aligned}A(B\to\rho\ell\nu) &= -i2\sqrt{2}G_f c_\rho^{-1}\langle\ell^-\bar\nu|(\bar\ell\gamma^\mu P_L\nu)|0\rangle \\ &\times\left(\frac{-V_{ub}^L+V_{ub}^R}{2}\left((M_B+M_\rho)A_1(q^2)\epsilon(P_\rho,\lambda_\rho)^*_\mu - \frac{2A_2(q^2)}{M_B+M_\rho}(q\epsilon(P_\rho,\lambda_\rho)^*)P_{B\mu}\right)\right. \\ &\left.+\frac{V_{ub}^L+V_{ub}^R}{2}\frac{2iV(q^2)}{M_B+M_\rho}\epsilon_{\mu\nu\eta\sigma}P_B^\nu P_\rho^\eta\epsilon(P_\rho,\lambda_\rho)^{*\sigma}\right). \qquad (319)\end{aligned}$$

We divide amplitude into W boson helicity λ_W. In off-shell, there is a following relation,

$$g_{\mu\nu} = \sum_{\lambda_W}\eta_{\lambda_W}\epsilon(q,\lambda_W)^*_\mu\epsilon(q,\lambda_W)_\nu \qquad \eta_{\lambda_W} = \begin{cases} -1 & \lambda_W = 0,\pm \\ 1 & \lambda_W = s\end{cases} \qquad (320)$$

with W boson polarized vector $\epsilon(q,\lambda_W)_\mu$. Thus we calculate $\{(\text{lepton part})\times\epsilon(q,\lambda_W)^{*\mu}\}$ and $\{\epsilon(q,\lambda_W)^\mu\times(\text{hadron part})\}$ separately.

At first, we calculate leptonic part. In the rest frame of W boson, momentum vectors are presented as

$$\begin{aligned}q^\mu &= (\sqrt{q^2},0,0,0) && (321)\\ P_B^\mu &= (E_B,0,0,p_B) && (322)\\ P_\rho^\mu &= (E'_\rho,0,0,p'_\rho) && (323)\\ P_l^\mu &= \frac{\sqrt{q^2}}{2}(1,\sin\theta,0,\cos\theta) && (324)\\ P_\nu^\mu &= \frac{\sqrt{q^2}}{2}(1,-\sin\theta,0,-\cos\theta) && (325)\\ \epsilon(q,\pm)^{*\mu} &= \mp\frac{1}{\sqrt{2}}(0,1,\pm i,0) && (326)\\ \epsilon(q,0)^{*\mu} &= (0,0,0,-1) && (327)\\ \epsilon(q,s)^{*\mu} &= (1,0,0,0). && (328)\end{aligned}$$

Hence we calculate leptonic part as follow,

$$\begin{aligned}&\langle\ell^-\bar\nu|\bar\ell\gamma_\mu P_L\nu|0\rangle\epsilon(q,\lambda_W)^{*\mu} \\ &= (\omega(P_l)_{\lambda_l}\xi(P_l)^*_{\lambda_l}\quad \omega(P_l)_{-\lambda_l}\xi(P_l)^*_{\lambda_l})\begin{pmatrix}0 & \sigma_{+\mu}\\ \sigma_{-\mu} & 0\end{pmatrix}\begin{pmatrix}0&0\\0&1\end{pmatrix}\begin{pmatrix}-\omega(P_\nu)_{\lambda_\nu}\xi(P_\nu)_{\lambda_\nu}\\ \omega(P_\nu)_{-\lambda_\nu}\xi(P_\nu)_{-\lambda_\nu}\end{pmatrix}\epsilon(q,\lambda_W)^{*\mu} \\ &= \omega(P_l)_{\lambda_l}\xi(P_l)^*_{\lambda_l}\sigma_{+\mu}\omega(P_\nu)_{-\lambda_\nu}\xi(P_\nu)_{-\lambda_\nu}\epsilon(q,\lambda_W)^{*\mu} \qquad (329)\end{aligned}$$

with $\xi_+ = \begin{pmatrix} \cos\frac{\theta}{2} \\ \sin\frac{\theta}{2} \end{pmatrix}$, $\xi_- = \begin{pmatrix} -\sin\frac{\theta}{2} \\ \cos\frac{\theta}{2} \end{pmatrix}$, $\sigma^\mu_\pm = (1, \pm\sigma_i)$, $\omega_\pm(p) = \sqrt{E \pm |\vec{p}|}$. Since ℓ, ν masses are 0, ω is calculated as

$$\omega(P_l)_\pm = \omega(P_\nu)_\pm = \begin{cases} (q^2)^{1/4} & + \\ 0 & - \end{cases} . \tag{330}$$

Therefore we calculate leptonic part as

$$\begin{aligned} \langle \ell^- \bar{\nu} | \bar{\ell} \gamma_\mu P_L \nu | 0 \rangle \epsilon(q, \lambda_W)^{*\mu} &= \sqrt{q^2} \xi(P_l)^*_- \sigma_{+\mu} \xi(P_\nu)_- \epsilon(q, \lambda_W)^{*\mu} \\ &= \sqrt{q^2}(0, -\cos\theta, -i, \sin\theta)\epsilon(q, \lambda_W)^{*\mu} \\ &= \begin{cases} -\sqrt{\frac{q^2}{2}}(1 \mp \cos\theta) = L_\pm & \lambda_W = \pm \\ -\sqrt{q^2}\sin\theta = L_0 & \lambda_W = 0 \\ 0 & \lambda_W = s \end{cases} . \end{aligned} \tag{331}$$

Next, we calculate hadronic part. In the rest frame of B meson, momentum vectors are presented as

$$P_B^\mu = (M_B, 0, 0, 0) \tag{332}$$

$$P_\rho^\mu = (E_\rho, 0, 0, p_\rho) \tag{333}$$

$$\epsilon(q, \pm) = \mp\frac{1}{\sqrt{2}}(0, 1, \mp i, 0) \tag{334}$$

$$\epsilon(q, 0)^\mu = \frac{1}{\sqrt{q^2}}(p_\rho, 0, 0, -M_B + E_\rho) \tag{335}$$

$$\epsilon(q, s)^\mu = \frac{1}{\sqrt{q^2}} q^\mu \tag{336}$$

$$\epsilon(P_\rho, \pm)^{*\mu} = \mp\frac{1}{\sqrt{2}}(0, 1, \pm i, 0) \tag{337}$$

$$\epsilon(P_\rho, 0)^{*\mu} = \frac{1}{M_\rho}(p_\rho, 0, 0, E_\rho). \tag{338}$$

If λ_W is s, leptonic part is 0. Hence we evaluate vector product with $\lambda_W = \pm$ or 0 and list as follow.

- $\lambda_W = \pm$

$$\epsilon(q, \pm)^\mu \epsilon(P_\rho, \lambda_\rho)^*_\mu = \begin{cases} -1 & \lambda_W = \lambda_\rho \\ 0 & \lambda_\rho \neq \lambda_W \end{cases} \tag{339}$$

$$\epsilon(q, \pm)^\mu P_{B\mu} = 0 \tag{340}$$

$$\epsilon(q, \pm)^\mu \epsilon_{\mu\nu\eta\sigma} P_B^\nu P_\rho^\eta \epsilon(P_\rho, \lambda_\rho)^{*\sigma} = \begin{cases} \pm i M_B p_\rho & \lambda_W = \lambda_\rho = \pm \\ 0 & \lambda_W \neq \lambda_\rho \end{cases} \tag{341}$$

- $\lambda_W = 0$

$$\epsilon(q,0)^\mu \epsilon(P_\rho,\lambda_\rho)^*_\mu = \begin{cases} \dfrac{E_\rho M_B - M_\rho^2}{\sqrt{q^2} M_\rho} & \lambda_W = \lambda_\rho = 0 \\ 0 & \lambda_W \neq \lambda_\rho \end{cases} \tag{342}$$

$$\epsilon(q,0)^\mu P_{B\mu} = \frac{M_B p_\rho}{\sqrt{q^2}} \tag{343}$$

$$\epsilon(q,0)^\mu \epsilon_{\mu\nu\eta\sigma} P_B^\nu P_\rho^\eta \epsilon(P_\rho,\lambda_\rho)^{*\sigma} = 0 \tag{344}$$

Thus we evaluate hadronic part with $\lambda_W = \pm$ and $\lambda_W = 0$, $H_\pm/2$ and $-H_0/2$, and obtain as follow,

$$\frac{1}{2}H_\pm = \left(\frac{V_{ub}^L - V_{ub}^R}{2}(M_B + M_\rho) A_1(q^2) \mp \frac{V_{ub}^L + V_{ub}^R}{2} \frac{2M_B p_\rho}{M_B + M_\rho} V(q^2) \right) \tag{345}$$

$$-\frac{1}{2}H_0 = -\frac{V_{ub}^L - V_{ub}^R}{2} \frac{M_B + M_\rho}{2\sqrt{q^2} M_\rho} \left((M_B^2 - M_\rho^2 - q^2) A_1(q^2) - \frac{4M_B^2 p_\rho^2}{(M_B + M_\rho)^2} A_2(q^2) \right). \tag{346}$$

Next, we calculate phase space dQ. dQ is $dq^2 dy/(128\pi^3)$ as same as $B \to \pi \ell \nu$. We translate y into $\cos\theta$ as

$$dy = d\left(\frac{2P_l P_B}{M_B^2} \right) = \frac{p_B \sqrt{q^2}}{M_B^2} d\cos\theta = \frac{\sqrt{\Omega_+ \Omega_-}}{2M_B^2} d\cos\theta \tag{347}$$

$$\Omega_\pm = (M_B \pm M_\rho)^2 - q^2, \tag{348}$$

and we obtain dQ as

$$dQ = \frac{1}{256\pi^3} \frac{\sqrt{\Omega_+ \Omega_-}}{M_B^2} dq^2 d\cos\theta. \tag{349}$$

For these calculation, differential decay rate is

$$\begin{aligned} d\Gamma &= \sum_{\lambda_l, \lambda_\rho} \frac{1}{2E_B} |\mathcal{M}^{\lambda_l}_{\lambda_\rho}|^2 dQ \\ \frac{d\Gamma}{dq^2 d\cos\theta} &= \frac{G_f^2 \sqrt{\Omega_+ \Omega_-} q^2}{256\pi^3 c_\rho^2 M_B^3} \left(|H_0|^2 \sin^2\theta + |H_+|^2 \frac{(1-\cos\theta)^2}{2} + |H_-|^2 \frac{(1+\cos\theta)^2}{2} \right) \\ &= \frac{G_f^2 p_\rho q^2}{128\pi^3 c_\rho^2 M_B^2} \left(|H_0|^2 \sin^2\theta + |H_+|^2 \frac{(1-\cos\theta)^2}{2} + |H_-|^2 \frac{(1+\cos\theta)^2}{2} \right) \end{aligned} \tag{350}$$

with $\mathcal{M}^{\lambda_l}_{\lambda_\rho} = -i2\sqrt{2}G_f c_\rho^{-1} \sum_{\lambda_W} L^{\lambda_l}_{\lambda_W} H^{\lambda_\rho}_{\lambda_W}$. p_ρ is 3-dimension momentum of ρ in the rest frame of B meson. We integrate it from $\cos\theta = -1$ to 1 and obtain following relation,

$$\frac{d\Gamma}{dq^2} = \frac{G_f^2 p_\rho q^2}{96\pi^3 c_\rho^2 M_B^2} \left(|H_0|^2 + |H_+|^2 + |H_-|^2\right). \tag{351}$$

After CP transforming, H_+ and H_- are exchanged each other by Eq. (341). However After integrating $\cos\theta$, decay rate is not affected.

App. C Renormalization for hadronic decays

Four quark operators are renormalized by QCD interaction [32]. An effective Hamiltonian is written as

$$\mathcal{H}_{\rm eff} = \frac{G_f}{\sqrt{2}} V_{ij} V_{lk}^* \sum_m C_m^{(0)} \mathcal{O}_m^{(0)} \tag{352}$$

$$\mathcal{O}_m^{(0)} = (\bar{u}_i^{(0)} d_j^{(0)} \bar{d}_k^{(0)} u_l^{(0)})_m \tag{353}$$

where $u^{(0)}$, $d^{(0)}$, $\mathcal{O}_m^{(0)}$ and $C_m^{(0)}$ are bare up-type and down-type quark field, four Fermi operator and Wlison coefficient respectively. The subscript m indicates combinations of color and chiral structure, and the subscript i, j, k and l show generations. Here we introduce field and operator renormalizations as

$$q^{(0)} \equiv Z_2^{1/2} q \qquad (q = u,\ d) \tag{354}$$

$$\mathcal{O}_i^{(0)} = Z_{ij} \mathcal{O}_j \tag{355}$$

where Z_2 and Z_{ij} are divergent. We evaluate the matrix element (amputated Green function) of $\mathcal{O}_m^{(0)}$ in QCD 1-loop level and find the following relation,

$$\langle \mathcal{O}_i^{(0)} \rangle = Z_2^{-2} Z_{ij} \langle \mathcal{O}_j \rangle. \tag{356}$$

We define renormalized Wilson coefficients, C_m, so that

$$\sum_m C_m^{(0)} \mathcal{O}_m^{(0)} = \sum_m C_m(\mu) \mathcal{O}_m(\mu) \tag{357}$$

where μ is the renormalization scale. Renormalization constants of Wilson coefficients Z_{ij}^c are defined by

$$C_i^{(0)} \equiv Z_{ij}^c C_j. \tag{358}$$

From Eq. (357), we obtain

$$Z_{ij}^c = Z_{ji}^{-1}. \tag{359}$$

Since the left-hand side of Eq. (358) does not depend on energy scale μ, we obtain the following renormalization group equation,

$$\frac{d}{d \ln \mu} C_k = \sum_j \gamma_{jk} C_j \tag{360}$$

where the anomalous dimension matrix γ_{ij} is given by

$$\gamma_{jk} = -\sum_i {Z^c_{ki}}^{-1} \left(\frac{d}{d\ln\mu} Z^c_{ij} \right) \tag{361}$$

$$= \sum_i {Z_{ji}}^{-1} \left(\frac{d}{d\ln\mu} Z_{ik} \right). \tag{362}$$

As we will show, at the 1-loop level, the μ dependence of $\gamma_{ij}(\mu)$ is factorized as follows,

$$\gamma_{ij}(\mu) \equiv \bar{\gamma}(\mu)\tilde{\gamma}_{ij}. \tag{363}$$

Then we can diagonalize $\tilde{\gamma}_{ij}$,

$$a_i \delta_{ij} \equiv U^{-1}_{ik} \left(\tilde{\gamma}^T\right)_{kl} U_{lj} \tag{364}$$

where U_{ij} is unitary matrix. The Wilson coefficient $\tilde{C}_i$ in the diagonal basis,

$$\tilde{C}_i \equiv \sum_j U^{-1}_{ij} C_j(\mu). \tag{365}$$

satisfies the following renormalization group equation (RGE),

$$\mu \frac{d}{d\mu} \tilde{C}_i(\mu) = a_i \bar{\gamma}(\mu) \tilde{C}_i(\mu). \tag{366}$$

The solution is

$$\tilde{C}_i(\mu) = \exp\left(a_i \int_{g_s(m)}^{g_s(\mu)} dg_s \frac{1}{\beta(g_s)} \bar{\gamma}(\mu) \right) \tilde{C}_i(m) \tag{367}$$

where the beta function $\beta(g_s)$ is given by

$$\beta(g_s) = \mu \frac{dg_s}{d\mu} = -\frac{g_s^3}{16\pi^2} \left(11 - \frac{2}{3} N_f \right), \tag{368}$$

and N_f is the number of flavors. The running coupling constant $g_s(\mu)$ is the solution of equation Eq. (368).

Next, we calculate Z_2. The 1-loop Feynman diagram for kinematic term of fermion $\bar{\psi}\partial\!\!\!/\psi$ is shown in Fig. 20 and this contribution r_ψ in $R\xi$ gauge is calculated as following equations,

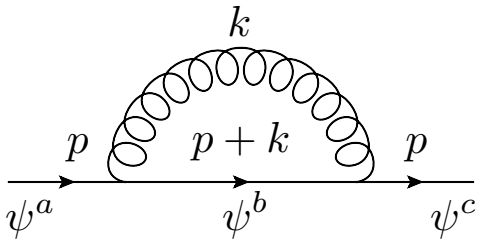

Fig.20 1-loop diagram of fermion field.

$$r_\psi = \mu^\epsilon \int \frac{d^n k}{(2\pi)^n} \frac{i}{\not p} i g_s T^A_{cb} \gamma^\mu i \frac{\not p + \not k}{(p+k)^2} i g_s T^A_{ba} \gamma^\nu \frac{i}{\not p} \frac{-i}{k^2} (g_{\mu\nu} - (1-\xi) k_\mu k_\nu / k^2) \quad (369)$$

$$= \frac{4}{3} \mu^\epsilon g_s^2 \delta_{ca} \frac{1}{\not p} (\gamma^\mu \gamma^\rho \gamma^\nu) \frac{1}{\not p} I_{\mu\nu\rho} \quad (370)$$

$$I_{\mu\nu\rho} \equiv \int \frac{d^n k}{(2\pi)^n} \frac{(p+k)_\rho}{(p+k)^2} \frac{1}{k^2} (g_{\mu\nu} - (1-\xi) k_\mu k_\nu / k^2) \quad (371)$$

$$\gamma^\mu \gamma^\rho \gamma^\nu = g^{\mu\rho}\gamma^\nu + g^{\nu\rho}\gamma^\mu - g^{\mu\nu}\gamma^\rho - i\epsilon^{\mu\rho\nu\eta}\gamma^5\gamma_\eta \quad (372)$$

$$T^A_{ca} T^A_{db} = \frac{1}{2}(\delta_{cb}\delta_{da} - \delta_{ca}\delta_{db}/3) \quad (373)$$

where a, b and c are color indices, T^A_{ab} is generator of SU(3) and $n = 4 - \epsilon$ is spacetime dimension. In minimal subtraction scheme, we use only divergent part. The divergent part of $I_{\mu\nu\rho}$, $I^{\rm div}_{\mu\nu\rho}$, is calculated as follow,

$$I^{\rm div}_{\mu\nu\rho} = \frac{i}{8\pi^2\epsilon} \left[\left(g_{\mu\nu} p_\rho \frac{1}{2} \right) + \frac{1}{2}(\xi - 1)[\frac{1}{3} g_{\mu\nu} p_\rho - \frac{1}{6} g_{\mu\rho} p_\nu - \frac{1}{6} g_{\nu\rho} p_\mu] \right]. \quad (374)$$

The divergent part of r_ψ, $r^{\rm div}_\psi$, is written as

$$r^{\rm div}_\psi = \frac{g_s^2 \xi}{6\pi^2\epsilon} \delta_{ca} \frac{i}{\not p}. \quad (375)$$

As the result, Z_2 is obtained as following equation,

$$Z_2 = 1 - \frac{g_s^2 \xi}{6\pi^2\epsilon} + O(g_2^4). \quad (376)$$

In the following subsection, we calculate QCD 1-loop diagrams in each case of $b_L \to u_L \bar{c}_L s_L$, $b_L \to u_L \bar{u}_L d_L$ and $b_R \to u_R \bar{c}_L s_L$ and obtain $C_i(m_b)$.

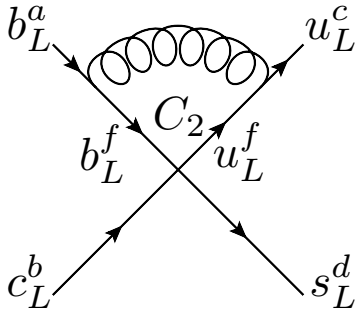

Fig.21

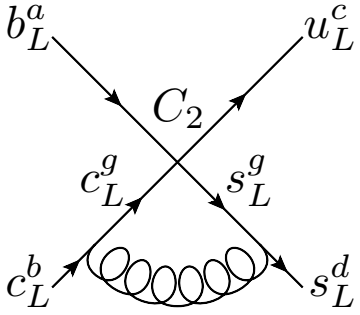

Fig.22

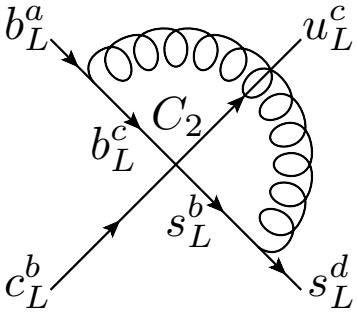

Fig.23

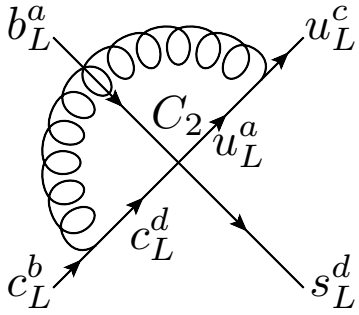

Fig.24

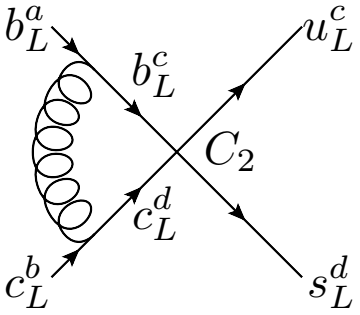

Fig.25

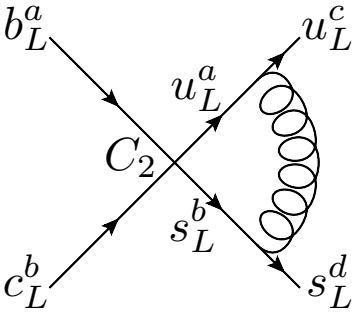

Fig.26

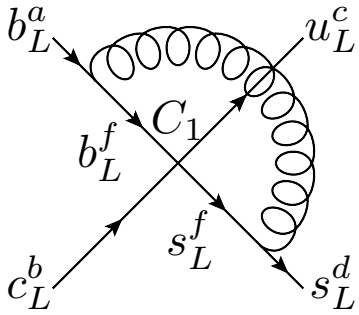

Fig.27

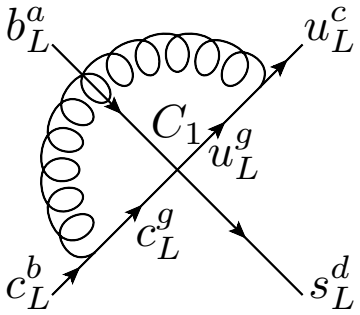

Fig.28

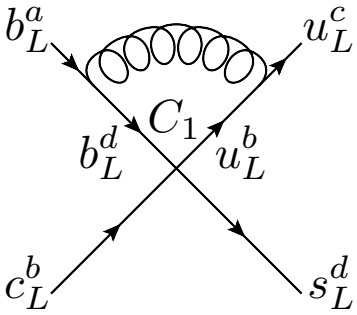

Fig.29

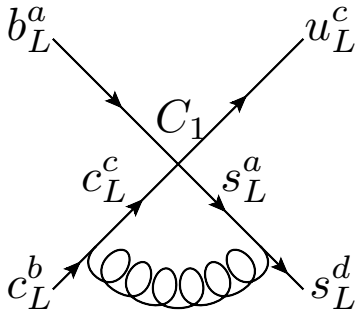

Fig.30

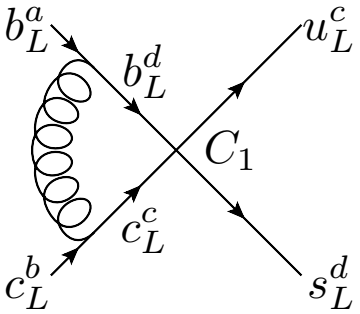

Fig.31

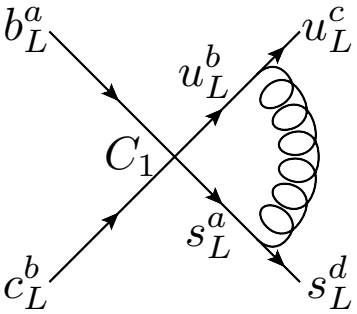

Fig.32

C.1 $b_L \to u_L \bar{c}_L s_L$

For $b_L \to u_L \bar{c}_L s_L$, the following two operators contribute:

$$\mathcal{O}_1 = (\bar{u}^a \gamma^\mu P_L b^b)(\bar{s}^b \gamma_\mu P_L c^a) \tag{377}$$

$$\mathcal{O}_2 = (\bar{u}^a \gamma^\mu P_L b^a)(\bar{s}^b \gamma_\mu P_L c^b). \tag{378}$$

All QCD 1-loop Feynman diagrams are shown in Figs. 21 - 32. We define $r_{ij}^{(k)}$ as the coefficient of $\mathcal{O}_i$ obtained with Feynman diagram Fig. k that arises from $\mathcal{O}_j$ and $r_{ij}^{(k)\mathrm{div}}$ as the divergent part of $r_{ij}^{(k)}$. Then the renormalization constant Z_{ij} is expressed by $Z_{ij}/Z_2^2 = 1 + \sum_k r_{ij}^{(k)\mathrm{div}}$. The coefficient $r_{ij}^{(21)\mathrm{div}}$ is calculated as following equations,

$$r_{i2}^{(21)} \mathcal{O}_i = \mu^\epsilon \int \frac{d^n k}{(2\pi)^n} \left(\bar{u}_L^c i g_s T_{cf}^A \gamma^\nu i \frac{\not{k} + m_u}{k^2 - m_u^2} \gamma^\mu i \frac{\not{k} + m_b}{k^2 - m_b^2} i g_s T_{fa}^A \gamma^\rho b_L^a \right) (\bar{s}_L^b \gamma_\mu c_L^b) \times \frac{-i}{k^2} \left(g_{\nu\rho} - (1-\xi) \frac{k_\nu k_\rho}{k^2} \right) \tag{379}$$

$$r_{i2}^{(21)\mathrm{div}} \mathcal{O}_i = \frac{g_s^2}{6\pi^2 \epsilon} \xi \mathcal{O}_2 \tag{380}$$

Thus we obtain $r_{ij}^{(21)\mathrm{div}}$ as follow,

$$r_{ij}^{(21)\mathrm{div}} = \begin{cases} \dfrac{g_s^2 \xi}{6\pi^2 \epsilon} & i = j = 2 \\ 0 & \text{otherwise} \end{cases} . \tag{381}$$

We calculate similarly $r_{ij}^{(22)\mathrm{div}}$, $r_{ij}^{(27)\mathrm{div}}$ and $r_{ij}^{(28)\mathrm{div}}$ and obtain following equation,

$$r_{ij}^{(21)\mathrm{div}} + r_{ij}^{(22)\mathrm{div}} + r_{ij}^{(27)\mathrm{div}} + r_{ij}^{(28)\mathrm{div}} = \frac{g_s^2 \xi}{3\pi^2 \epsilon}. \tag{382}$$

$r_{ij}^{(23)\mathrm{div}}$ is calculated as following equations,

$$r_{i2}^{(23)}\mathcal{O}_i =\mu^\epsilon \int \frac{d^n k}{(2\pi)^n} \left(\bar{u}_L^c \gamma^\mu i \frac{\not{k} - m_b}{k^2 - m_b^2} i g_s T_{ca}^A \gamma^\nu b_L^a\right) \left(\bar{s}_L^d i g_s T_{db}^A \gamma^\rho i \frac{\not{k} - m_s}{k^2 - m_s^2} \gamma_\mu c_L^b\right) \times \frac{-i(g_{\nu\rho} - (1-\xi)k_\nu k_\rho/k^2)}{k^2} \tag{383}$$

$$r_{i2}^{(23)\mathrm{div}}\mathcal{O}_i = - i g_s^2 T_{ca}^A T_{db}^A \left(\bar{u}_L^c \gamma^\mu \gamma^\sigma \gamma^\nu b_L^a\right) \left(\bar{s}_L^d \gamma^\rho \gamma^\delta \gamma_\mu c_L^b\right) I_{\sigma\delta\nu\rho} \tag{384}$$

$$I_{\sigma\delta\nu\rho} \equiv \int \frac{d^n k}{(2\pi)^n} \frac{k_\sigma k_\delta (g_{\nu\rho} - (1-\xi)k_\nu k_\rho/k^2)}{(k^2)^3} \tag{385}$$

$$= \frac{i}{8\pi^2\epsilon}(g_{\sigma\delta} g_{\nu\rho}/4 - (1-\xi) g_{\sigma\delta\nu\rho}/24) \tag{386}$$

$$g_{\sigma\delta\nu\rho} \equiv g_{\sigma\delta} g_{\nu\rho} + g_{\sigma\nu} g_{\rho\delta} + g_{\sigma\rho} g_{\nu\delta}. \tag{387}$$

The $r_{ij}^{(24)\mathrm{div}}$, $r_{ij}^{(25)\mathrm{div}}$ and $r_{ij}^{(26)\mathrm{div}}$ are evaluated as following equations,

$$r_{i2}^{(24)\mathrm{div}}\mathcal{O}_i = - i g_s^2 T_{ca}^A T_{db}^A \left(\bar{u}_L^c \gamma^\nu \gamma^\sigma \gamma^\mu b_L^a\right) \left(\bar{s}_L^d \gamma_\mu \gamma^\delta \gamma^\rho c_L^b\right) I_{\sigma\delta\nu\rho} \tag{388}$$

$$r_{i2}^{(25)\mathrm{div}}\mathcal{O}_i = i g_s^2 T_{ca}^A T_{db}^A \left(\bar{u}_L^c \gamma^\mu \gamma^\sigma \gamma^\nu b_L^a\right) \left(\bar{s}_L^d \gamma_\mu \gamma^\delta \gamma^\rho c_L^b\right) I_{\sigma\delta\nu\rho} \tag{389}$$

$$r_{i2}^{(26)\mathrm{div}}\mathcal{O}_i = i g_s^2 T_{ca}^A T_{db}^A \left(\bar{u}_L^c \gamma^\nu \gamma^\sigma \gamma^\mu b_L^a\right) \left(\bar{s}_L^d \gamma^\rho \gamma^\delta \gamma_\mu c_L^b\right) I_{\sigma\delta\nu\rho} \tag{390}$$

by similar calculations. Their sum is obtained as follow,

$$\begin{aligned}
&(r_{i2}^{(23)\mathrm{div}} + r_{i2}^{(24)\mathrm{div}} + r_{i2}^{(25)\mathrm{div}} + r_{i2}^{(26)\mathrm{div}})\mathcal{O}_i \\
=& i g_s^2 T_{ca}^A T_{db}^A \left(\bar{u}_L^c (\gamma^\mu \gamma^\sigma \gamma^\nu - \gamma^\nu \gamma^\sigma \gamma^\mu) b_L^a\right) \left(\bar{s}_L^d (\gamma_\mu \gamma^\delta \gamma^\rho - \gamma^\rho \gamma^\delta \gamma_\mu) c_L^b\right) I_{\sigma\delta\nu\rho} \qquad (391)\\
=& - \frac{g_s^2}{8\pi^2\epsilon}(3\mathcal{O}_1 - \mathcal{O}_2). \qquad (392)
\end{aligned}$$

Moreover we obtain following result about $r_{i1}^{(29)\mathrm{div}}$, $r_{i1}^{(30)\mathrm{div}}$, $r_{i1}^{(31)\mathrm{div}}$ and $r_{i1}^{(32)\mathrm{div}}$ by similar calculation,

$$(r_{i1}^{(29)\mathrm{div}} + r_{i1}^{(30)\mathrm{div}} + r_{i1}^{(31)\mathrm{div}} + r_{i1}^{(32)\mathrm{div}})\mathcal{O}_i = -\frac{g_s^2}{8\pi^2\epsilon}(3\mathcal{O}_2 - \mathcal{O}_1). \tag{393}$$

As the result, Z_{ij} for $b_L \to u_L \bar{c}_L s_L$ is written as follow,

$$Z_{ij}/Z_2^2 = 1 + \frac{g_s^2}{3\pi^2\epsilon} - \frac{g_s^2}{8\pi^2\epsilon} \begin{pmatrix} -1 & 3 \\ 3 & -1 \end{pmatrix} + O(g^4) \tag{394}$$

$$Z_{ij} = 1 - \frac{g_s^2}{8\pi^2\epsilon} \begin{pmatrix} -1 & 3 \\ 3 & -1 \end{pmatrix} + O(g^4). \tag{395}$$

Thus γ_{ij} is obtained as

$$\gamma_{ij} = Z_{ij}^{-1}\mu\frac{d}{d\mu}Z_{ij} \tag{396}$$

$$= \frac{g_s^2}{8\pi^2}\begin{pmatrix} -1 & 3 \\ 3 & -1 \end{pmatrix} + O(g_s^4) \tag{397}$$

using following relations, $g_s(\mu) = \mu^{-\epsilon/2}Z_g(\mu)g_s^{(0)}$ and $dZ_g(\mu)/d\mu \propto O(g^3)$. Finally, we obtain the following solution of RGE,

$$C_1(m_b) = (\tilde{C}_+(m_b) + \tilde{C}_-(m_b)) \tag{398}$$

$$= \frac{1}{2}\left(\left(\frac{\alpha_s(m_b)}{\alpha_s(m_W)}\right)^{-6/23} - \left(\frac{\alpha_s(m_b)}{\alpha_s(m_W)}\right)^{12/23}\right) = -0.27 \tag{399}$$

$$C_2(m_b) = (\tilde{C}_+(m_b) - \tilde{C}_-(m_b)) \tag{400}$$

$$= \frac{1}{2}\left(\left(\frac{\alpha_s(m_b)}{\alpha_s(m_W)}\right)^{-6/23} + \left(\frac{\alpha_s(m_b)}{\alpha_s(m_W)}\right)^{12/23}\right) = 1.12 \tag{401}$$

where

$$\alpha_s(m_W) = 0.12, \qquad \alpha_s(m_b) = 0.23 \tag{402}$$

$$C_1(m_W) = 0, \qquad C_2(m_W) = 1 \tag{403}$$

are used.

C.2 $b_R \to u_R\bar{c}_L s_L$

For $b_R \to u_R\bar{c}_L s_L$, following operators,

$$\mathcal{O}_{1R} = (\bar{u}^\alpha\gamma^\mu P_R b^\beta)(\bar{s}^\beta\gamma_\mu P_L c^\alpha) \tag{404}$$

$$\mathcal{O}_{2R} = (\bar{u}^\alpha\gamma^\mu P_R b^\alpha)(\bar{s}^\beta\gamma_\mu P_L c^\beta), \tag{405}$$

arise. The Feynman diagrams are obtained with changing $b_L \to b_R$ and $u_L \to u_R$ in those of $b_L \to u_L\bar{c}_L s_L$. By similar calculation to $b_L \to u_L\bar{c}_L s_L$, we obtain following equations,

$$(r_{i2}^{(21)\mathrm{div}} + r_{i2}^{(22)\mathrm{div}})\mathcal{O}_i = \frac{g_s^2\xi}{3\pi^2\epsilon}\mathcal{O}_2 \tag{406}$$

$$(r_{i2}^{(23)\mathrm{div}} + r_{i2}^{(24)\mathrm{div}} + r_{i2}^{(25)\mathrm{div}} + r_{i2}^{(26)\mathrm{div}})\mathcal{O}_i$$

$$= i\mu^\epsilon g_s^2 T^A_{ca}T^A_{db}\left(\bar{u}_R^c 2i\epsilon^{\mu\sigma\nu\eta}\gamma^5\gamma_\eta b_R^a\right)\left(\bar{s}_L^d 2i\epsilon_\mu{}^{\delta\rho\alpha}\gamma^5\gamma_\alpha c_L^b\right) I_{\sigma\delta\nu\rho} \tag{407}$$

$$= -\frac{g_s^2}{8\pi^2\epsilon}(-3\mathcal{O}_2 + \mathcal{O}_1). \tag{408}$$

The sign of Eq. (408) differs from Eq. (393) in $b_L \to u_L \bar{c}_L s_L$ because of γ_5 behavior. Next, we calculate $r_{ij}^{(27)\mathrm{div}}$ and obtain

$$\begin{aligned} r_{i1}^{(27)}\mathcal{O}_i =& \mu^\epsilon \int \frac{d^n k}{(2\pi)^n} \left(\bar{u}_R^b \gamma^\mu i \frac{\not{k} - m_b}{k^2 - m_b^2} i g_s \gamma^\nu T_{fa}^A b_R^a \right) \\ & \times \left(\bar{d}_L^d i g_s \gamma^\rho T_{df}^A i \frac{\not{k} - m_d}{k^2 - m_d^2} \gamma_\mu c_L^b \right) \frac{-i}{k^2} \left(g_{\nu\rho} - (1-\xi)\frac{k_\nu k_\rho}{k^2} \right) \end{aligned} \tag{409}$$

$$r_{i1}^{(27)\mathrm{div}}\mathcal{O}_i = \frac{g_s^2(1+\xi/3)}{2\pi^2\epsilon}\mathcal{O}_{1R} \tag{410}$$

and also we obtain following equation,

$$r_{i1}^{(28)\mathrm{div}}\mathcal{O}_i = \frac{g_s^2(1+\xi/3)}{2\pi^2\epsilon}\mathcal{O}_{1R} \tag{411}$$

by the similar calculation. $r_{ij}^{(29)\mathrm{div}}$ is calculated as

$$\begin{aligned} r_{i1}^{(29)}\mathcal{O}_i =& \mu^\epsilon \int \frac{d^n k}{(2\pi)^n} \left(\bar{u}_R^c i g_s \gamma^\nu T_{cb}^A i \frac{\not{k} - m_u}{k^2 - m_u^2} \gamma^\mu i \frac{\not{k} - m_b}{k^2 - m_b^2} i g_s \gamma^\rho T_{da}^A b_R^a \right) \left(\bar{d}_L^d \gamma_\mu c_L^b \right) \\ & \times \frac{-i}{k^2} \left(g_{\nu\rho} - (1-\xi)\frac{k_\nu k_\rho}{k^2} \right) \end{aligned} \tag{412}$$

$$r_{i1}^{(29)\mathrm{div}}\mathcal{O}_i = \frac{g_s^2 \xi}{8\pi^2\epsilon} T_{cb}^A T_{da}^A \left(\bar{u}_R^c \gamma^\mu b_R^a \right) \left(\bar{d}_L^d \gamma_\mu c_L^b \right) \tag{413}$$

and similarly we obtain

$$r_{i1}^{(30)\mathrm{div}}\mathcal{O}_i = \frac{g_s^2 \xi}{8\pi^2\epsilon} T_{cb}^A T_{da}^A \left(\bar{u}_R^c \gamma^\mu b_R^a \right) \left(\bar{d}_L^d \gamma_\mu c_L^b \right) \tag{414}$$

$$r_{i1}^{(31)\mathrm{div}}\mathcal{O}_i = \frac{-g_s^2 \xi}{8\pi^2\epsilon} T_{cb}^A T_{da}^A \left(\bar{u}_R^c \gamma^\mu b_R^a \right) \left(\bar{d}_L^d \gamma_\mu c_L^b \right) \tag{415}$$

$$r_{i1}^{(32)\mathrm{div}}\mathcal{O}_i = \frac{-g_s^2 \xi}{8\pi^2\epsilon} T_{cb}^A T_{da}^A \left(\bar{u}_R^c \gamma^\mu b_R^a \right) \left(\bar{d}_L^d \gamma_\mu c_L^b \right). \tag{416}$$

Hence we obtain the following relation,

$$(r_{i1}^{(27)\mathrm{div}} + r_{i1}^{(28)\mathrm{div}} + r_{i1}^{(29)\mathrm{div}} + r_{i1}^{(30)\mathrm{div}} + r_{i1}^{(31)\mathrm{div}} + r_{i1}^{(32)\mathrm{div}})\mathcal{O}_i = \frac{g_s^2(1+\xi/3)}{\pi^2\epsilon}\mathcal{O}_{1R}. \tag{417}$$

Thus we obtain

$$Z_{ij} = 1 - \frac{g^2}{8\pi^2\epsilon}\begin{pmatrix} -8 & 0 \\ -3 & 1 \end{pmatrix} \tag{418}$$

$$\gamma_{ij} = \frac{g^2}{8\pi^2}\begin{pmatrix} -8 & 0 \\ -3 & 1 \end{pmatrix} + O(g^4). \tag{419}$$

Then, $C_{1R}(m_b)$ and $C_{2R}(m_b)$ are obtained as follow,

$$C_{1R}(m_b) = \tilde{C}_{-R}(m_b) - \tilde{C}_{+R}(m_b) \tag{420}$$

$$= \frac{1}{3}\left(\left(\frac{\alpha_s(m_b)}{\alpha_s(m_W)}\right)^{24/23} - \left(\frac{\alpha_s(m_b)}{\alpha_s(m_W)}\right)^{-3/23}\right) = 0.34 \tag{421}$$

$$C_{2R}(m_b) = 3\tilde{C}_{+R}(m_b) \tag{422}$$

$$= \frac{1}{3}\left(3\left(\frac{\alpha_s(m_b)}{\alpha_s(m_W)}\right)^{-3/23}\right) = 0.92, \tag{423}$$

using the following equations,

$$C_{1R}(m_W) = 0 \tag{424}$$

$$C_{2R}(m_W) = 1. \tag{425}$$

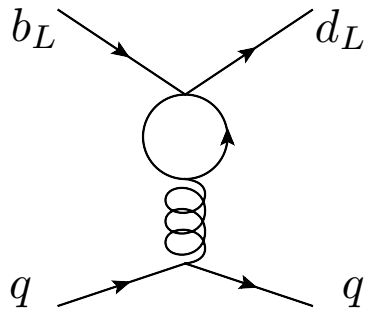

Fig.33 One of additional 1-loop Feynman diagrams for $b_L \to u_L \bar{u}_L d_L$.

C.3 $b_L \to u_L \bar{u}_L d_L$

For $b_L \to u_L \bar{u}_L d_L$, we must consider following operators,

$$\mathcal{O}_1 = (\bar{d}_L^a \gamma^\mu b_L^a)(\bar{u}_L^b \gamma_\mu u_L^b) \tag{426}$$

$$\mathcal{O}_2 = (\bar{d}_L^a \gamma^\mu b_L^b)(\bar{u}_L^b \gamma_\mu u_L^a) \tag{427}$$

$$\mathcal{O}_3 = \sum_q (\bar{d}_L^a \gamma^\mu b_L^a)(\bar{q}_L^b \gamma_\mu q_L^b) \tag{428}$$

$$\mathcal{O}_4 = \sum_q (\bar{d}_L^a \gamma^\mu b_L^b)(\bar{q}_L^b \gamma_\mu q_L^a) \tag{429}$$

$$\mathcal{O}_5 = \sum_q (\bar{d}_L^a \gamma^\mu b_L^a)(\bar{q}_R^b \gamma_\mu q_R^b) \tag{430}$$

$$\mathcal{O}_6 = \sum_q (\bar{d}_L^a \gamma^\mu b_L^b)(\bar{q}_R^b \gamma_\mu q_R^a) \tag{431}$$

because penguin diagrams can contribute. Hence, in addition to Fig. 21 - 32, figure 33 arise. The γ_{ij} is calculated from these Feynman diagrams as follow [33]

$$\gamma_{ij} = \frac{g^2}{8\pi^2} \left(\begin{array}{cc|cccc} -1 & 3 & 0 & 0 & 0 & 0 \\ 3 & -1 & -1/9 & 1/3 & -1/9 & 1/3 \\ \hline 0 & 0 & -11/9 & 11/3 & -2/9 & 2/3 \\ 0 & 0 & 3 - N_f/9 & -1 + N_f/3 & -N_f/9 & N_f/3 \\ 0 & 0 & 0 & 0 & 1 & -3 \\ 0 & 0 & -N_f/9 & N_f/3 & -N_f/9 & -8 + N_f/3 \end{array} \right), \tag{432}$$

All elements in left below part of γ_{ij} are zero. It means that $\mathcal{O}_{3,4,5,6}$ do not contribute renormalization of $\mathcal{O}_{1,2}$ so it is sufficient that we consider only $\mathcal{O}_{1,2}$ for evaluating $C_{1,2}$. They are already calculated in Subsec.C.1.

App. D Isospin analysis in $B \to \pi\pi$ and $\rho_L\rho_L$

When we measure ϕ_2 with $B \to \pi\pi$ or $B \to \rho_L\rho_L$, ρ_L is longitudinal mode of ρ meson, we use isospin analysis for excluding effect of penguin diagram. In this section, we explain how to use isospin analysis. It is almost same for $B \to \pi\pi$ and $B \to \rho_L\rho_L$, so we explain about $B \to \pi\pi$ case. When there is differencial point as $B \to \rho_L\rho_L$, then, we will mention it.

The time dependent CP asymmetry of $B \to \pi\pi$ ($\pi^+\pi^-$ or $\pi^0\pi^0$) is written as

$$\frac{\Gamma(B^0 \to \pi\pi) - \Gamma(\bar{B}^0 \to \pi\pi)}{\Gamma(B^0 \to \pi\pi) + \Gamma(\bar{B}^0 \to \pi\pi)} = C_{\pi\pi}\cos(\Delta M_{B_d} t) - S_{\pi\pi}\sin(\Delta M_{B_d} t)$$

$$C_{\pi\pi} = \frac{1 - |\bar{\rho}(\pi\pi)|^2}{1 + |\bar{\rho}(\pi\pi)|^2} \tag{433}$$

$$S_{\pi\pi} = \frac{2\mathrm{Im}\left(\frac{q}{p}\bar{\rho}(\pi\pi)\right)}{1 + |\bar{\rho}(\pi\pi)|^2} \tag{434}$$

$$\bar{\rho}(\pi\pi) = \frac{A(\bar{B}^0 \to \pi\pi)}{A(B^0 \to \pi\pi)}. \tag{435}$$

Thus $C_{\pi\pi}$ and $S_{\pi\pi}$ are observables. $B - \bar{B}$ mixing parameter q/p is known as

$$\frac{q}{p} = \frac{V_{td}V_{tb}^*}{V_{td}^*V_{tb}}. \tag{436}$$

If $B \to \pi\pi$ is affected by only tree diagram,

$$\bar{\rho}(\pi\pi)_{\text{no penguin}} = \frac{V_{ub}V_{ud}^*}{V_{ub}^*V_{ud}}. \tag{437}$$

Then,

$$\begin{aligned} S_{\pi\pi\,\text{no penguin}} &= \sin\left(\arg\left(\frac{V_{td}V_{tb}^*}{V_{td}^*V_{tb}}\frac{V_{ub}V_{ud}^*}{V_{ub}^*V_{ud}}\right)\right) \\ &= \sin(2\phi_2). \end{aligned} \tag{438}$$

Thus we can measure ϕ_2 from $S_{\pi\pi}$. However, in fact, penguin diagram can also affect $B \to \pi\pi$ as shown in Fig. 10.

Since π^+ and π^0 are made from quark combination, $u\bar{d}$ and $(u\bar{u} - d\bar{d})/\sqrt{2}$, these

are represented to isospin states as follow,

$$|\pi^{\pm}\rangle = |1, \pm 1\rangle \tag{439}$$

$$|\pi^{0}\rangle = |1, 0\rangle \,. \tag{440}$$

We combine these state and define 2π states as following equations.

$$|\pi^{+}\pi^{-}\rangle = \frac{1}{\sqrt{2}} \left(|1, -1\rangle \otimes |1, 1\rangle + |1, 1\rangle \otimes |1, -1\rangle \right) = \frac{1}{\sqrt{3}} |2, 0\rangle + \sqrt{\frac{2}{3}} |0, 0\rangle \tag{441}$$

$$= \frac{1}{\sqrt{2}} (|\pi^{-}(p)\rangle \otimes |\pi^{+}(-p)\rangle + |\pi^{+}(p)\rangle \otimes |\pi^{-}(-p)\rangle) \tag{442}$$

$$|\pi^{0}\pi^{0}\rangle = |1, 0\rangle \otimes |1, 0\rangle = \sqrt{\frac{2}{3}} |2, 0\rangle - \frac{1}{\sqrt{3}} |0, 0\rangle \tag{443}$$

$$= |\pi^{0}(p)\rangle \otimes |\pi^{0}(-p)\rangle \tag{444}$$

$$|\pi^{+}\pi^{0}\rangle = \frac{1}{\sqrt{2}} \left(|1, 0\rangle \otimes |1, 1\rangle + |1, 1\rangle \otimes |1, 0\rangle \right) = |2, 1\rangle \tag{445}$$

$$= \frac{1}{\sqrt{2}} (|\pi^{0}(p)\rangle \otimes |\pi^{+}(-p)\rangle + |\pi^{+}(p)\rangle \otimes |\pi^{0}(-p)\rangle) \tag{446}$$

Combine spin 1 and 1

$$|2, \pm 2\rangle = |1, \pm 1\rangle \otimes |1, \pm 1\rangle \tag{447}$$

$$|2, \pm 1\rangle = \sqrt{\frac{1}{2}} \, |1, 0\rangle \otimes |1, \pm 1\rangle + \sqrt{\frac{1}{2}} \, |1, \pm 1\rangle \otimes |1, 0\rangle \tag{448}$$

$$|2, 0\rangle = \sqrt{\frac{1}{6}} \, |1, -1\rangle \otimes |1, 1\rangle + \sqrt{\frac{2}{3}} \, |1, 0\rangle \otimes |1, 0\rangle + \sqrt{\frac{1}{6}} \, |1, 1\rangle \otimes |1, -1\rangle \tag{449}$$

$$|1, \pm 1\rangle = \sqrt{\frac{1}{2}} \, |1, 0\rangle \otimes |1, \pm 1\rangle - \sqrt{\frac{1}{2}} \, |1, \pm 1\rangle \otimes |1, 0\rangle \tag{450}$$

$$|1, 0\rangle = \sqrt{\frac{1}{2}} \, |1, -1\rangle \otimes |1, 1\rangle - \sqrt{\frac{1}{2}} \, |1, 1\rangle \otimes |1, -1\rangle \tag{451}$$

$$|0, 0\rangle = \sqrt{\frac{1}{3}} \, |1, -1\rangle \otimes |1, 1\rangle - \sqrt{\frac{1}{3}} \, |1, 0\rangle \otimes |1, 0\rangle + \sqrt{\frac{1}{3}} \, |1, 1\rangle \otimes |1, -1\rangle \tag{452}$$

The distinction of first term and second term is momentum of π in B meson rest

frame. Definitions of amplitude with these state are

$$A^{+-} = A(B^0 \to \pi^+\pi^-) \tag{453}$$
$$= \frac{1}{\sqrt{3}}\langle 2,0|\mathcal{H}^{\Delta I=3/2}|\frac{1}{2},-\frac{1}{2}\rangle + \sqrt{\frac{2}{3}}\langle 0,0|\mathcal{H}^{\Delta I=1/2}|\frac{1}{2},-\frac{1}{2}\rangle \tag{454}$$
$$= \frac{1}{\sqrt{3}}A_2 + \sqrt{\frac{2}{3}}A_0 \tag{455}$$
$$A^{+0} = A(B^+ \to \pi^+\pi^0) \tag{456}$$
$$= \langle 2,1|\mathcal{H}^{\Delta I=3/2}|\frac{1}{2},\frac{1}{2}\rangle$$
$$= A_2' \tag{457}$$
$$A^{00} = A(B^0 \to \pi^0\pi^0) \tag{458}$$
$$= \sqrt{\frac{2}{3}}\langle 2,0|\mathcal{H}^{\Delta I=3/2}|\frac{1}{2},-\frac{1}{2}\rangle - \frac{1}{\sqrt{3}}\langle 0,0|\mathcal{H}^{\Delta I=1/2}|\frac{1}{2},-\frac{1}{2}\rangle \tag{459}$$
$$= \sqrt{\frac{2}{3}}A_2 - \frac{1}{\sqrt{3}}A_0 \tag{460}$$

with amplitude from $B^0(|1/2,-1/2\rangle)$ to isospin$=i$ state ($|i,0\rangle$), A_i ($i=0,2$). Since these amplitude do not depend final state momentum p because $B\to\pi\pi$ is two body decays, we obtain as

$$\langle\pi^i(p)\pi^j(-p)|\mathcal{H}|B\rangle = \langle\pi^j(p)\pi^i(-p)|\mathcal{H}|B\rangle \qquad i,j=0,\pm. \tag{461}$$

As the result, decay rates with these amplitude are calculated as follow,

$$\Gamma(B^0\to\pi^+\pi^-) = \frac{1}{2M_B}\int d\Phi|\langle\pi^+(p)\pi^-(-p)|\mathcal{H}|B^0\rangle|^2 \tag{462}$$
$$= \frac{1}{2M_B}\int d\Phi|\frac{1}{2}\langle\pi^+(p)\pi^-(-p)|\mathcal{H}|B^0\rangle + \frac{1}{2}\langle\pi^-(p)\pi^+(-p)|\mathcal{H}|B^0\rangle|^2$$
$$= \frac{1}{2}\frac{1}{2M_B}\int d\Phi|\frac{1}{\sqrt{2}}(\langle\pi^+(p)\pi^-(-p)| + \langle\pi^-(p)\pi^+(-p)|)\mathcal{H}|B^0\rangle|^2$$
$$= \frac{1}{2}\frac{1}{2M_B}\int d\Phi|A^{+-}|^2 \tag{463}$$
$$\Gamma(B^+\to\pi^+\pi^0) = \frac{1}{2}\frac{1}{2M_B}\int d\Phi|A^{+0}|^2 \tag{464}$$
$$\Gamma(B^0\to\pi^0\pi^0) = \frac{1}{2}\frac{1}{2M_B}\int d\Phi|\langle\pi^0(p)\pi^0(-p)|\mathcal{H}|B^0\rangle|^2 \tag{465}$$
$$= \frac{1}{2}\frac{1}{2M_B}\int d\Phi|A^{00}|^2. \tag{466}$$

That is, we must multiply 1/2 because identical particle for $\pi^0\pi^0$ and symmetrization for $\pi^+\pi^-$ and $\pi^+\pi^0$.

Next, we evaluate $\frac{q}{p}\bar{\rho}(\pi^+\pi^-)$ as following relation,

$$\begin{aligned}\frac{q}{p}\bar{\rho}(\pi^+\pi^-) &= \frac{A(\bar{B}^0 \to \pi^+\pi^-)}{A(B^0 \to \pi^+\pi^-)} \\ &= \frac{q}{p}\frac{\bar{A}_2 + \sqrt{2}\bar{A}_0}{A_2 + \sqrt{2}A_0}\end{aligned} \tag{467}$$

where $\bar{A}_i$ is amplitude of $\bar{B}^0(|1/2, +1/2\rangle)$ decay. Strong interaction conserve isospin symmetry, so tree diagram affects to both $\mathcal{H}^{\Delta I=3/2}$ and $\mathcal{H}^{\Delta I=1/2}$ and penguin diagram affects only $\mathcal{H}^{\Delta I=1/2}$. For this reason, it can be calculated as follow.

$$\frac{q}{p}\bar{\rho}(\pi^+\pi^-) = \frac{q}{p}\frac{\bar{A}_2}{A_2}\left(\frac{1+\sqrt{2}\bar{A}_0/\bar{A}_2}{1+\sqrt{2}A_0/A_2}\right) = \frac{q}{p}\frac{\bar{A}_2}{A_2}\left(\frac{1+\bar{z}}{1+z}\right) = e^{2i\phi_2}\left(\frac{1+\bar{z}}{1+z}\right) \tag{468}$$

$$\mathrm{Im}\left(\frac{q}{p}\bar{\rho}(\pi^+\pi^-)\right) = \left|\frac{1+\bar{z}}{1+z}\right|\sin\left(2\phi_2 + \arg\left(\frac{1+\bar{z}}{1+z}\right)\right) \tag{469}$$

$$z = \sqrt{2}\frac{A_0}{A_2} \qquad \bar{z} = \sqrt{2}\frac{\bar{A}_0}{\bar{A}_2}. \tag{470}$$

A relation between A_2 and A_2' is calculated by combining spin 1/2(B meson) and spin 3/2(Hamiltonian) and obtain as follow,

$$A_2' = \sqrt{\frac{3}{2}}A_2. \tag{471}$$

Relation between A_2' and A_2

For evaluating coefficient $\langle 2,1|\mathcal{H}^{\Delta I=3/2}|\frac{1}{2},\frac{1}{2}\rangle$ and $\langle 2,0|\mathcal{H}^{\Delta I=3/2}|\frac{1}{2},-\frac{1}{2}\rangle$, we compose spin1/2 and spin3/2. We want to know terms of $|2,0\rangle$ and $|2,1\rangle$ after composing. Then we check only $|\frac{3}{2},\pm\frac{1}{2}\rangle\times|\frac{1}{2},\mp\frac{1}{2}\rangle$, $|\frac{3}{2},\frac{1}{2}\rangle\times|\frac{1}{2},\frac{1}{2}\rangle$ and $|\frac{3}{2},\frac{3}{2}\rangle\times|\frac{1}{2},-\frac{1}{2}\rangle$. Using $I^2=(I_1+I_2)^2=I_1^2+I_2^2+2I_{1z}I_{2z}+4(I_{1+}I_{2-}+I_{1-}I_{2+})$ and $I_z=I_{z1}+I_{z2}$, we make combination satisfying following equations,

$$I^2|2,0\rangle = 2(2+1)|2,0\rangle \tag{472}$$
$$I^2|2,1\rangle = 2(2+1)|2,1\rangle \tag{473}$$
$$I_z|2,0\rangle = 0 \tag{474}$$
$$I_z|2,1\rangle = |2,1\rangle, \tag{475}$$

and thus result is follow.

$$|2,0\rangle = \frac{1}{\sqrt{2}}|\frac{3}{2},\frac{1}{2}\rangle\times|\frac{1}{2},-\frac{1}{2}\rangle+\frac{1}{\sqrt{2}}|\frac{3}{2},-\frac{1}{2}\rangle\times|\frac{1}{2},\frac{1}{2}\rangle \tag{476}$$
$$|2,1\rangle = \frac{\sqrt{3}}{2}|\frac{3}{2},\frac{1}{2}\rangle\times|\frac{1}{2},\frac{1}{2}\rangle+\frac{1}{2}|\frac{3}{2},\frac{3}{2}\rangle\times|\frac{1}{2},-\frac{1}{2}\rangle \tag{477}$$

Each first terms are related to definition of A_2 and A_2' and we obtain Eq. (471).

we summarize these relation of amplitude and obtain following relation

$$\frac{A^{+-}}{\sqrt{2}}+A^{00}=A^{+0}. \tag{478}$$

Moreover we show $A_{0,2}$ in complex plane as Fig. 34. $|A^{+-}|,|A^{00}|,|A^{+0}|$ can be calculated by decay rate. Then we obtain z from these and $\bar{z}$ is calculated in the same way.

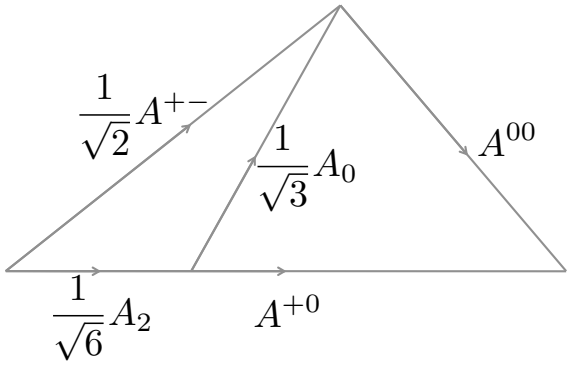

Fig.34 Relation between amplitudes in complex plane

Next, we calculate ϕ_2. The relation between observables, ϕ_2, z and $\bar{z}$ is as follow.

$$C_{\pi^+\pi^-} = \left(1 - \left|\frac{1+\bar{z}}{1+z}\right|^2\right) / \left(1 + \left|\frac{1+\bar{z}}{1+z}\right|^2\right) \tag{479}$$

$$S_{\pi^+\pi^-} = 2\left|\frac{1+\bar{z}}{1+z}\right| \sin\left(2\phi_2 + \arg\left(\frac{1+\bar{z}}{1+z}\right)\right) / \left(1 + \left|\frac{1+\bar{z}}{1+z}\right|^2\right) \tag{480}$$

$$C_{\pi^0\pi^0} = \left(1 - \left|\frac{2-\bar{z}}{2-z}\right|^2\right) / \left(1 + \left|\frac{2-\bar{z}}{2-z}\right|^2\right) \tag{481}$$

$$S_{\pi^0\pi^0} = 2\left|\frac{2-\bar{z}}{2-z}\right| \sin\left(2\phi_2 + \arg\left(\frac{2-\bar{z}}{2-z}\right)\right) / \left(1 + \left|\frac{2-\bar{z}}{2-z}\right|^2\right) \tag{482}$$

$$\frac{BR(B^0 \to \pi^+\pi^-)}{BR(B^+ \to \pi^+\pi^0)} \frac{\tau^+}{\tau^0} = \frac{1}{9}(|1+z|^2 + |1+\bar{z}|^2) \tag{483}$$

$$\frac{BR(B^0 \to \pi^0\pi^0)}{BR(B^+ \to \pi^+\pi^0)} \frac{\tau^+}{\tau^0} = \frac{1}{18}(|2-z|^2 + |2-\bar{z}|^2) \tag{484}$$

We mention that $S_{\pi^0\pi^0}$ can not be measured, because it is too difficult to measure

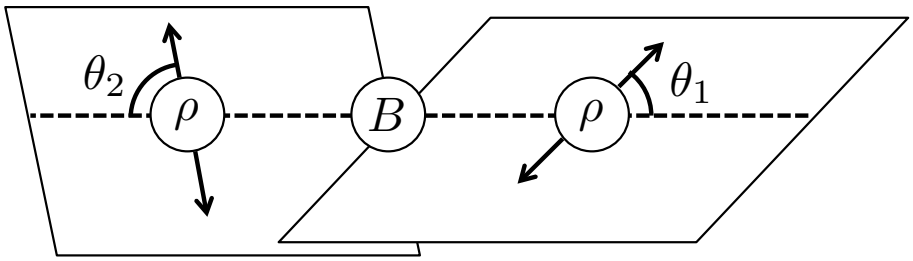

Fig.35

in experiment. However Belle II experiment may be able to measure. Thus we are going to theoretical calculation. z, $\bar{z}$ and ϕ_2 are calculated as following equations,

$$\mathrm{Re}[z] = \frac{3}{4}(1+C_{\pi^+\pi^-})\frac{BR(B^0\to\pi^+\pi^-)}{BR(B^+\to\pi^+\pi^0)}\frac{\tau^+}{\tau^0} - \frac{3}{2}(1+C_{\pi^0\pi^0})\frac{BR(B^0\to\pi^0\pi^0)}{BR(B^+\to\pi^+\pi^0)}\frac{\tau^+}{\tau^0} + \frac{1}{2}$$

$$|\mathrm{Im}[z]| = \sqrt{\frac{9}{2}(1+C_{\pi^+\pi^-})\frac{BR(B^0\to\pi^+\pi^-)}{BR(B^+\to\pi^+\pi^0)}\frac{\tau^+}{\tau^0} - (\mathrm{Re}[z]+1)^2} \tag{485}$$

$$\mathrm{Re}[\bar{z}] = \frac{3}{4}(1-C_{\pi^+\pi^-})\frac{BR(B^0\to\pi^+\pi^-)}{BR(B^+\to\pi^+\pi^0)}\frac{\tau^+}{\tau^0} - \frac{3}{2}(1-C_{\pi^0\pi^0})\frac{BR(B^0\to\pi^0\pi^0)}{BR(B^+\to\pi^+\pi^0)}\frac{\tau^+}{\tau^0} + \frac{1}{2}$$

$$|\mathrm{Im}[\bar{z}]| = \sqrt{\frac{9}{2}(1-C_{\pi^+\pi^-})\frac{BR(B^0\to\pi^+\pi^-)}{BR(B^+\to\pi^+\pi^0)}\frac{\tau^+}{\tau^0} - (\mathrm{Re}[\bar{z}]+1)^2} \tag{486}$$

$$\arcsin\left[\frac{S_{\pi^+\pi^-}}{\sqrt{1-C^2_{\pi^+\pi^-}}}\right] = \frac{\pi}{2} \pm \left[2\phi_2 + \arg\left(\frac{1+\bar{z}}{1+z}\right) - \frac{\pi}{2}\right] \tag{487}$$

$$\arcsin\left[\frac{S_{\pi^0\pi^0}}{\sqrt{1-C^2_{\pi^0\pi^0}}}\right] = \frac{\pi}{2} \pm \left[2\phi_2 + \arg\left(\frac{2-\bar{z}}{2-z}\right) - \frac{\pi}{2}\right]. \tag{488}$$

The results of isospin analysis in $B\to\pi\pi, \rho_L\rho_L$ are shown in Fig. 36 and 37. In Fig. 36, it seems that there are 6 solutions, but in fact, there are 8 solutions. (3 sign selections that come from $|\mathrm{Im}[z]|, |\mathrm{Im}[\bar{z}]|$ and arcsin make 8 solution because of $2^3 = 8$.) The reason of solution decrease are two couple of very near solutions. On the other hand, in Fig. 37, there are only 2 solutions. This means effect of $S_{\rho^0_L\rho^0_L}$ that can not be measured in $B\to\pi\pi$ or triangle in Fig. 34 does not have area. In this case, the second one affect. That is,penguin diagram in $B\to\rho_L\rho_L$ does not occur to shift phase and only arcsin divide into 2 solutions.

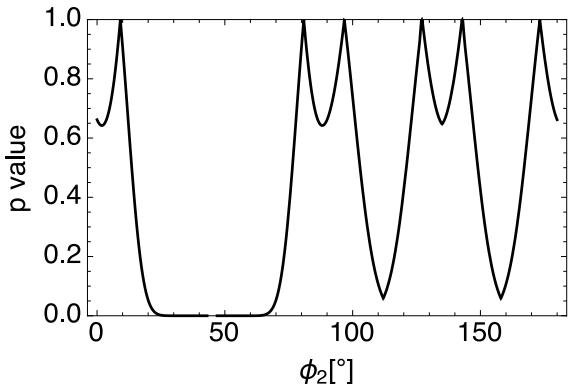

Fig.36 p value of ϕ_2 measured from $B \to \pi\pi$.

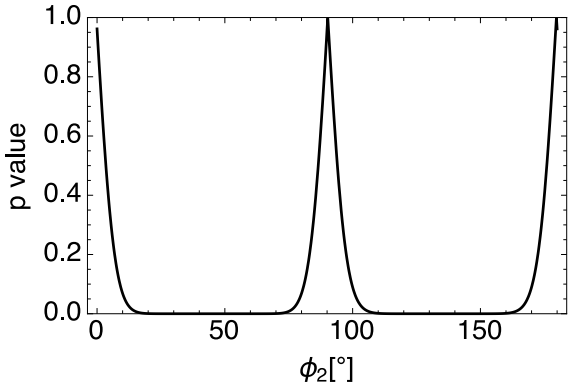

Fig.37 p value of ϕ_2 measured from $B \to \rho_L\rho_L$.

How to measure f_L

ρ is vector meson so there are longitudinal and transverse parts. For measuring f_L, we must consider about $\rho \to \pi\pi$ after $B \to \rho\rho$. Then, partial decay rate is

$$\frac{d^2\Gamma}{\Gamma d\cos\theta_1 d\cos\theta_2} = \frac{9}{4}\{\frac{1}{4}(1-f_L)\sin^2\theta_1\sin^2\theta_2 + f_L\cos^2\theta_1\cos^2\theta_2\} \tag{489}$$

with angle θ_1, θ_2 defined as Fig. 35. Thus f_L can be calculated from this distribution. Then it is known that longitudinal part almost occupy in $B \to \rho\rho$ decays as follow.

$$f_L^{+0} = 0.950 \pm 0.016 [17,\ 18] \tag{490}$$
$$f_L^{00} = 0.618 \pm 0.118 [19,\ 20] \tag{491}$$
$$f_L^{+-} = 0.990 \pm 0.020 [21,\ 22] \tag{492}$$

App. E Dalitz Plot Analysis in $B \to DK$

A one of the angle of unitarity triangle ϕ_3 is measured from $B \to DK$ decays. Then three methods for extraction of ϕ_3 are known, that is, GLW method using $D \to \pi\pi$ and KK decays [23, 24], ADS method using $D \to K\pi$ decays [25] and dalitz plot analysis using $D \to K_s\pi\pi$ [26]. In this section, we study dalitz plot analysis.

Feynman diagrams contributing $B \to DK$ are shown in Fig. 38. With Wolfenstein parameterization in CKM matrix, only V_{ub} and V_{td} have weak phase and argument of V_{ub} is -ϕ_3. Hence amplitudes of $B \to DK$ are written as following relation,

$$A(B^- \to D^0 K^-) = \mathcal{A}_B \tag{493}$$
$$A(B^- \to \bar{D}^0 K^-) = \mathcal{A}_B r_B e^{i(-\phi_3+\delta_B)} \tag{494}$$
$$A(B^+ \to \bar{D}^0 K^+) = \mathcal{A}_B \tag{495}$$
$$A(B^+ \to D^0 K^+) = \mathcal{A}_B r_B e^{i(\phi_3+\delta_B)}, \tag{496}$$

where δ_B is strong phase. About $D \to K_s\pi\pi$, we obtain following relation from CP symmetry,

$$A(D^0 \to K_s(p_1)\pi^+(p_2)\pi^-(p_3)) \overset{\text{CP}}{=} A(\bar{D}^0 \to K_s(p_1)\pi^-(p_2)\pi^+(p_3)). \tag{497}$$

It is known that there is CP violation in decay and mixing of D meson [10], but we ignore it because it is small. With definition with $s_{ij} \equiv (p_i + p_j)^2$, there is a following

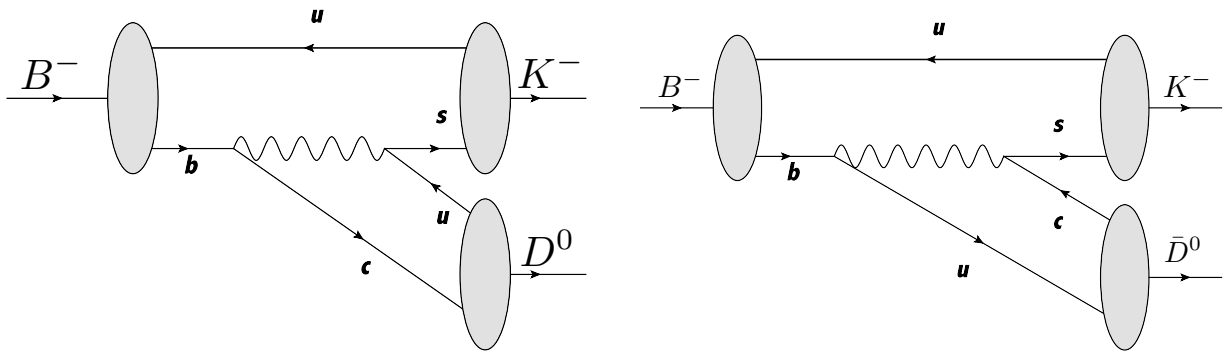

(a) $B^- \to D^0 K^-$ (b) $B^- \to \bar{D}^0 K^-$

Fig.38 Feynman diagram of $B^- \to D^0(\bar{D}^0)K^-$.

relation,

$$s_{23} = m_D^2 + m_K^2 + 2m_\pi^2 - s_{12} - s_{13}, \tag{498}$$

Hence $D \to K_s\pi\pi$ decay is described by two parameters s_{12} and s_{13}. Thus we obtain following relations,

$$A(D^0 \to K_s(p_K)\pi^+(p_+)\pi^-(p_-)) = A(s_{12}, s_{13}) \tag{499}$$
$$A(\bar{D}^0 \to K_s(p_K)\pi^+(p_+)\pi^-(p_-)) = A(s_{13}, s_{12}). \tag{500}$$

By Eqs.(493-496, 500), amplitudes of $B \to DK \to (K_s\pi\pi)_D K$ decays are written as follow,

$$\begin{aligned} &A(B^- \to (K_s(p_K)\pi^+(p_+)\pi^-(p_-))_D K^-) \\ =&\mathcal{A}_B \left(A(s_{12}, s_{13}) + r_B e^{i(-\phi_3+\delta_B)} A(s_{13}, s_{12}) \right) \end{aligned} \tag{501}$$

$$\begin{aligned} &A(B^+ \to (K_s(p_K)\pi^+(p_+)\pi^-(p_-))_D K^+) \\ =&\mathcal{A}_B \left(A(s_{13}, s_{12}) + r_B e^{i(\phi_3+\delta_B)} A(s_{12}, s_{13}) \right). \end{aligned} \tag{502}$$

From this relation, we obtain differential decay rate $d\Gamma$ as follow,

$$\begin{aligned} &d\Gamma(B^- \to (K_s(p_K)\pi^+(p_+)\pi^-(p_-))_D K^-)/\mathrm{dp} \\ =&|\mathcal{A}_B|^2 \left(|A(s_{12}, s_{13})|^2 + {r_B}^2 |A(s_{13}, s_{12})|^2 + 2r_B \mathrm{Re}(e^{i(-\phi_3+\delta_B)} A(s_{12}, s_{13})^* A(s_{13}, s_{12})) \right) \end{aligned} \tag{503}$$

$$\begin{aligned} &d\Gamma(B^+ \to (K_s(p_K)\pi^+(p_+)\pi^-(p_-))_D K^+)/\mathrm{dp} \\ =&|\mathcal{A}_B|^2 \mathscr{P}^2 \left(|A(s_{13}, s_{12})|^2 + {r_B}^2 |A(s_{12}, s_{13})|^2 + 2r_B \mathrm{Re}(e^{i(\phi_3+\delta_B)} A(s_{13}, s_{12})^* A(s_{12}, s_{13})) \right), \end{aligned} \tag{504}$$

where dp is phase space integration. We divide the phase space into bins as illustrated in Fig. 39. ith bins and $-i$th bins are symmetric about diagonal line $s_{12} = s_{13}$. We

define integration of interference and noninterference term in these bins as follow,

$$c_i \equiv \int_i dp|\mathcal{A}_B|^2 \mathrm{Re}\left(A(s_{12},s_{13})^* A(s_{13},s_{12})\right)/\sqrt{T_i T_{-i}} \tag{505}$$

$$= c_{-i} \tag{506}$$

$$s_i \equiv -\int_i dp|\mathcal{A}_B|^2 \mathrm{Im}\left(A(s_{12},s_{13})^* A(s_{13},s_{12})\right)/\sqrt{T_i T_{-i}} \tag{507}$$

$$= -s_{-i} \tag{508}$$

$$T_i \equiv \int_i dp|\mathcal{A}_B|^2 |A(s_{12},s_{13})|^2 \tag{509}$$

$$T_{-i} = \int_i dp|\mathcal{A}_B|^2 |A(s_{13},s_{12})|^2. \tag{510}$$

Using c_i, s_i and T_i, integrated decay rate in each bin is written as following equations,

$$\Gamma_i^- = \int_i d\Gamma(B^- \to (K_s\pi^+\pi^-)_D K^-) \tag{511}$$

$$= T_i + {r_B}^2 T_{-i} + 2r_B\sqrt{T_i T_{-i}}\left(\cos(-\phi_3+\delta_B)c_i + \sin(-\phi_3+\delta_B)s_i\right) \tag{512}$$

$$\Gamma_{-i}^- = \int_{-i} d\Gamma(B^- \to (K_s\pi^+\pi^-)_D K^-) \tag{513}$$

$$= T_{-i} + {r_B}^2 T_i + 2r_B\sqrt{T_i T_{-i}}\left(\cos(-\phi_3+\delta_B)c_i - \sin(-\phi_3+\delta_B)s_i\right) \tag{514}$$

$$\Gamma_i^+ = \int_i d\Gamma(B^+ \to (K_s\pi^+\pi^-)_D K^+) \tag{515}$$

$$= T_{-i} + {r_B}^2 T_i + 2r_B\sqrt{T_i T_{-i}}\left(\cos(\phi_3+\delta_B)c_i - \sin(\phi_3+\delta_B)s_i\right) \tag{516}$$

$$\Gamma_{-i}^+ = \int_{-i} d\Gamma(B^+ \to (K_s\pi^+\pi^-)_D K^+) \tag{517}$$

$$= T_i + {r_B}^2 T_{-i} + 2r_B\sqrt{T_i T_{-i}}\left(\cos(\phi_3+\delta_B)c_i + \sin(\phi_3+\delta_B)s_i\right). \tag{518}$$

In these, there are $4n$ equations and $2n+3$ unknown parameters, ϕ_3, δ_B, c_i and s_i, with $n \geq i$ since Γ_i and T_i are observables. This is, if n is larger than two, we can solve these equations and obtain ϕ_3. Also even if $c_i = 0$ of $s_i = 0$ is satisfied by strong phase, there are $2n$ equations and $n+3$ unknown parameters. Thus we can solve these equations with $n \geq 3$. Observables corresponding to Γ_i and T_i are measured by Belle collaboration [27]. We rewrite Γ_i and T_i to number of signals in each bins as follow,

$$\Gamma_{\pm i}^+ h = N_{\pm i}^+ \tag{519}$$

$$\Gamma_{\mp i}^- h = N_{\pm i}^- \tag{520}$$

$$T_{\pm i} h = K_{\pm i}, \tag{521}$$

by multiplying constant h and we obtain following equations,

$$\begin{aligned}
N_i^+ =& K_{-i} + {r_B}^2 K_i + 2r_B\sqrt{K_i K_{-i}}\,(\cos(\phi_3+\delta)c_i - \sin(\phi_3+\delta)s_i)\\
N_i^- =& K_{-i} + {r_B}^2 K_i + 2r_B\sqrt{K_i K_{-i}}\,(\cos(-\phi_3+\delta)c_i - \sin(-\phi_3+\delta)s_i)\\
N_{-i}^+ =& K_i + {r_B}^2 K_{-i} + 2r_B\sqrt{K_i K_{-i}}\,(\cos(\phi_3+\delta)c_i + \sin(\phi_3+\delta)s_i)\\
N_{-i}^- =& K_i + {r_B}^2 K_{-i} + 2r_B\sqrt{K_i K_{-i}}\,(\cos(-\phi_3+\delta)c_i + \sin(-\phi_3+\delta)s_i)\,. \qquad (522)
\end{aligned}$$

We note that $N_{\pm i}^+ = N_{\pm i}^-$ is satisfied in the limit $r_B = 0$. In addition, c_i and s_i are measured by CLEO collaboration [28]. In the result, we can obtain $\phi_3 = (74.5\pm15.1)^\circ$ and show p value in Fig. 40 by using these measured value.

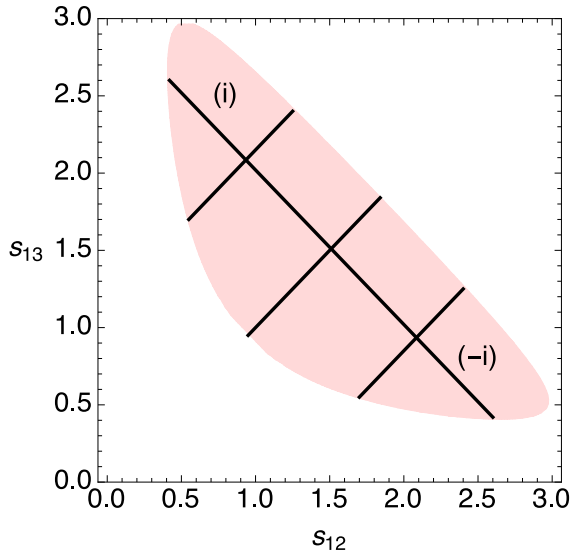

Fig.39 An example of binning phase space.

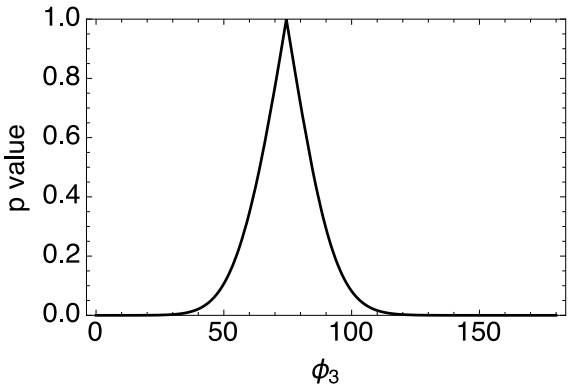

Fig.40 The p value of ϕ_3 extracted using Dalitz plot analysis.

App. F Input list

- Heavy Flavor Averaging Group[10]
  - HFAG-Oscillations/prepared for the PDG2014 Review of Particle Physics

    $T_{B^0} = 1.520(4) \times 10^{-12}$ s

    $T_{B^+} = 1.638(4) \times 10^{-12}$ s

    $\Delta M_{B^0} = 0.5055(20)$ ps^{-1}

    $\Delta M_{B_s} = 17.757(21)$ ps^{-1}
  - HFAG-Semileptonic, Summer 2014/PDG 2014

    $\mathrm{Br}(B \to \pi\ell\nu)|_{16\mathrm{GeV}^2>q^2>0} = (1.06 \pm 0.04) \times 10^{-4}$

    $V_{ub}^{B\to X_u\ell\nu} = (4.39 \pm 0.31) \times 10^{-3}$
  - HFAG,Rare Decays, 2014, Charmless Mesonic

    $\mathrm{Br}(B^0 \to \pi^+\pi^-) = (5.10 \pm 0.19) \times 10^{-6}$

    $\mathrm{Br}(B^0 \to \pi^0\pi^0) = (1.17 \pm 0.13) \times 10^{-6}$

    $\mathrm{Br}(B^+ \to \pi^+\pi^0) = (5.48 \pm 0.345) \times 10^{-6}$

    $\mathrm{Br}(B^0 \to \rho^+\rho^-) = (24.2 \pm 3.15) \times 10^{-6}$

    $\mathrm{Br}(B^0 \to \rho^0\rho^0) = (0.97 \pm 0.24) \times 10^{-6}$

    $\mathrm{Br}(B^+ \to \rho^+\rho^0) = (24.0 \pm 1.95) \times 10^{-6}$
  - HFAG, Rare Decays, 2014, Radiative and leptonic

    $\mathrm{Br}(B \to \tau\nu) = (114 \pm 22) \times 10^{-6}$
  - HFAG,Rare Decays, 2014, ACP

    $A_{\pi^+\pi^0} = -0.026 \pm 0.039$

    $A_{\pi^0\pi^0} = 0.43 \pm 0.24$

    $A_{\rho^+\rho^0} = -0.051 \pm 0.054$
  - HFAG, Unitarity Triangle, Summer2015

    $C_{\pi^+\pi^-} = -0.31 \pm 0.05$

    $S_{\pi^+\pi^-} = -0.66 \pm 0.06$

    $\sin 2\phi_1 = 0.691 \pm 0.017$

    $S_{\rho^+\rho^-} = -0.14 \pm 0.13$

    $C_{\rho^+\rho^-} = 0.00 \pm 0.09$

    $S_{\rho^0\rho^0} = 0.3 \pm 0.7 \pm 0.2$

    $C_{\rho^0\rho^0} = 0.2 \pm 0.8 \pm 0.3$

- CKM fitter[34]
  - Preliminary results as of Summer 2015 (EPS-HEP 2015 conference)

    $\lambda = 0.22543^{+0.00042}_{-0.00031}$

    $A = 0.8227^{+0.0066}_{-0.0136}$
- PDG2015[9]
  - Reviews, Tables, Plots(2014)

    $G_f = 1.1663787(6) \times 10^{-5}\text{GeV}^{-2}$

    $\hbar = 6.58211928(15) \times 10^{-25}\text{GeV s}$
  - Summary Tables

    $M_Z = 91.1876(21)\text{GeV}$

    $M_W = 80.385(15)\text{GeV}$

    $M_{\pi^\pm} = 0.13957018(35)\text{GeV}$

    $M_{\rho^\pm} = 0.77526(25)\text{GeV}$

    $M_{\omega^\pm} = 0.78265(12)\text{GeV}$

    $M_{K_S} = 0.497611(13)\text{GeV}$

    $M_{D^0} = 1.86484(5)\text{GeV}$

    $M_{B^\pm} = 5.27937(15)\text{GeV}$

    $M_{B^0} = 5.27961(15)\text{GeV}$

    $M_{B_s} = 5.36681(23)\text{GeV}$

    $M_\tau = 1.77686(12)\text{GeV}$

    $m_q = (m_u + m_d)/2 = (3.5^{+0.7}_{-0.2}) \times 10^{-3}\text{GeV}$
- Flavor Lattice Averaging Group[11]

  $F_B = 0.1905 \pm 0.0042\text{GeV}$

  $\xi = 1.268 \pm 0.063$

  $\alpha_s{}^{(5)}_{\overline{MS}}(M_Z) = 0.1184 \pm 0.0012$
- longitudinal polarization fraction of $B \to \rho\rho$

$$f_L^{+0} = 0.950 \pm 0.016[17,\ 18] \tag{523}$$

$$f_L^{00} = 0.618 \pm 0.118[19,\ 20] \tag{524}$$

$$f_L^{+-} = 0.990 \pm 0.020[21,\ 22] \tag{525}$$

- Quark mass[35]

  $m_b(\overline{MS}) = 4.20 \pm 0.07\text{GeV}$

  $m_b(1S) = 4.91 \pm 0.12\text{GeV}$

$m_c(1S) = 1.77 \pm 0.14\text{GeV}$

- $|V_{ub}|$ measured by $B \to \rho\ell\nu, \omega\ell\nu$[13]

$$
\begin{aligned}
|V_{ub}| &= 3.56 \pm 0.11 \pm 0.09^{+0.54}_{-0.37} \quad B^- \to \rho^0\ell^-\nu \\
|V_{ub}| &= 3.51 \pm 0.16 \pm 0.13^{+0.53}_{-0.36} \quad B^0 \to \rho^+\ell^-\nu \\
|V_{ub}| &= 3.08 \pm 0.29 \pm 0.11^{+0.44}_{-0.31} \quad B^- \to \omega^0\ell^-\nu
\end{aligned}
$$

Acknowledgement

I thank Minoru Tanaka for the continuous support of my Ph.D study and related research, and Ryoutaro Watanabe for his insightful comments and encouragement.

Reference

[1] N. Cabibbo *Phys. Rev. Lett.* **10** (1963) 531–533. [,648(1963)].

[2] M. Kobayashi and T. Maskawa *Prog. Theor. Phys.* **49** (1973) 652–657.

[3] **Belle** Collaboration, I. Adachi *et al. Phys. Rev. Lett.* **110** (2013), no. 13 131801, [1208.4678].

[4] C.-H. Chen and S.-h. Nam *Phys. Lett.* **B666** (2008) 462–466, [0807.0896].

[5] A. Crivellin *Phys. Rev.* **D81** (2010) 031301, [0907.2461].

[6] A. J. Buras, K. Gemmler, and G. Isidori *Nucl. Phys.* **B843** (2011) 107–142, [1007.1993].

[7] **Belle** Collaboration, A. Abdesselam *et al.*, *Measurement of the branching fraction of $B^+ \to \tau^+\nu_\tau$ decays with the semileptonic tagging method and the full Belle data sample*, in *8th International Workshop on the CKM Unitarity Triangle (CKM 2014) Vienna, Austria, September 8-12, 2014*, 2014. 1409.5269.

[8] T. Enomoto and M. Tanaka *Phys. Rev.* **D91** (2015), no. 1 014033, [1411.1177].

[9] **Particle Data Group** Collaboration, K. A. Olive *et al. Chin. Phys.* **C38** (2014) 090001.

[10] **Heavy Flavor Averaging Group (HFAG)** Collaboration, Y. Amhis *et al.* 1412.7515.

[11] S. Aoki *et al. Eur. Phys. J.* **C74** (2014) 2890, [1310.8555].

[12] P. Ball and R. Zwicky *Phys. Rev.* **D71** (2005) 014015, [hep-ph/0406232].

[13] **Belle** Collaboration, A. Sibidanov *et al. Phys. Rev.* **D88** (2013), no. 3 032005, [1306.2781].

[14] L. Wolfenstein *Phys. Rev. Lett.* **51** (1983) 1945.

[15] I. I. Y. Bigi and A. I. Sanda, *CP violation*, vol. 9. 2000.

[16] M. Gronau and D. London *Phys. Rev. Lett.* **65** (1990) 3381–3384.

[17] **Belle** Collaboration, J. Zhang *et al. Phys. Rev. Lett.* **91** (2003) 221801, [hep-ex/0306007].

[18] **BaBar** Collaboration, B. Aubert *et al. Phys. Rev. Lett.* **102** (2009) 141802, [0901.3522].

[19] **Belle** Collaboration, A. Somov *et al. Phys. Rev. Lett.* **96** (2006) 171801, [hep-ex/0601024].

[20] **BaBar** Collaboration, B. Aubert *et al. Phys. Rev.* **D76** (2007) 052007, [0705.2157].

[21] **Belle** Collaboration, P. Vanhoefer *et al.* 1510.01245.

[22] **BaBar** Collaboration, B. Aubert *et al. Phys. Rev.* **D78** (2008) 071104, [0807.4977].

[23] M. Gronau and D. London *Phys. Lett.* **B253** (1991) 483–488.

[24] M. Gronau and D. Wyler *Phys. Lett.* **B265** (1991) 172–176.

[25] D. Atwood, I. Dunietz, and A. Soni *Phys. Rev. Lett.* **78** (1997) 3257–3260, [hep-ph/9612433].

[26] A. Giri, Y. Grossman, A. Soffer, and J. Zupan *Phys. Rev.* **D68** (2003) 054018, [hep-ph/0303187].

[27] **Belle** Collaboration, H. Aihara *et al. Phys. Rev.* **D85** (2012) 112014, [1204.6561].

[28] **CLEO** Collaboration, J. Libby *et al. Phys. Rev.* **D82** (2010) 112006, [1010.2817].

[29] A. Crivellin and U. Nierste *Phys. Rev.* **D79** (2009) 035018, [0810.1613].

[30] **LHCb** Collaboration, R. Aaij *et al. Nature Phys.* **11** (2015) 743–747, [1504.01568].

[31] F. U. Bernlochner, Z. Ligeti, and S. Turczyk *Phys. Rev.* **D90** (2014), no. 9 094003, [1408.2516].

[32] G. Buchalla, A. J. Buras, and M. E. Lautenbacher *Rev. Mod. Phys.* **68** (1996) 1125–1144, [hep-ph/9512380].

[33] R. D. C. Miller and B. H. McKellar *Phys. Rept.* **106** (1984) 169–296.

[34] J. Charles *et al. Phys. Rev.* **D91** (2015), no. 7 073007, [1501.05013].

[35] Z.-z. Xing, H. Zhang, and S. Zhou *Phys. Rev.* **D77** (2008) 113016, [0712.1419].